



Max Planck Institut für Kolloid und Grenzflächenforschung



Towards Greener Stationary Phases: Thermoresponsive and Carbonaceous Chromatographic Supports

Dissertation

zur Erlangung des akademischen Grades
“doctor rerum naturalium”
(Dr. rer. nat.)
in der Wissenschaftsdisziplin Kolloidchemie

eingereicht an der
Mathematisch-Naturwissenschaftlichen Fakultät
der Universität Potsdam

von
Irene Tan

This work is licensed under a Creative Commons License:
Attribution - Noncommercial - Share Alike 3.0 Germany
To view a copy of this license visit
<http://creativecommons.org/licenses/by-nc-sa/3.0/de/>

Published online at the
Institutional Repository of the University of Potsdam:
URL <http://opus.kobv.de/ubp/volltexte/2011/5313/>
URN [urn:nbn:de:kobv:517-opus-53130](http://nbn-resolving.org/urn:nbn:de:kobv:517-opus-53130)
<http://nbn-resolving.org/urn:nbn:de:kobv:517-opus-53130>

*“Du must das Leben nicht verstehen,
dann wird es werden wie ein Fest.”*

Rainer Maria Rilke (1875-1926)

TABLE OF CONTENTS

1	INTRODUCTION	1
2	THEORY AND BACKGROUND	5
2.1	Stationary Phases for High Performance Liquid Chromatography	5
2.1.1	Silica Monoliths	5
2.1.2	Polymer Immobilized on Silica Stationary Supports.....	7
2.1.3	Porous Graphitic Carbon.....	9
2.2	Stimuli Responsive Polymers.....	10
2.2.1	Thermoresponsive Polymers.....	11
2.3	Controlled/ Living Radical Polymerization Techniques	13
2.3.1	Reversible Addition Fragmentation Chain Transfer Polymerization	14
2.3.2	Atom Transfer Radical Polymerization	16
2.4	Hydrothermal Synthesis of Biomass Derived Carbonaceous Materials.....	18
3	CHARACTERIZATION METHODS.....	21
3.1	Nitrogen Sorption	21
3.2	Electron Microscopy	23
3.3	High Performance Liquid Chromatography	25
4	RESULTS AND DISCUSSION	30
4.1	Modification of Silica Monoliths with Thermoresponsive Polymers for Chromatography	30
4.1.1	In-situ Grafting of PEGylated Copolymer to Silica Monoliths	31
4.1.2	Synthesis and Characterization	32
4.1.3	Chromatographic Characterization	40
4.1.3.1	Effect of Temperature on the Performance of the Column	42
4.1.3.2	Effect of Grafting Density on the Performance of the Column.....	45

4.1.3.3	Effect of Molecular Weight of Grafted Copolymers on the Performance of the Column.....	50
4.1.3.4	Effect of Varying Comonomers on the Performance of the Column	52
4.1.3.5	Performance of the Column in the Separation of Proteins	53
4.1.3.6	Determination of the Hydrophobicity of the Monolithic Columns	54
4.1.3.7	Effect of Polymer Type on the Performance of the Column.....	56
4.1.4	Summary and Outlook	63
4.2	Biomass Derived Carbonaceous Materials for Chromatography.....	65
4.2.1	Hydrothermal Carbonization and the Incorporation of Functional Monomers	66
4.2.2	Synthesis and Characterization	68
4.2.3	Chromatographic Characterization	83
4.2.4	Summary and Outlook	89
5	CONCLUSION.....	91
6	APPENDIX.....	97
7	REFERENCES	109

1 INTRODUCTION

Dating back to the 4th century, pharmacology is known as the oldest discipline in health sciences. Humans back then had already formulated cures for various illnesses; for example, plants had been known to be used as remedies for as long as 60,000 years. How these remedial properties function had been a topic that was redefined over centuries, starting with the traditional beliefs of Hippocrates and Galen to modern theories and principles of drug action that govern today's origin of pharmacology¹. One principle states that each remedy has an identifiable essence that is obtained from the natural product by chemical extraction. Till recent times, the separation of biological compounds such as proteins and enzymes is still important in order to study their properties individually for various applications in life sciences. Thus, in the last century, a huge research area was dedicated to this field.

Conventionally, biomolecules are separated by electrophoresis and liquid chromatography. Electrophoresis is commonly used for separating biological macromolecules such as proteins or small nucleic acids (DNA, RNA, oligonucleotides) under denaturing conditions². In liquid chromatography, biomolecules can be separated with reversed phase liquid chromatography (RPLC)³⁻⁵, ion-exchange chromatography (IEC)^{6, 7} or hydrophobic interaction chromatography (HIC)⁸⁻¹⁰. Some trends accompanying current 'state of the art' techniques in the development of high performance liquid chromatography (HPLC) are mentioned below.

'Normal' phase (NP) HPLC is one of the first chromatographic techniques developed, with a hydrophilic surface chemistry using underivatized silica or alumina having a high affinity for hydrophilic compounds. However, it is not commonly used due to its limitations in complex bioseparation schemes like in proteomics as the use of purely non-polar solvents is employed. Besides factors related with the high costs and less availability of organic solvents (acetonitrile), non-specific interactions on normal phase columns cause the retention and separation of highly hydrophilic and uncharged compounds to be inefficient. These compounds also face solvophilic problems in non-polar mobile phases.

Since the 1970s, 'reversed' phase (RP) HPLC accounts for the vast majority of analyses performed in liquid chromatography. It is any chromatography method that uses a non-polar stationary phase; for example, by introducing alkyl chains bonded covalently to unmodified polar silica support surface, reversing the order of elution compared to NP-HPLC. This

column retains non-polar compounds more strongly while the polar substances elute first. To date, one of the more popular commercially available RP columns is the octadecyl carbon chain (C_{18}) bonded silica, with 297 columns commercially available. It is a powerful technique used for a large range of molecules, especially in the pharmaceutical industries due to its suitability towards broad numbers of useful drug analytes. However, RP-HPLC has major drawbacks when it comes to process scaling of proteins and the separation of hydrophilic compounds.

In order to address the shortcoming of normal phase chromatography, a new mode of separation known as hydrophilic interaction chromatography (HILIC) emerged in the early 1990s. The name was coined by Alpert¹¹ which describes the separation mechanism as liquid-liquid partition chromatography. HILIC phases basically resemble NP chromatography; they consist of polar stationary phases except that the eluents used are partially aqueous. Usually, a small amount of water or miscible aprotic solvents are added and the analytes are distributed between the water-rich polar stationary phase and the hydrophobic mobile phase, thus enabling the retention of the polar compounds on the polar column. Thus it was shown that the main advantage of HILIC phases over NP phases is attributed solely to solvability factors of solutes. HILIC chromatography allows the separation of complex polar compounds such as carbohydrates, peptides¹² and nucleic acids which NPC cannot perform efficiently.

The search for alternative stationary phases is not limited to only silica-bonded materials. Carbon and polymeric stationary phases are also intensively used and investigated since silica-based stationary phases show certain disadvantages. The main problem associated with silica is its low chemical resistance when exposed to extremely alkaline conditions. In 1986, Knox *et al.*¹³ published the first paper on the use of porous graphitic carbon (PGC) as a stationary phase. The peculiarity of such a stationary phase was the fact that it could function in both normal and reversed phase modes in HPLC. PGCs boast superior mechanical strength and perform well in chromatography, thus this was the starting point when a large field of research started to be dedicated to carbon supports.

In addition to surface chemistries, the morphologies of chromatographic supports have also evolved over the years in order to suit changing separation needs. Pore size and particle diameter are important aspects to investigate since diffusion and mass transfer kinetics play a

role in enhancing separation. The structural transition from micrometer-sized (3-10 μm) sphere packing to single-pieced monoliths introduced improved mass transfer properties and physical stability. Non-porous micro-particulate (typically 0.7-2 μm) supports later emerged in order to provide high column efficiencies attributed to small particle sizes¹⁴. These ‘pellicular’ mono-dispersed supports have already been carried out for the separation of large biomolecules such as proteins, polynucleotides and peptides^{15, 16}. More trends in changing morphologies from micrometer sphere packing to monoliths will be discussed further in Chapter 2.

As mentioned, the most commonly employed columns for protein separation in classical liquid chromatography are RP-18, in which the analytes are gradient-eluted with low pH and organic mobile phases such as acetonitrile. The use of such organic eluents tends to, in certain cases, cause denaturation in protein separations. For such proteins which do not spontaneously re-fold after elution, their solute biological activities would be destroyed upon prolonged contact with organic phases and acidic conditions. Peptides and proteins have numerous functional groups, and they can possess either net positive or negative charges in varying solution pH. Ion-exchange chromatography (IEC) separates proteins according to their net charges via electrostatic interactions, which are dependent on the composition of the mobile phase. Elution is in this case achieved by increasing the ionic strength of the solvent, thus allowing the analytes to unbind from the column surfaces. In a conventional hydrophobic interaction chromatography (HIC) system, separations are based on the surface hydrophobicity of proteins and peptides. Usually, they were performed using a starting mobile phase of very high salt concentration to promote ‘salting out’ effect on the analytes, thus promoting hydrophobic binding to the column. Subsequently, this binding is reduced by lowering the salt concentration and thus decreasing the hydrophobic effect on the analytes. These processes however, possibly induce alterations to the protein structures, resulting in decreased product yields and reduced bioactivity.

Recent advances in liquid chromatography explore the separation of mixtures of biomolecules in purely aqueous environment under isocratic conditions, which could be compared to the efficiency of the RP-18 column. Kanazawa¹⁷ and Roohi *et al*¹⁸ have demonstrated that a group of steroids could be separated well in water by immobilizing a temperature sensitive polymer on the stationary phase. The harsh conditions previously used for biomolecule separation

could then be avoided; in addition, gradient elution commonly used in RPLC, IEC and HIC can effectively be excluded. This special feature involving a simple temperature switch for the separation of steroids under ‘green’ conditions prompted the continuation of this work towards the investigation of more versatile approaches towards proteomics.

The main focus of the present work involves the development of thermoresponsive stationary phases for the separation of biocompounds (*eg.* steroids and proteins) in purely aqueous and isocratic conditions on the HPLC. The first part of the thesis describes the modification of silica monoliths with temperature sensitive copolymer poly(oligo(ethylene glycol) methacrylate-*co*-2-(2-methoxyethoxy)ethyl methacrylate) (P(OEGMA-*co*-MEO₂MA)) and the effect of varying parameters on bioanalyte separation is discussed. The advantages of using a PEG-derived copolymer are illustrated by its biocompatibility and its tunability of its lower critical solution temperature (LCST) in water. Moreover, the column’s performance is compared to benchmark poly(*N*-isopropyl acrylamide) (PNIPAAm)-modified monoliths.

The second chapter of the thesis introduces the generation of carbonaceous products with modifiable surface groups from a process known as hydrothermal carbonization. The product was investigated as promising column packing material for liquid chromatography. A series of basic HPLC studies was done to study the efficiency of the column, for example as RP and NP modes. Finally, PNIPAAm was grafted on the particles’ surfaces and separations based on the thermoresponsive composite were also conducted in parallel.

2 THEORY AND BACKGROUND

2.1 Stationary Phases for High Performance Liquid Chromatography

High performance liquid chromatography (HPLC) is a chromatographic method that was developed later from classical column chromatography. The differences between both are distinguished by their operating techniques: In classical chromatography, columns were made out of glass with big diameters and were packed with stationary materials with large particle sizes. Modern liquid chromatography employs short stainless steel columns (30-150 mm) with small diameters (commonly 4.6 mm) and the stationary phase materials which are packed into the columns usually have small particle sizes (3-10 μm average diameter). Instead of using hydrostatic pressures like in classical chromatography, the mobile phases are pumped through columns with a high pressure in HPLC. Therefore, the term 'high pressure' and 'high performance' can be used synonymously. The improved dimensions enable HPLC to achieve better separation times and performance.

Solid supports used as stationary phases consist normally of different porous materials with varying particle sizes. The differences in particle diameter sizes and porosity determine their applications, for example, packing with 3-5 μm sizes are ideal for fast separation analyses. The materials can basically be classified into three groups¹⁹: Inorganic packing such as silica, carbon, hydroxyapatites and alumina, organic polymer gels such as crosslinked copolymers of polymethylmethacrylate and bonded packing material which is a composite of both. The development of efficient packing materials is classified structurally according from beads to core/shell particles and later to monoliths.

For my research, silica monoliths with meso- and macroporosity were used and the modification of their surfaces with polymers is shown below. Carbonaceous particles as packing materials for HPLC are also discussed.

2.1.1 Silica Monoliths

Inorganic-based packing materials such as silica gels are popular as a support matrix due to their mechanical strength and stability under high pressures as compared to organic polymer-based gels. For more than 20 years, silica-based supports have been widely used preferably in LC as it is commercially available in a wide range of spherical particle sizes and pore sizes.

Its ease of derivatization also enables its surfaces to be tailored accordingly with different functionalities.

An important breakthrough in chromatographic science was the discovery of monolithic materials as an alternative to the spherical particles. Since their introduction in the 1980s, monolithic materials which are a single piece of porous material, continue to be an important advancement in liquid chromatography. Such hierarchically porous materials show superior mass transfer properties and thus they can operate at reduced pressures and can provide shorter analysis times as compared to particulate packed columns^{4, 20, 21}.

Such single-piece silica gel monolith with porosity spanning over multiple length scales for liquid chromatography are synthesized using the sol-gel methodology²². This process involves the hydrolysis of alkoxysilanes $\text{Si}(\text{O-R})_4$ (where $\text{R} = \text{CH}_3, \text{C}_2\text{H}_5$ etc.) in the presence of a water-soluble polymer such as polyethylene oxide (PEO) under acidic conditions. Well-defined and interconnected macroporous structures form as a result of phase separation and spinodal decomposition during polycondensation to form a viscous hydrogel. This bicontinuous structure can be observed on the SEM micrograph in Figure 2-2(a). The macropore sizes of the preformed monolith can be tailored by varying parameters such as soft template polymers used in the synthesis or time allowed for the phase separation process to occur.

On the surface of the structures, hydrophilic groups in the form of silanol ($-\text{Si}-\text{OH}$) are present. Figure 2-1 shows the different hydroxyl groups on the surface of silica that may be formed during the sol-gel process. The reactive hydrophilic surface enables the ease of chemical modification with different functional groups for suitable applications. There are recent reports on surface functionalization of silica monoliths for HILIC mode separation of polar compounds with reagents such as polyacrylamide²³, while the most popular octadecyl- (C_{18}), octyl- (C_8), cyano- and phenyl-bonded phases are reported for RP-HPLC.

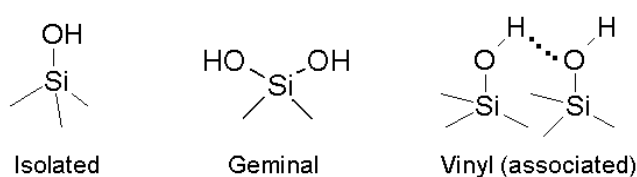


Figure 2-1: Types of hydroxyl groups on silica surface

Subsequently, solvent exchange was applied to the wet gels to tailor mesoporosity on its Si-O-Si backbone. The next steps include solvent removal and heat treatment to finally give silica monolith with designed bimodal macro- and mesoporosity. The current commercial packings have well-defined pore sizes in the range of 0.7 to 30 nm and with specific surface areas from 50 to 250 m²/g are obtained using such previously described procedures. Mesopores can be observed from the TEM micrograph in Figure 2-2(b) and they provide the necessary high surface area for analytical separations.

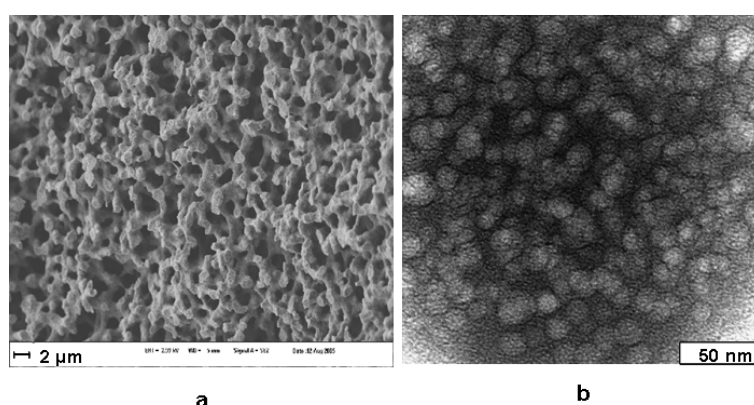


Figure 2-2: Scanning Electron Micrograph (SEM) (a) and Transmission Electron Micrograph (TEM) (b) of a macro- and mesoporous silica monolith (Chromolith Si 100-4.6 mm, MERCK, Darmstadt)

2.1.2 Polymer Immobilized on Silica Stationary Supports

There are several limitations to underivatized silica surfaces, thus many post-functionalization processes have been applied resulting in the so-called chemical-bonded silica phases. As previously mentioned, the stability of the silica skeleton presents a limitation when using aggressive alkaline conditions, thus silica-based stationary supports should not be exposed for a long period of time to mobile phases with a pH larger than 8. In the case of chemically-bonded silica-based phases, the Si-C bonds can also be easily hydrolyzed upon the use of highly acidic conditions. Several manufacturers have indeed reported the use of unmodified silica columns in HILIC mode separation for basic polar analytes^{24, 25}, usually coupled with a mass spectrometer (MS) detector. However, separation mechanisms are often complicated especially for polar solutes present in complex matrices and the highly polar residual silanol groups easily cause severe irreversible adsorptions in columns.

However, the advantage of the reactive silanol groups is the ease of functionalization of silica surface. The surface behavior can thus be altered and novel properties can be introduced, such

as change in polarity or stimuli-responsivity. Currently, there are many studies which explore the grafting of various reagents such as chiral selectors²⁶, zwitterionic²⁷ and thermoresponsive polymers¹⁸. Immobilization of organic polymers on silica stationary supports appears as an ideal solution to overcome the drawbacks mentioned above about the use of raw silica, allowing a versatile decoration of the silica supports with tailored functionality. The resulting silica-polymer composite packings combine then the excellent mechanical strength of the inorganic silica together with the chemical functionality and selectivity of the organic polymers. Another advantage would be the increase of stability of the final packing due to masking effects against silica dissolution as well as an effective shielding of residual silanol groups, avoiding thus non-specific binding.

There are two main approaches for polymer immobilization: physisorption and chemical coupling (see Figure 2-3). The first method may include coating by precipitation where dissolved polymers can be deposited on silica gel after the removal of this solvent. This method can result in relatively stable materials if the polymer is insoluble in the mobile phases used. Examples of hydrophilic polymer layers immobilized by coating are polyallylamine²⁸ or proteins for chiral separations in LC²⁹. In order to improve the stability of adsorption, deposited polymers can be crosslinked thus resulting in stable layers that are insoluble in eluents.

In contrast to physisorption, covalent couplings are more stable and the grafted polymers are strongly anchored on the surface of silica gels. Covalent attachment can be done using two different methods, the ‘grafting from’ and the ‘grafting to’ procedures (See Figure 2-3). ‘Grafting to’ approach allows tailored end-functionalized polymers B to react with a suitable functional surface substrate A. The synthesis of homogenous and stable polymer B with narrow molecular weight distribution can be done first for example by ‘living’ radical polymerization or ring opening metathesis polymerization (ROMP). Silica surface can also be modified accordingly for appropriate reactive groups to couple with polymer B terminal groups^{30, 31}, forming stable bonds such as the amide bond. The ‘grafting from’ method has attracted considerable attention in recent years in the preparation of tethered polymers on solid substrate surface. It involves immobilizing an initiator on the surface and allowing monomers in solution M to undergo controlled polymerization directly onto the activated

surface. The latter approach results in higher grafting densities since all reactive groups on surface participate in the grafting process.

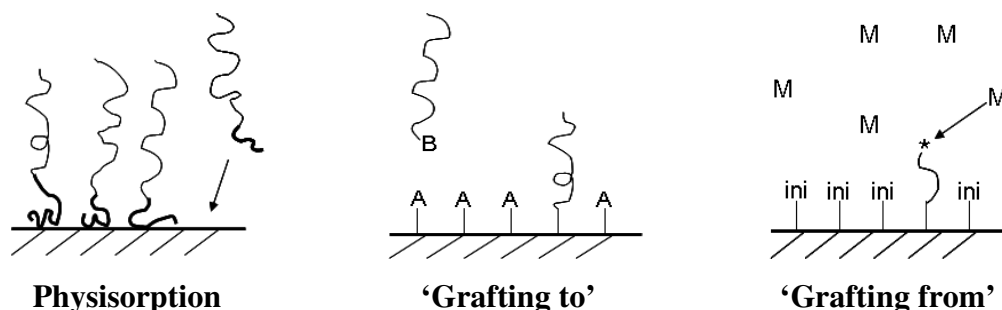


Figure 2-3: Schematic approaches for the preparation of polymer immobilization to surfaces

Controlled radical polymerizations including atom transfer radical polymerization (ATRP)³², reversible addition fragmentation transfer (RAFT)³³, 2,2,6,6-tetramethylpiperidine-1-oxyl (TEMPO)-mediated and iniferter³⁴ radical polymerizations have been used to synthesize polymer brushes on solid surfaces³⁵⁻⁴⁰. Recently, stimuli responsive polymers have been a class of polymers widely applied in this area.

2.1.3 Porous Graphitic Carbon

Since the 70s, the drawbacks of silica-based stationary phases mentioned above have driven the search towards carbon as an alternative chromatography support. However, the ideal carbon phase is difficult to reproduce; they often exhibit high retentiveness, and it is very difficult to synthesize homogenous surfaces. Attempts to combine good mechanical strength and chromatographic performance for such a phase did not exist till Knox *et al.* pioneered porous graphitic carbon (PGC)^{13, 41}.

Generally, the preparation of PGC requires relatively high temperatures (>2500 °C) and the use of a porous silica gel as a sacrificial template. Spherical silica was in this case impregnated with a melt of phenol and hexamine and then promptly heated to 80-160 °C to form phenol-formaldehyde resin within the pores of the gel. The polymer formed is then pyrolysed under inert atmosphere up to 1500 °C and subsequently the silica was removed with hot aqueous potash solution. Highly porous graphitized carbon which retains the porosity and shape of the silica template resulted after further heating to 2500 °C. The choice of porosity and shape largely depends on the template selected. Over the years, manufacturing processes

have been refined to produce other carbonaceous phases to achieve varied separation requirements^{42, 43}.

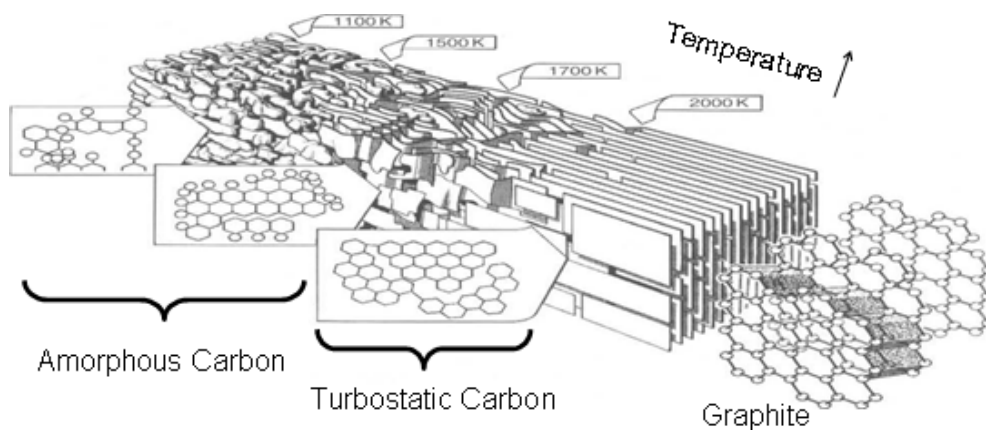


Figure 2-4: Behavior of the carbon structure upon pyrolysis

PGC has unique mixed properties which enable it to perform as a stationary phase in various applications, including both NP-HPLC and RP-HPLC. Due to its graphitic backbone, increasingly hydrophobic compounds are more retained which suggests a RP behavior analogous to those of non-polar phases. In addition, the delocalization of electrons between graphitized sheets of PGC also induces a polar retention effect⁴⁴ responsible for the retention of polar and ionic analytes. Some original characteristics of such a phase include redox ability⁴⁵, conducting properties used in electrically modulated liquid chromatography (EMLC)⁴⁶ and resistance to aggressive conditions which gives it an advantage over silica-based phases. Thus, these particular properties confer the unique chromatographic separation ability of PGC. PGC columns have already been demonstrated in a number of important applications: the separation of isomers^{47, 48}, carbohydrates⁴⁹⁻⁵¹, several bioactive compounds such as taxol⁵² and pharmaceuticals such as antihypoxia drugs⁵³, etc.

2.2 Stimuli Responsive Polymers

Stimuli responsive polymers respond towards external changes in their environmental factors such as temperature, pH, electrical and magnetic field, chemicals, ionic strength and light⁵⁴⁻⁵⁶. These responses manifest as dramatic changes in shape, solubility, surface characteristics, self assembly of molecules or a sol to gel transition. Some polymers have the properties to respond towards two or more stimuli and their properties can also be easily incorporated in synthetic polymers to give hybrid gels. The rapid progress in polymer science has given rise

to the class of ‘smart’ polymers which have found extensive applications in the areas of biotechnology. Some of the more significant examples of this include the delivery of therapeutics, tissue engineering, cell culture, bioseparations in chromatography, sensors and actuators. Recently, thermo-switchable stationary phases for HPLC have been described as an interesting option for controlling the separation of bioanalytes⁵⁷. These types of phases are generated by grafting temperature-sensitive polymers on silica or polymer-based beads or monoliths^{18, 58}.

2.2.1 Thermoresponsive Polymers

A thermoresponsive polymer undergoes physical change when exposed to thermal stimuli. The ability to show such changes under easily controlled conditions can be exploited for many analytical techniques, especially in separation chemistry. For most polymers such as polyethylene oxide (PEO) or polyethylene glycol (PEG), they exhibit a property known as upper critical solution temperature (UCST), where their dissolution occurs upon heating and vigorous stirring (see Figure 2-5(a)). In contrary to the behavior of most compounds in aqueous solution, the class of temperature-sensitive polymers exhibit lower critical solution temperatures (LCST). This is the temperature value at which the polymer is dissolved in solution below its LCST while upon elevating the temperature, the polymer becomes increasingly non-soluble and precipitates out of the solution (see Figure 2-5(b)). Normally, this property may depend on factors such as molecular weight of polymer, concentration in solution, pH and ionic strength in solutions.

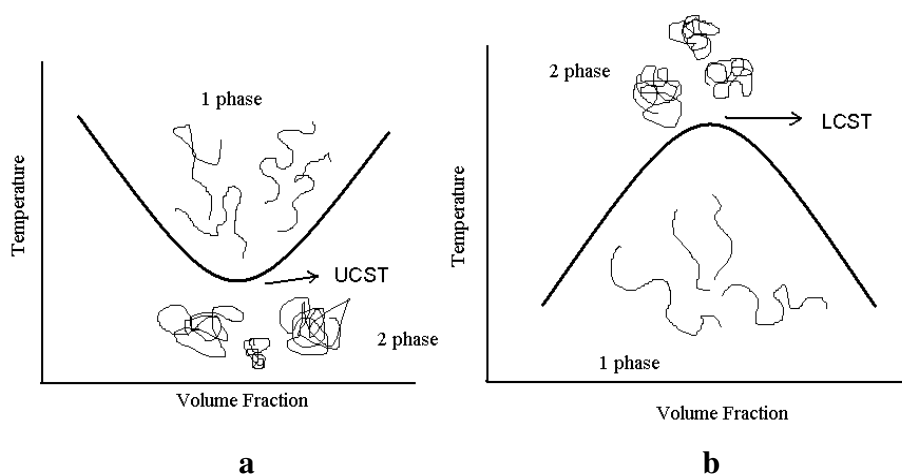
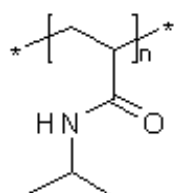


Figure 2-5: Phase diagram plots of polymer-solution phase behaviour including: (a) UCST; (b) LCST

One of the most commonly known thermoresponsive polymer is poly(*N*-isopropyl acrylamide) (PNIPAAm) (structure shown in Figure 2-6) and it has been mainly exploited for drug delivery applications as well as for preparing smart stationary phases⁵⁹. Heskins and Guillet⁶⁰ established the LCST of PNIPAAm to be 32 °C as early as the 1960s, and this temperature, being relatively close to body temperature, enables it to be widely explored for preparing switchable materials for biological applications⁶¹. Another reason for its biomedical popularity is its insensitivity towards slight environmental changes such as pH or concentration which makes it desirable for hyperthermia-induced drug delivery studies⁶².



LCST: 32 °C

Figure 2-6: Chemical structure of PNIPAAm

Another class of thermoresponsive polymer is represented by poly(oxazoline)s. Oxazolines are structural isomers of NIPAAm; the N moiety of the former appears within the backbone chains instead when polymerized by ‘living’ cationic ring opening polymerization (Figure 2-7)⁶³. The cloud point of each polymer varies with differences in the extended alkyl chain of monomers, concentration of polymer in solution, molecular weight and addition of salts. Due to its biocompatibility, poly(2-oxazoline)s are widely studied for its potential for use as biomaterials like in drug delivery systems or thermoresponsive materials⁶⁴. It was found that by copolymerizing each different monomer, the LCST and individual properties of each copolymer could be specifically tuned to a desired LCST in water.

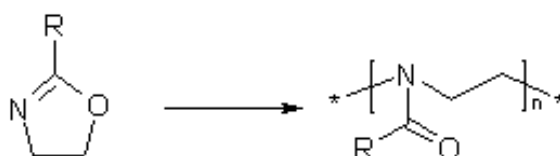


Figure 2-7: Polymerization scheme of poly(2-oxazoline)s, where R = *N*-propyl (LCST 23.8 °C); isopropyl (LCST 38.7 °C); *N*-ethyl (LCST 60 °C); for concentration of 1 wt.% in solution

Recently, oligo(ethylene glycol)-based thermoresponsive polymers have been proposed by the group of Lutz *et al.*⁶⁵ as interesting alternatives to PNIPAAm. Indeed, these polymers display

reversible phase transitions in water and in addition, are mainly composed of bioinert ethylene oxide units (i.e., poor hydrogen bond donors and highly hydrated acceptors). Moreover, these interesting macromolecules can be easily synthesized using commercially available monomers (Figure 2-8) by surface-initiated atom transfer radical polymerization (ATRP) in the presence of the initiator *N*-succinimidyl 2-bromoisobutyrate⁶⁶. For instance, random copolymers of 2-(2-methoxyethoxy)ethyl methacrylate (MEO₂MA) and oligo(ethylene glycol) methacrylate (OEGMA; *M_n* ~ 475 g/mol) exhibit an LCST in water, which can be precisely adjusted by varying the comonomer composition⁶⁷. Thus, thermoresponsive P(MEO₂MA-*co*-OEGMA) copolymers have been recently exploited for preparing a variety of smart biocompatible materials⁶⁸. In particular, it has been demonstrated lately that these polymers allow reversible control over bioadhesion^{69, 70}. Thus, it was tempting to use these smart biocompatible coatings for developing innovative stationary phases.

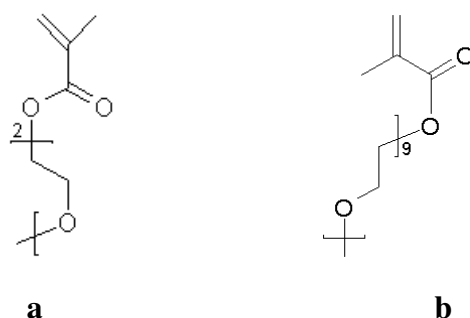


Figure 2-8: Chemical structures of (a) 2-(2-methoxyethoxy) ethyl methacrylate (MEO₂MA); LCST: 26°C; (b) oligo(ethylene glycol) methacrylate (OEGMA; *M_n* ~ 475 g/mol); LCST 90 °C

2.3 Controlled Free Radical/ Living Polymerization Techniques

The traditional free radical polymerization is determined by chain termination and chain transfer reactions, thus this normally accounts for less control over the growing polymer chains resulting in broad polydispersity indexes (PDI). The molar masses of the resultant polymer cannot be pre-determined as the rate of termination is not constant; termination can occur by several different mechanisms⁷¹. Therefore, radical processes where these steps can be avoided or strongly inhibited are much sought after.

In 1956, Szwarc *et al.*^{72, 73} discovered ‘living’ anionic polymerization which later led to major developments in both synthetic polymer chemistry and polymer physics. A polymerization process is considered ‘living’ when the molecular weight (*M_n*) is a linear function of conversion and the polymerization proceeds till the monomer is used up in solution.

Polymerization can be carried out in stages where different monomers can be easily added to the end of the polymer chains when polymerization gets re-initiated. Living polymerization or controlled radical polymerization is thus shown to give rise to narrow polymer molecular weights and it is an especially popular technique used for synthesizing block copolymers. These studies were a platform to the production of well-defined polymers with controlled molecular architectures such as end-functionalized telechelic polymers and nano-structured morphologies.

An example of living polymerization can be seen in nitroxide mediated polymerization (NMP), which was invented by Solomon and Rizzardo in the middle of the 1980s⁷⁴. The reaction is initiated by classical radicals such as peroxides or azo compounds and the termination of growing chains are done with a radical scavenger known as 2,2,6,6-tetramethylpiperidine-1-oxyl (TEMPO) (Figure 2-8). The bonds formed between TEMPO and the polymer chain ends are reversibly cleavable, thus suppressing the termination of propagating chains.

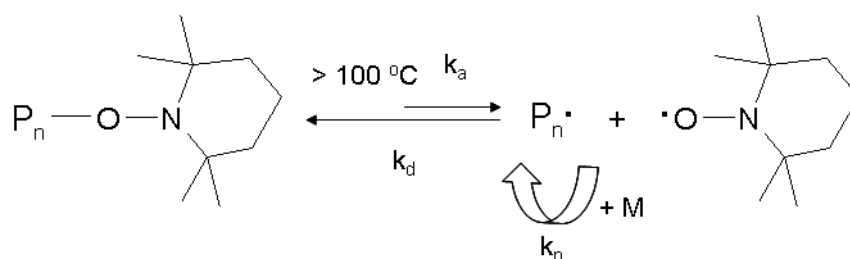


Figure 2-9: Reaction scheme of nitroxide mediated polymerization (NMP) where $P_n\bullet$ = growing polymer chain; M = monomer; k_a = rate of activation; k_d = rate of deactivation; k_p = rate of propagation

Besides NMP, other important living polymerizations include ring opening metathesis (ROMP), reversible addition fragmentation chain transfer (RAFT), atom transfer radical polymerization (ATRP) and iniferter polymerization techniques, in which among these, RAFT and ATRP were basically used for the synthesis and grafting of polymers on solid supports in my research and will be further discussed in the following sub-chapters.

2.3.1 Reversible Addition Fragmentation Chain Transfer Polymerization

‘Reversible addition fragmentation chain transfer’ or RAFT was invented by Krstina *et al.*⁷⁵ in 1995. As its name suggests, this living radical polymerization undergoes a reversible chain transfer mechanism. It is a versatile technique with regards to its compatibility with a wide

range of reaction temperatures, monomers and solvents, including water systems⁷⁶. The reaction is initiated by a low concentration of radical initiators such as azobisisobutyronitrile (AIBN) and typically, the growing chain $P_n\bullet$ reacts with substituted RAFT agents of thiocarbonylthio compounds (Figure 2-10) such as dithioesters⁷⁷, dithiocarbamates⁷⁸, trithiocarbonates⁷⁹ and xanthates⁸⁰ by ‘radical transesterification’ to an equilibrium between activated and deactivated species. It has thus been the focus of intensive research over the last few years since RAFT allows the engineering of macromolecules with complex architectures including block, graft, brush, star and dendrimer structures⁸¹. End functionalities and molecular weights are also easy to control with this technique.

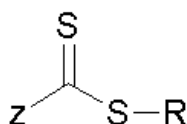


Figure 2-10: Generic structure of RAFT agents

The application of different RAFT agents depends on the suitability of monomers used during polymerization. The Z and R groups perform different functions in the RAFT agent; Z group controls the reactivity of the C=S bond and influences the rate of radical addition and fragmentation while the R group is a free radical leaving group which must be able to reinitiate polymerization. An example of a RAFT compound suitable for methacrylates and methacrylamides is the 4-cyano-4-(phenylcarbonothioylthio) pentanoic acid (which was used for the synthesis of our thermoresponsive PNIPAAm). RAFT polymerization consists of four main steps: initiation, addition-fragmentation, reinitiation and equilibration. The scheme is shown in Figure 2-11. In the initiation step, an active polymer chain $P_n\bullet$ was created by radical initiators $I\bullet$ and the addition-fragmentation step sees the active species reacting with the RAFT agent, forming an intermediate species which the R group can reversibly be cleaved. The active leaving group reinitiates monomer M in solution, leading to more active polymer chain $P_m\bullet$ which may either undergo the addition-fragmentation step again or proceed to equilibration. Equilibration stage finally traps the active propagating chains to the dormant thiocarbonyl compound while the other chain is active in polymerization, thus eliminating termination steps.

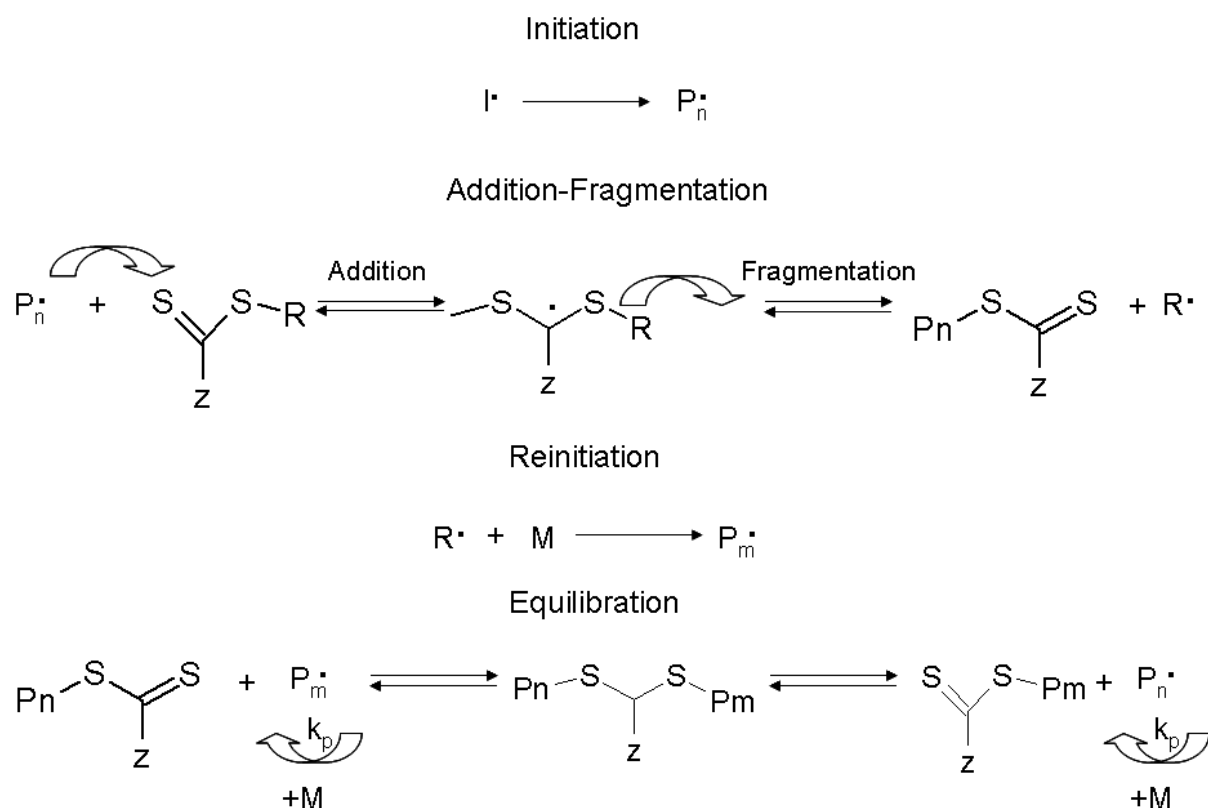


Figure 2-11: General reaction scheme of RAFT polymerization using dithio-RAFT agent

2.3.2 Atom Transfer Radical Polymerization

Recently, Matyjaszewski *et al.*⁸² described atom transfer radical polymerization (ATRP) as a catalytic process, where the amount of radicals and rate of propagation can be controlled by the activity and the amount of catalyst present. It is typically a reversible redox process where the repetitive addition of a monomer to growing radicals is generated from dormant alkyl halides (R-X), and polymerization is catalyzed by transition metal compounds like copper halides complexed with two 2,2'-bipyridine molecules. The monomers are added to the growing polymer chain by the radicals that were reversibly terminated by halide (X^{2-}) readdition from Cu(II) species. Like its name implies, the atom transfer step is the key to uniform polymer chain growth and the general reaction scheme is shown in Figure 2-12.

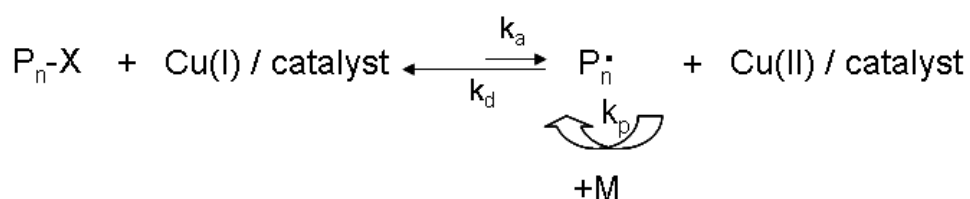


Figure 2-12: General reaction scheme of ATRP process

The active $P_n\bullet$ polymer chains are relatively small in concentration as compared to the dormant P_n-X species due to the dynamic equilibrium between the two species. Since the association constant is relatively small, disproportionation process between two active polymer chains is considerably reduced, thus only a small degree of these chains are irreversibly terminated.

The main role of alkyl halides ($R-X$) used in ATRP is to generate growing chains quantitatively as an initiator⁸³. Normally, alkyl bromides are more reactive than alkyl chlorides since it must rapidly migrate between the growing chain and the transition metal. By using them with functional groups as initiators, terminal functional groups can be created on the polymers, thus ATRP can be used for architecture control for the synthesis of block, star or graft copolymers.

The main species to the key of success for ATRP are the catalyst and ligands used in polymerization. An important factor in selecting good ATRP catalysts depends on whether it can determine the equilibrium position and dynamics of exchange between the dormant and active species. This equilibrium determines the rate of polymerization and catalysts involving copper are the most successful as it does not inhibit polymerization nor cause a high distribution of chain length regardless of monomers used. The task of the ligand would be to dissolve the metal salt in organic solutions and to control its redox potential with respect to reactivity and one such ligand used are 2,2,6,2-terpyridines⁸⁴.

ATRP is promisingly the most robust among living polymerization methods since it can be used for a large variety of monomers including styrenes, methacrylates, acrylonitriles and dienes⁸⁵.

2.4 Hydrothermal Synthesis of Biomass Derived Carbonaceous Materials

It was described in earlier sub-chapters how porous graphitic carbon has been an important topic in recent years in the field of liquid chromatography. However, the production of PGC requires high temperatures ($>2500\text{ }^{\circ}\text{C}$) and because of high temperatures, the surface is inert and hydrophobic as mentioned before. However, it could be an advantage not to fully carbonize the precursors so that some polar functional groups are left on the surface. In addition, these precursors could be derived from biomass natural sources which would make the resulting materials more sustainable in terms of lower toxicity and lower costs.

Therefore, in this study, we employed a more sustainable method for converting cheap natural precursors to produce functional carbonaceous materials, namely hydrothermal carbonization (HTC)⁸⁶. HTC employs mild carbonization conditions ($<200\text{ }^{\circ}\text{C}$; $<20\text{ hr}$) converting biomass or biomass derived precursors into carbon in water under self-generated pressure. Carbohydrates such as glucose, xylose, maltose, sucrose and starch or carbohydrate decomposition products such as hydroxymethylfurfural and furfural have been used as a carbon source. When such compounds are hydrothermally treated at $180\text{ }^{\circ}\text{C}$, they first lose water molecules and dehydrate to form 5-hydroxymethyl-furfural-1-aldehyde (HMF). Upon further reaction, a cascade of polymerization-condensation process finally produces carbonaceous spheres composed of a polyfurane hydrophobic core and a hydrophilic surface shell decorated with a high number of polar functionalities such as hydroxyl and carbonyl groups etc.⁸⁷. The general HTC reaction scheme for hexoses is shown below in Figure 2-13.

Since such carbonaceous structures are stable in strong acidic or basic media, are spherically shaped in the micrometer range and in addition, their surface contains polar functional groups, they could then be targeted as potential stationary phases for liquid chromatography. Their surface properties could then be tailored with desired properties like it was described previously for the silica solid supports. Surface functionalities can be altered for example by the simple addition of a small amount of organic monomers such as acrylic acid⁸⁸ or acrylamide to the HTC solution. Under HTC conditions, the monomers undergo a mechanism known as cycloaddition between the double bond of the monomer and the conjugated polyfurane network, thus resulting in the incorporation of desired surface groups. In addition, the final carbon product is stabilized, and nanostructuring occurs with additives. Finally,

properties such as particle size, the rate of synthesis (addition of catalysts) and agglomeration can also be easily tailored by varying reaction conditions.

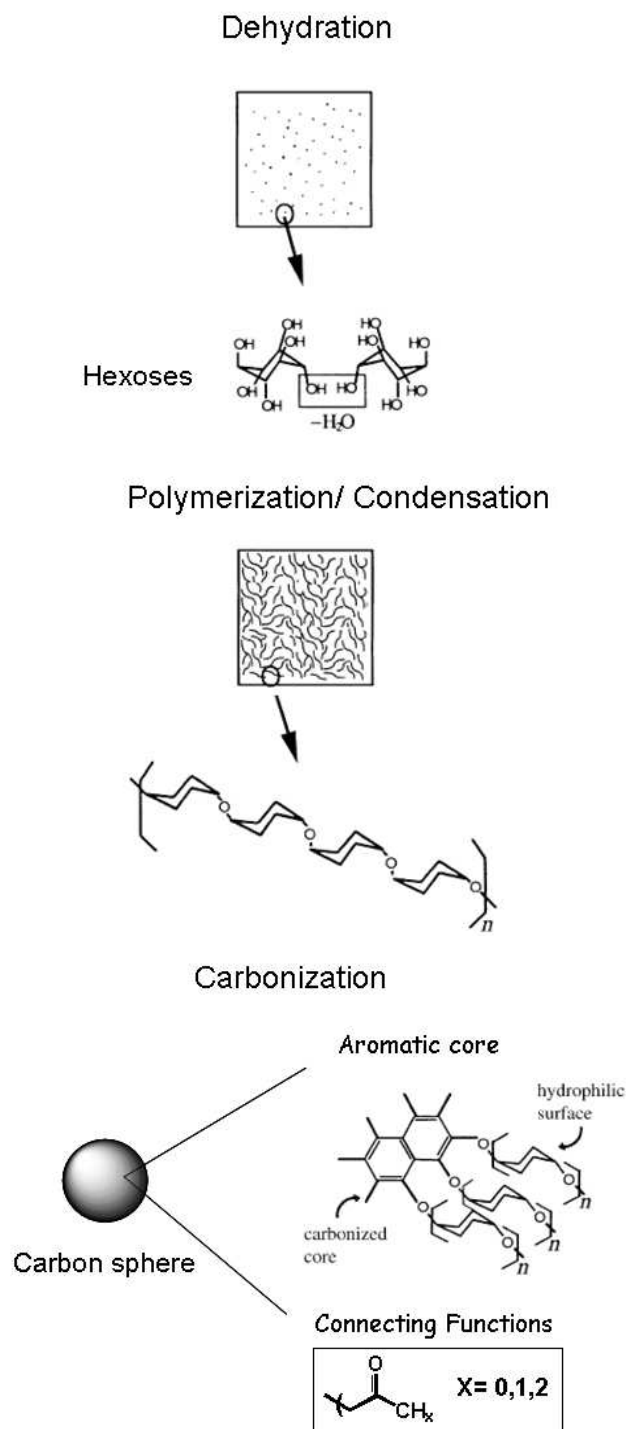


Figure 2-13: General schematic reaction mechanism of hydrothermal carbonization of hexoses

Other materials which can be synthesized by the HTC method include mesoporous and hollow spheres by silica-templating⁸⁹, nitrogen-doped carbons from chitin taken from prawn shells⁹⁰ and hybrid materials for the encapsulation of noble metal nanoparticles⁹¹ for fuel cells or catalysis.

3 CHARACTERIZATION METHODS

3.1 Nitrogen Sorption

Through the physical adsorption (Van der Waals interactions) of gas molecules such as nitrogen, hydrogen, argon, carbon dioxide and krypton on a solid surface, properties of porous materials such as surface area, pore volume and pore size distribution can be determined. The gas which is adsorbed is called an ‘adsorbate’ and the solid where adsorption takes place is known as the ‘adsorbent’. An important analytical technique which serves as a basis for explaining such measurements is the BET theory which was published by Brunauer, Emmett and Teller in 1938⁹². The concept of this theory was derived from the Langmuir theory for monolayer to multilayer molecular adsorption, with assumptions that gas molecules physically adsorb on a solid in layers infinitely, that there is no interaction between each of these layers and that the Langmuir theory can be applied to each layer. Basically, the theory stipulates that the amount of adsorbed gas (typically nitrogen) is measured as a function to the relative pressure ratio P/P_o at a constant temperature T . The resulting BET equation for calculating surface area is expressed in Equation 3-1:

$$\frac{P/P_o}{n(1-P/P_o)} = \frac{1}{n_m C} + \frac{C-1}{n_m C} (P/P_o) \quad \text{Equation 3-1}$$

where P and P_o are the equilibrium and saturation pressures of adsorbates at the temperature of adsorption; n is the total amount of adsorbed gas quantity; n_m is the monolayer capacity and C is the BET constant which is expressed by Equation 3-2.

$$C = \exp\left(\frac{E_1 - E_L}{RT}\right) \quad \text{Equation 3-2}$$

E_1 is the heat of adsorption for the first layer; E_L is that for the second and higher layers which is equivalent to the heat of liquefaction.

Equation 3-1 can be plotted as a linear graph known as the BET plot, and the linear relationship is maintained in the range of $0.05 < P/P_o < 0.35$. C and n_M can finally be determined from the intercept and gradient from the BET graph. Finally, the specific surface

area S_{BET} (m^2/g) from the BET model can be calculated according to the following equation 3-3:

$$S_{\text{BET}} = \frac{n_{\text{M}} N_{\text{A}}}{V_{\text{m(g)}} a} \quad \text{Equation 3-3}$$

where N_{A} is the Avogadro's number; $V_{\text{m(g)}}$ is the molar volume of adsorbent gas and a is the mass of adsorbent in grams. However, the final results largely depend on the correctness of the assumptions. The values of relative pressures may not always be right and the presence of micropores in the materials may give values which deviate largely away from the correct values.

The Barrett-Joyner-Halenda (BJH)⁹³ method is one of the earliest methods used for the characterization of pore volume and size distribution of mesoporous solids. This method assumes that pores are cylindrical and adsorption on mesoporous materials follows a sequential process of building up of adsorbed layer followed by capillary condensation. Equation 3-4 shows BJH calculations:

$$r_{\text{p}}(P/P_{\text{o}}) = \frac{2\gamma V_{\text{m(l)}}}{RT \ln(P/P_{\text{o}})} + t(P/P_{\text{o}}) \quad \text{Equation 3-4}$$

where r_{p} is the pore radius, γ is the surface tension, $V_{\text{m(l)}}$ the molar volume of the liquid, R the universal gas constant and t is the thickness of the physisorbed film before capillary condensation. Currently, there are other mathematical models for the calculations for the materials of different porosities: Dollimore Heal (DH) method for mesoporous materials; Non Local Density Functional Theory (NLDFT) and Monte Carlo simulation method for micro- and mesoporous materials; Dubinin Astakhov, Horvath-Kawazoe (HK) and Saito Foley methods for microporous solids.

Before a calculation model can be applied to calculate specific surface areas, pore sizes and volume distributions, an isotherm related to porosity of materials has to be first obtained. According to the definition by IUPAC, microporous materials consist of pores which are smaller than 2 nm, mesoporosity ranges from 2 to 50 nm and those with pores larger than 50

nm are macroporous. Figure 3-1 shows the six main physisorption (adsorption-desorption) isotherms, and they differ because each system shows different gas or solid interactions.

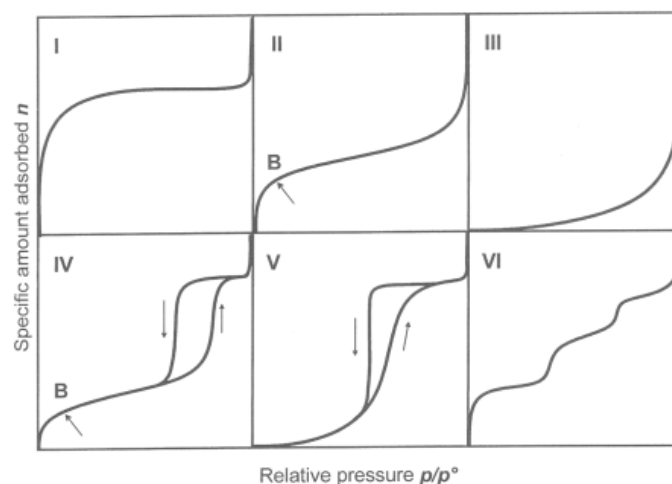


Figure 3-1: Standard IUPAC types of adsorption-desorption isotherms

Type I isotherm is mainly exhibited for microporous solids (<2 nm) and chemisorption behavior. Types II and III are typical for non-porous or macroporous materials (>50 nm) and type II shows unrestricted monolayer-multilayer adsorption, with point B indicating the relative pressure at which monolayer coverage is complete. Types IV and V show hysteresis loops which identify mesoporosity in materials, although type V curve is uncommon. This hysteresis was generated by capillary condensation of adsorbate in the mesopores of the materials and gives information such as shapes about the porosities. Finally, the rare type VI isotherm shows a step-wise multilayer adsorption on homogeneous non-porous solids such as special carbons⁹⁴.

3.2 Electron Microscopy

An electron microscope (EM) is an instrument that uses signals derived from the interactions between the electron beam and the samples to closely study structure, morphology and composition in the micro and nano scale. A beam of electrons that have wavelengths about 100 000 times shorter than photons was used to illuminate the sample and the microscope uses electrostatic and electromagnetic ‘lenses’ to focus the beams. Interactions occur inside the irradiated sample, thus affecting the electron beam and create high resolution images out of it. The resolving power is thus much higher than as compared to that of a light-powered optical microscope. EMs are used to observe a wide range of biological and inorganic

specimens such as microorganisms, cells, metals and crystals. There are different techniques of EM depending on the purpose of observation: in order to study a material's structure closely, transmission electron microscope (TEM), high resolution TEM and electron diffraction (ED) can be used. Scanning electron microscope (SEM) is normally used to study the materials' morphology. For observations on composition of material, energy-dispersive X-ray spectroscopy (EDXS) or electron energy loss spectroscopy (EELS) is commonly used.

In TEM, electrons are transmitted through thin films of specimens, thus enabling the observation of the structures closely. Electrons are first emitted from a cathode (wavelength 0.005-0.002 nm) and are accelerated at a high voltage (60-200 kV) due to the high potential difference of the anode. They pass through condenser lens which focuses the beam onto the sample which is held on a special microgrid or on a grid coated with supporting film. While the beams are passing through the sample, the electrons are scattered on the detector. The object image is then formed on the objective lens and finally, the projection lens magnifies the images received. The image is then recorded on a screen or photographically. The path of the electron beam for TEM is not very different from the light beam path used for the light microscope (LM) and this was shown on the diagram sketch in Figure 3-2.

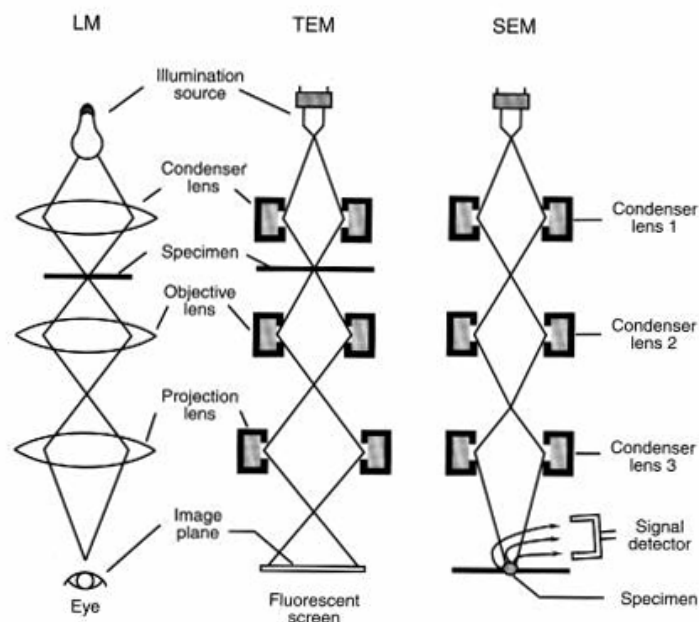


Figure 3-2: Sketch of photon beam path for LM and electron beam path for TEM and SEM

As for SEM, the source of electron beam comes from a thermoionic or field emission cathode and the primary electrons are accelerated at a lower voltage of 1-50 kV. A series of condenser lenses focus a very fine beam on a small area on the specimen surface. The beam moves across the sample due to deflection coils and the scattered electrons are detected. Surface morphology can be observed using the secondary electrons emitted from the specimen surface.

3.3 High Performance Liquid Chromatography

As mentioned before, high performance liquid chromatography (HPLC) is a chromatographic technique used to separate a mixture of compounds for analytical purposes such as to identify, quantify and purify each component¹⁹. A HPLC instrument consists of several modules and the block diagram of the system is as shown in Figure 3-3 below. Typically, it utilizes a high pressure pump (up to 400 atmospheres) rather than gravity to move mobile phases from a reservoir with degasser and analytes injected from a sampler through different types of densely-packed stationary phases. The performance of the pumps is measured on their abilities to yield a consistent and reproducible flow rate, although it also depends on the type and size of particle packing used as stationary supports. The eluate then passes through a detector that provides characteristic retention time for the analytes. The detector measures the adsorption of light of the samples at a chosen wavelength either in the ultraviolet (UV) or visible light (Vis) absorbance range and the information is finally sent and recorded in output systems such as on a computer or a recorder. Other detectors that can be coupled to the HPLC system include refractive index, electrochemical detectors and mass spectrometry. The analyte retention time (t_R) is the time taken for the injected compound to be retained in the column until it travels out of it and usually, it varies depending on the strength of its physical or chemical interactions with the stationary phase, the composition and flow rates of the mobile phases used.

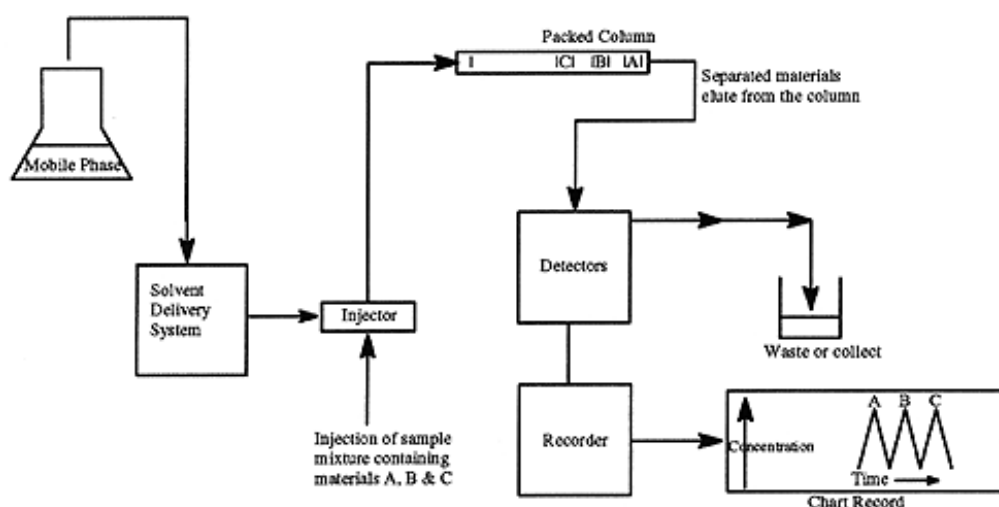


Figure 3-3: Block diagram of the HPLC system with its components

The type of column packing is an important tool for the HPLC and they can be classified into five different types of chromatography:

Normal Phase Chromatography (NPC): This type of phase uses a polar stationary phase and a non-polar, non-aqueous mobile phase and separates hydrophilic analytes based on adsorption to the surface and due to its polarity. However, efficiency of the separation occurs only when the samples dissolve readily in the non-polar solvents. The use of NPC is less common with the development of RPC, but begins to get popular again after the HILIC-bonded phases are discovered.

Reversed Phase Chromatography (RPC): This phase is the most widely used among the other chromatography techniques, especially in the pharmaceutical industries. The column consists of a non-polar stationary phase such as silica treated with $C_{18}H_{37}$ or C_8H_{17} , and the mobile phases used are aqueous and moderately polar. It is used for the separation of non-polar analytes due to the hydrophobic-hydrophobic interactions with the solid support. The more hydrophobic a compound is, the stronger it is retained in the column before it is eluted. The retention time can also be varied by the addition of polar or non-polar solvents into the mobile phases.

Size Exclusion Chromatography (SEC): This method separates the compounds on the basis of their sizes and is especially used for determining the molecular weights of polymers and proteins. Smaller compounds get retained through the adsorption on the pores while larger

molecules pass through quickly. Another word for this chromatography method is gel permeation chromatography (GPC), and this is normally reserved for 'last-step' purification processes as the resolutions are low.

Ion Exchange Chromatography (IEC): This technique employs the use of charges bound to the surface of the support to interact with counter ions in the solution. Ions of the same charges are eluted more quickly. The binding effects can be changed by varying pH factor in the mobile phase. IEC is typically used for the analyses of proteins and carbohydrates.

Affinity Chromatography: This process operates by using immobilized compounds that have an affinity to the analytes of interest. Interactions can include Van der Waals, electrostatic, dipole-dipole, hydrophobic forces or hydrogen-bonding.

Another important factor to consider is the choice of the mobile phase, whether a gradient or isocratic solution is to be used, and additives to be added largely depends on the nature of the column and samples to be analyzed. Common solvents used include an aqueous mixture of water and organic solvents like acetonitrile or methanol, and ion-pairing agents like salts and buffers can also be added to assist in the separation of analytes. By varying the mobile phase composition during the analysis, a gradient elution is achieved. This can be done to achieve a better resolution of peaks when a sample contains a mixture of hydrophilic and hydrophobic compounds, where the elution typically starts off with a water phase and with the slow increase of the percentage of hydrophobic organic phase to it.

The important parameters to consider when characterizing chromatograms are retention and selectivity factors of analytes, theoretical plate numbers of columns and concentration of compounds.

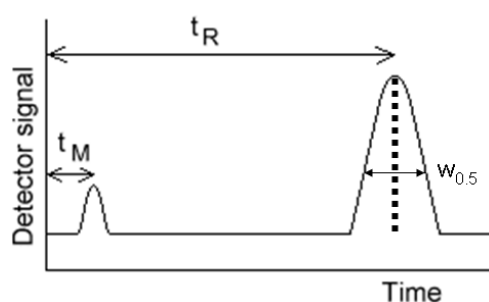


Figure 3-4: Schematic illustration of chromatogram peak

The retention factor k is the partition coefficient defining the molar concentration of analyte being retained in the stationary phase divided by the molar concentration of the analyte staying in the mobile phase. It is measured from the time the sample is injected to the time at which the display shows a maximum peak height for that compound and is often used to describe the rate of migration of the analyte through the column. It is defined in Equation 3-5:

$$k = (t_R - t_M) / t_M \quad \text{Equation 3-5}$$

where t_R is the retention time of analyte and t_M is the dead time where it is the time taken for the mobile phase to pass through the column. This is usually measured by using markers that are not retained in the column, for example, salts, deuterated solvents, uracil for RP and benzene for NP chromatography. Several factors can affect the t_R : pressure, nature of the stationary phase, composition of the solvent and temperature of the column. The selectivity of the more retained analyte B over analyte A can be described with the selectivity factor a as shown on Equation 3-6:

$$a = k_B / k_A \quad \text{Equation 3-6}$$

where k_A is the retention factor of analyte A, k_B is the retention factor of analyte B and $a > 1$.

In order to measure the efficiency of the column, factors called theoretical plate number N and height equivalent to a theoretical plate (HETP) can be measured. It is postulated that a column consists of separate layers called ‘theoretical plates’ in which in each ‘plate’, an equilibrium of the sample between the stationary phase and the mobile phase forms when the analyte moves down the column by transfer of equilibrated mobile phase from one to the next. Parameters N (m^{-1}) and HETP can only be found after examining a chromatogram (Figure 3-4) and the following equations 3-7 and 3-8 can be used:

$$N = 5.55 \times (t_R / w_{0.5})^2 \quad \text{Equation 3-7}$$

$$\text{HETP} = L / N \quad \text{Equation 3-8}$$

where $w_{0.5}$ is the peak width at half height obtained from the chromatogram of the elution profile and L is the length of the column in meters. Theoretically, a column is more efficient when N has a larger number of plates and HETP should be the smaller the better. Different solutes in the mixture will affect the behaviour of the column in these parameters.

The area under a peak is proportional to the concentration of the compound adsorbed by the UV detector and can be computed quantitatively from the output display of the system.

4 RESULTS AND DISCUSSION

4.1 Modification of Silica Monoliths with Thermoresponsive Polymers for Chromatography

As already mentioned in the previous chapter, in addition to the remarkable selectivity for biomolecules, another reason for the development and the wide usage of ‘reversed’ phase (RP) chromatography is due to the use of moderately polar solvents as opposed to purely organic solvents used in ‘normal’ phase (NP) modes. However, the use of such organic solvent gradients as mobile phases tends to destroy the biological activities of biomolecules to be separated.

Recently, advances in liquid chromatography show the separation of biomolecules in RP-HPLC such as steroids in purely aqueous and isocratic environment. In this study done within our working group, the surface properties of silica stationary supports were modified by immobilizing thermoresponsive polymers; namely poly(*N*-isopropyl acrylamide) (PNIPAAm) layers could be grafted and the resulting solid phase showed thermoresponsive characteristics¹⁸. The chromatography mode utilized here is RP-HPLC but it has the ‘greener’ advantage over classical RP of using pure aqueous mobile phases.

Kanazawa *et al.*¹⁷ first proposed brush-grafted PNIPAAm onto stationary supports, specifically on silica beads having surface reactive functional groups which can terminally couple with the polymer layers. The advantage of using ‘living’ radical polymerization as described before equips it with the possibility of adding more functional monomers to the existing block of polymer. Thus, there are several reports from Kanazawa’s group describing the incorporation of a more hydrophobic moiety butyl methacrylate (BMA) for the preparation of P(NIPAAm-*co*-BMA) for separating amino acids^{95, 96}. Okano *et al.* has also reported the grafting of a thermoresponsive polymer incorporated with a pH sensitive group such as poly(acrylic acid) on silica bead surfaces for the separation of ionic bioactive compounds⁷.

Recognizing the potential underlying thermoresponsive polymers for preparing smart switchable stationary phases, different polymers exhibiting a lower critical solution temperature (LCST) in water are explored for this purpose. In this chapter of my thesis, silica monoliths (MERCK, Darmstadt) instead of particulate silica beads were used and the

modification of the monolithic surfaces with a series of PEG-derived P(MEO₂MA-co-OEGMA) copolymers using the ‘grafting to’ method are reported. Due to its bio-inert ethylene oxide units, the oligo(ethylene oxide)-based thermoresponsive polymer should exhibit high biocompatibility. The copolymer can be first synthesized by ‘living’ atom transfer radical polymerization (ATRP) and for each copolymer, the LCST can be specifically tailored by varying parameters such as polymer molecular weight and comonomer composition. The silanol surface groups of a silica monolith are first modified with amino groups which can later couple the polymers ‘in-situ’ with chemical bonds. The resulting thermoresponsive modified column is then used in a series of separations for hydrophobic analytes such as steroids and proteins in purely aqueous isocratic HPLC conditions. The chromatographic performance was compared to previous studies of PNIPAAm-modified monoliths, and the added advantages in terms of biocompatibility and tunability of LCST are demonstrated. Column hydrophobicity was also evaluated by comparing it to benchmark C18 columns (MERCK, Darmstadt).

In addition, in order to study and compare how the different structures of each thermoresponsive polymer affect the aqueous-based steroid separation, the silica monoliths were also modified with a series of poly(2-oxazoline)s with varying LCSTs and the results compared in one sub-chapter (Chapter 4.1.3.7 (b)).

4.1.1 In-situ Grafting of PEGylated Copolymer to Silica Monoliths

As described in the introductory chapter, polymers can be chemically immobilized onto silica monoliths using the ‘grafting to’ or the ‘grafting from’ approaches. Although the latter technique gives a more evenly distributed and higher grafting densities onto surfaces, the ‘grafting to’ method presents a simple and quick way to attach polymers onto pre-formed chromatographic supports. This method was thus chosen to achieve quick modification of surface monolithic materials in our case. The monolithic surface has to be firstly modified with suitable functional sites which can be coupled with the desired polymer to be grafted. The polymers are grafted randomly onto these sites and the grafting density can be controlled by limiting the concentration of the polymer solution in contrast to the ‘grafting from’ approach in which polymerization is more difficult to control. We call our chemical attachment process ‘in-situ grafting’ as this is attributed solely to the technique used; the

chemical bonding reaction takes place within an end-capped monolithic column after the polymer solution was pumped through it by an analytical HPLC pump (JASCO, Darmstadt).

Up to date, PEG-based thermoresponsive polymers have not yet been exploited in preparing smart stationary phases and this will be the first report on using a variety of P(MEO₂MA-*co*-OEGMA) copolymers⁹⁷ for developing innovative stationary phases for efficient bioseparation. The synthesis and characterization of such a PEGylated monolith are reported below.

4.1.2 Synthesis and Characterization

A series of P(MEO₂MA-*co*-OEGMA) copolymers (composites a-f) with variable chain lengths and compositions were synthesized by ATRP in the presence of the initiator *N*-succinimidyl 2-bromoisobutyrate and using the catalytic system involving copper(I)/ bipyridine in ethanol at 60 °C under very dry conditions⁶⁷. The ratio of concentrations of [Initiator]:[CuBr]:[Bipy] during the reaction was 1:1:2. The formed copolymers were characterized by gel permeation chromatography (GPC) using NMP as a solvent and polystyrene as a standard, proton nuclear magnetic resonance (¹H NMR) and cloud point measurements. The six different copolymers with their respective comonomer composition ([OEGMA]/[MEO₂MA]), theoretical degree of polymerization (DP_{n,th}) measured by ([OEGMA] + [MEO₂MA]) / [Initiator], molecular weight (M_n), polydispersity index (PDI) and lower critical solution temperature (LCST) at 1 wt.% concentration are presented in a table below (Table 4-1). The final copolymer product was tailored with reactive *N*-succinimidyl ester chain end functionality.

	[OEGMA]/[MEO ₂ MA]	DP _{n th}	M _n	PDI	LCST (°C)	Grafting Density (µg/m ²)	Grafting Density (chains/nm ²)
a	10:90	100	18100	1.28	41	233	0.00714
b	10:90	75	15690	1.41	38	402	0.01770
c	10:90	50	12310	1.30	39	371	0.02480
d	10:90	25	6220	1.36	40	305	0.03920
e	5:95	100	18120	1.66	33	250	0.00926
f	15:85	100	17040	1.41	43	235	0.00715

Table 4-1: Characterization of the copolymers P(MEO₂MA-*co*-OEGMA) and the corresponding grafting densities on modified silica monoliths (calculated for one cycle polymer grafting; 250mg polymer/ cycle)

Proof of the thermo-sensitivity of the synthesized polymers is shown by their behaviours in water from turbidity measurements taken at 1°C/min from 5-60 °C. The LCSTs of components a-d are measured and the heating and cooling cycles are observed to undergo sharp transitions on Figure 4-1. At temperatures below the copolymer's LCST, light transmittance is high since the polymer is completely dissolved in water in their hydrophilic state. By increasing the temperature, the solution became turbid thus causing the transmittance value to fall. The cloud points are observed to be retained (39-41 °C) when the comonomer compositions are kept the same ([OEGMA]:[MEO₂MA]=10:90), proving that the LCSTs of P(MEO₂MA-*co*-OEGMA) are not affected drastically by polymer chain length or concentration variations.

Figure 4-2 shows the ¹H NMR spectrum of composite e dissolved in deuterated chloroform (CDCl₃) (δ=7.27), which proves the copolymer's structure. The broad peak at point e (δ=2.45) shows the intramolecular H interactions at close proximity between the brush side chains of the copolymer. The rest of the signals are as follows: For the MEO₂MA unit, δ=0.8, 3H(CH₃); δ=1.75, 2H(CH₂); δ=3.56, 2H(CH₂); δ=3.66, 2H(CH₂); δ=3.38, 6H(CH₃). For the OEGMA unit, δ=1.16, 3H(CH₃); δ=1.8, 2H(CH₂); δ=3.75, 2H(CH₂); δ=4.31 2H(CH₂).

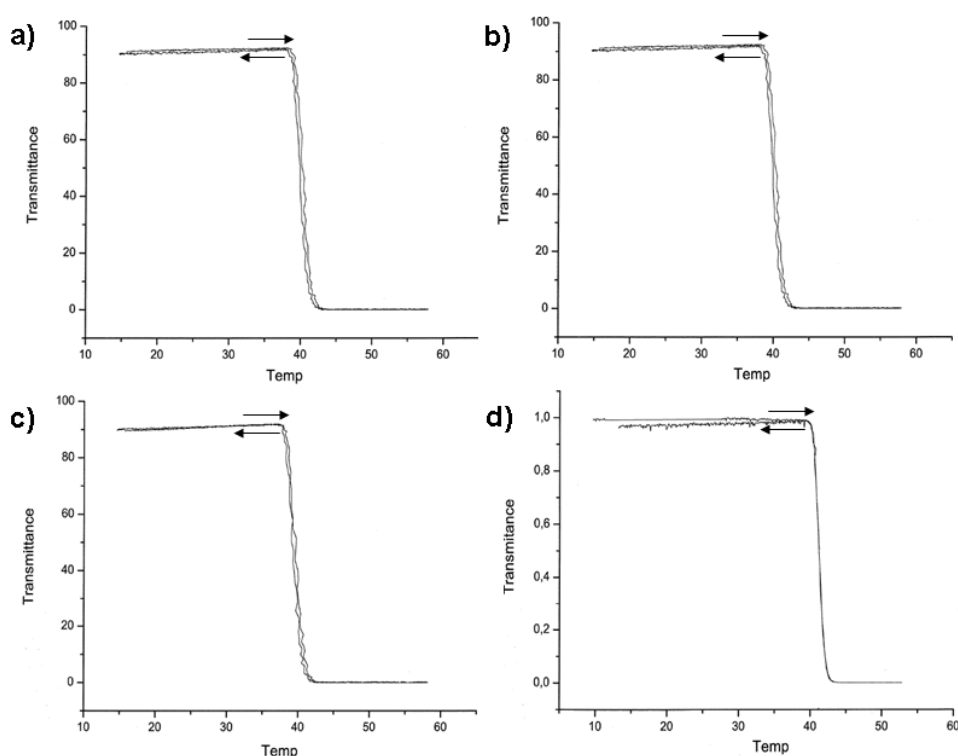


Figure 4-1: Turbidity curve (heating and cooling cycles) of composites a-d taken at 1 wt.% in water, 1°C/min

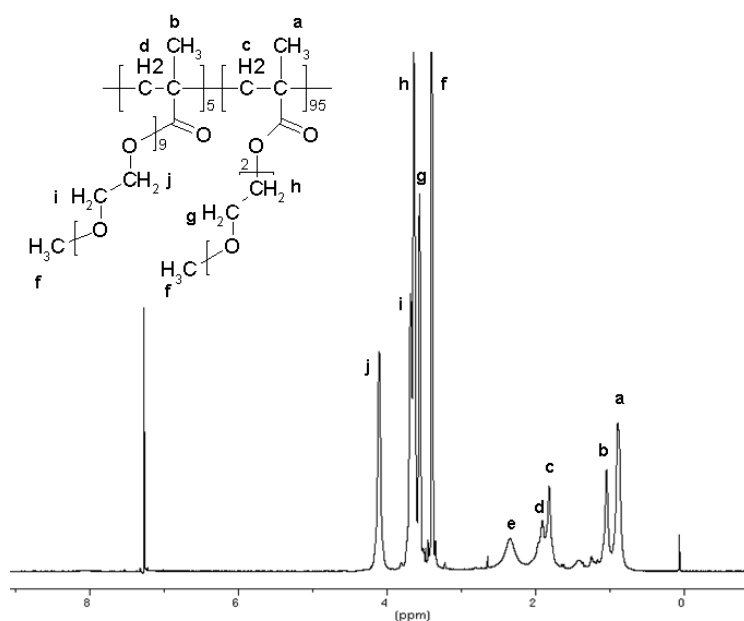


Figure 4-2: ^1H NMR spectrum of composite e in CDCl_3

Rehydroxylated silica monoliths were first ‘in-situ’ modified with typically 500 μg of 3-aminopropyl-triethoxysilane (APS) using a HPLC pump, thus functionalizing the surface with amino groups which can undergo standard amide coupling with the succinimide groups on the polymer chains. The general reaction scheme of the polymerization of P(MEO₂MA-co-

OEGMA) by ATRP, preparation of aminated silica monolith and polymer grafting to silica is as shown in Figure 4-3.

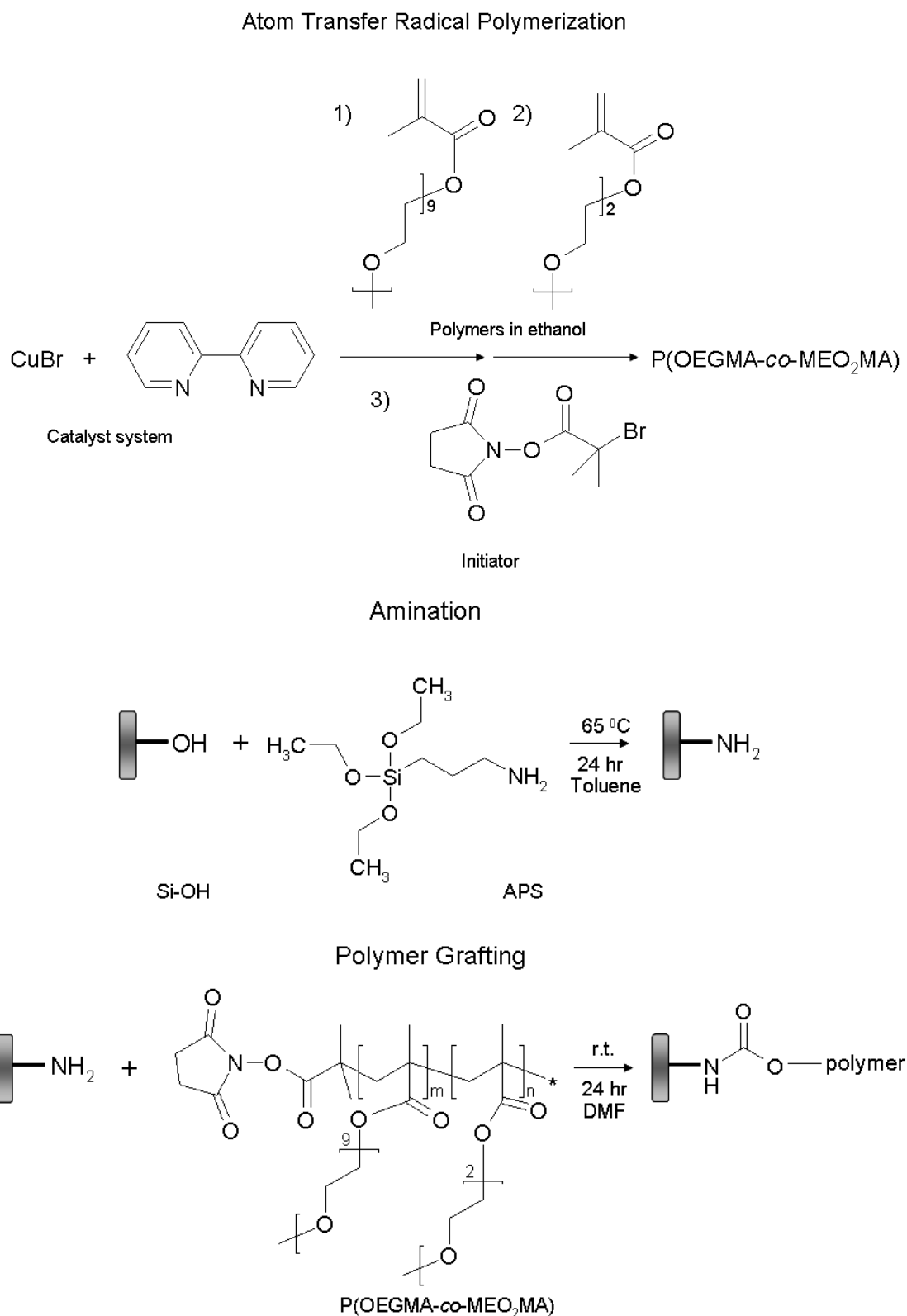


Figure 4-3: Reaction scheme of the polymerization and functionalization of silica monolith with P(OEGMA-co-MEO₂MA)

Parallel to the 'in-situ' grafting of the copolymer, modification was also performed on a free-standing piece of monolith. Grafting densities were calculated from elemental analyses data using the following formulas below. The amount of amino groups immobilized on the rehydroxylated silica after amination with APS can be computed with Equations 4-1 and 4-2:

$$m_C = \frac{\Delta C}{100 - [\Delta C \times M_{w,APS} / M_C]} \quad \text{Equation 4-1}$$

$$D_{s,APS} = m_C / M_C \quad (\text{mol/g}) \quad \text{Equation 4-2}$$

Where m_C is the weight of carbon content of the grafted APS per gram of bare silica support, ΔC is the %C increase after amination, $M_{w,APS}$ is the weighted average molecular weight of APS, M_C is the weighted average molecular weight of the C fraction of APS, $D_{s,APS}$ is the grafting density of APS on silica monolith. The amount of polymer immobilized on silica can be calculated with Equations 4-3 and 4-4 below:

$$m_p = \frac{\%C_p \times 10^6}{\%C_{p,theory} [1 - \%C_p / \%C_{p,theory} - \%C_i / \%C_{i,theory}] \times S} \quad (\mu\text{g}/\text{m}^2) \quad \text{Equation 4-3}$$

$$D_{s,p} = \frac{m_p \times 10^{-6} \times N_A}{M_{w,polymer}} \quad (\text{chains}/\text{m}^2) \quad \text{Equation 4-4}$$

Where m_p is the amount of grafted polymer in μg per m^2 of support, $\%C_p$ is the increase in C% after grafting of polymers, $\%C_{p,theory}$ is the calculated weight %C in a monomer repeat unit, $\%C_i$ is the increase in C% after amination, $\%C_{i,theory}$ is the calculated weight %C in one initiator APS unit, S is the specific surface area of the solid support in m^2/g , $D_{s,p}$ is the grafting density of the polymer in chains/m^2 , N_A is the Avogadro's constant at 6.022×10^{23} and $M_{w,p}$ is the molecular weight of the polymer grafted. The calculation of m_p is presented in $\mu\text{g}/\text{m}^2$, thus equation includes 10^6 converting result from g/m^2 . The calculation of $D_{s,p}$ is presented in chains/m^2 , thus equation includes 10^{-6} converting result from $\mu\text{g}/\text{m}^2$.

According to the elemental analyses, the concentration of amino groups on the silica monolith was $453 \mu\text{g}/\text{m}^2$. The polymers were then loaded in cycles, each coupling with 250 mg per cycle. After the coupling of P(MEO₂MA-co-OEGMA) thermoresponsive polymers, grafting densities in the range of $233\text{--}402 \mu\text{g}/\text{m}^2$ were measured (Table 4-1) for the first cycle polymer loading. The fact that the polymers were successfully grafted onto the monolith surfaces was also confirmed by Fourier transform infrared spectroscopy (FT-IR) (Figure 4-4). For instance, the spectrum of the modified monolith showed new adsorption bands corresponding to the amide functions at 1700 cm^{-1} ($\nu_{\text{C=O}}$) and 1540 cm^{-1} ($\delta_{\text{N-H}}$).

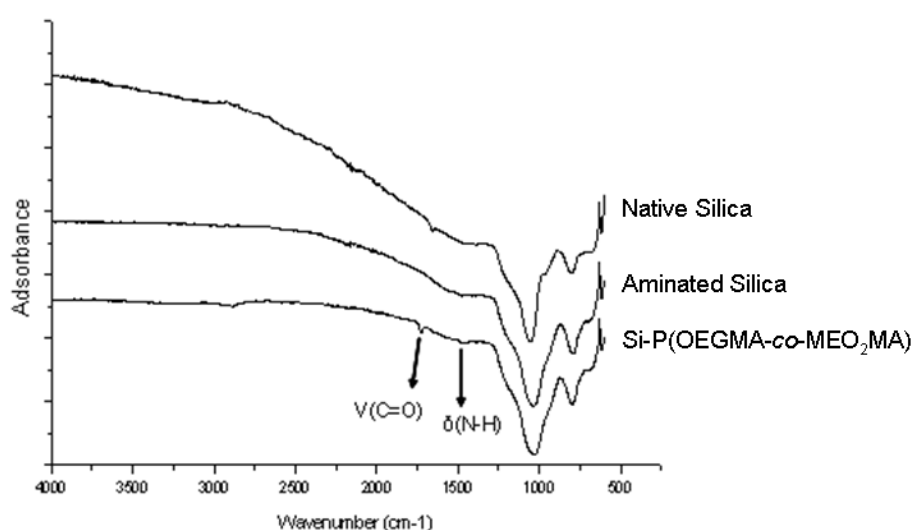


Figure 4-4: FT-IR spectras of rehydroxylated silica monolith, aminated silica and thermoresponsive composite

The thermo-gravimetric analysis (TGA) profiles of the starting silica, aminated silica and the thermoresponsive composite are shown in Figure 4-5. The results also prove the modification and attachment of the polymer on the silica surface. A mass loss difference of approximately 18% was observed between the thermoresponsive column and the starting silica material. From the values obtained from TGA and using Equation 4-5, the thickness of the polymer layer was calculated to be 4.6 nm.

$$d = \frac{\Delta m \times D \times 10^4}{a_s}$$

Equation 4-5

Where Δm is the mass difference between the grafted polymer and the starting material obtained from TGA. D is the weighted average density of monomers (g/ml) and a_s is the specific surface area of silica (350 m²/g).

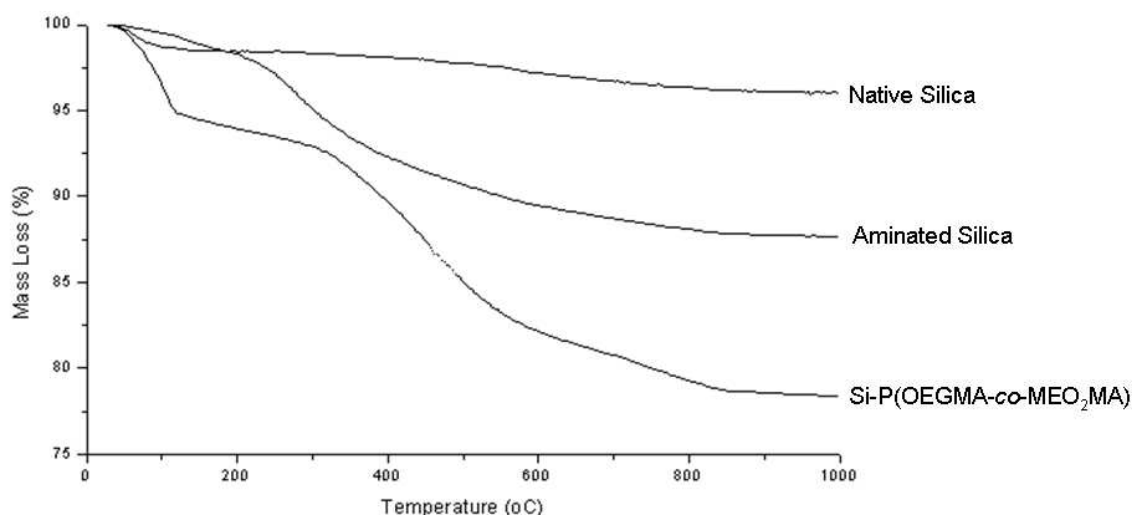


Figure 4-5: TGA profiles of the starting silica, aminated silica and the final thermoresponsive composite

Table 4-2 compares the thickness of the polymer film obtained from values calculated by elemental analyses (Equations 4-1 to 4-4) and TGA (Equation 4-5), in which the polymer layer is assumed to be homogeneously grafted onto silica.

	Specific surface area (m ² /g)	Average pore size diameter (nm)	d _{E.A.} (nm)	d _{TGA} (nm)
Native Si	317.8	16		
Si-Polymer	170	5	4.5	4.7

Table 4-2: Pore structural characterization of the native silica and polymer modified silica

Figure 4-6 shows the Brunauer, Emmett and Teller (BET) nitrogen adsorption-desorption isotherms from both the starting silica and the final composite. Both curves show the typical type IV isotherm for mesoporous materials since mesoporous silica monolith was used. As expected, the attachment of the polymer causes the volume of nitrogen adsorbed to decrease as the pores of the monolith were filled up in the grafting process. The average pore radius shrinks from 16 nm to 5 nm, and polymer grafting also decreases the accessible surface area of silica from 317.8 m²/g to 170 m²/g. Thus, it is rather important to find an optimal amount

of polymer to be grafted on the silica monolith; one which does not block the mesopores that are required for separation performance on proteins and steroids in HPLC. This will be further elaborated in one sub-chapter later on.

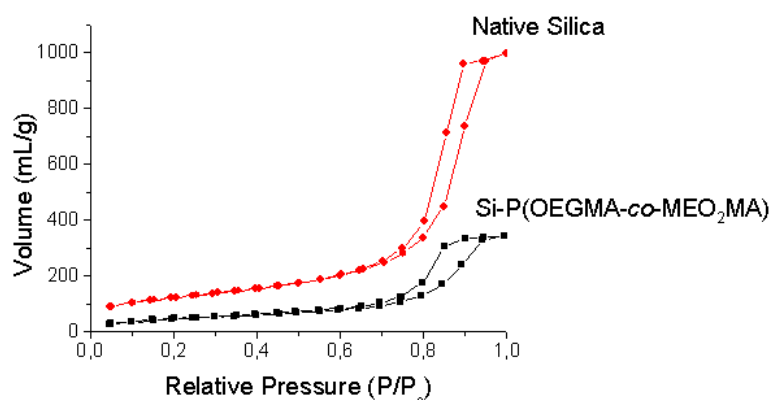


Figure 4-6: Nitrogen sorption data of the starting silica and the final thermoresponsive composite

Both scanning electron microscopy (SEM) and transmission electron microscopy (TEM) were also measured for both materials; Figure 4-7 (A and B) proves that post-grafting of the polymer does not affect the morphology of the silica monolith, which is important since the solid support must be stable upon introduction of other moieties. On Figure 4-7 (C and D), certain extent of the blocking of the mesopores is observed after modification, and the polymer is shown to be grafted homogeneously rather than concentrated on an area. Thus, mesopores will be increasingly blocked and active surfaces reduced when more polymers are introduced into the column. These results coincide with the results of the BET sorption curves.

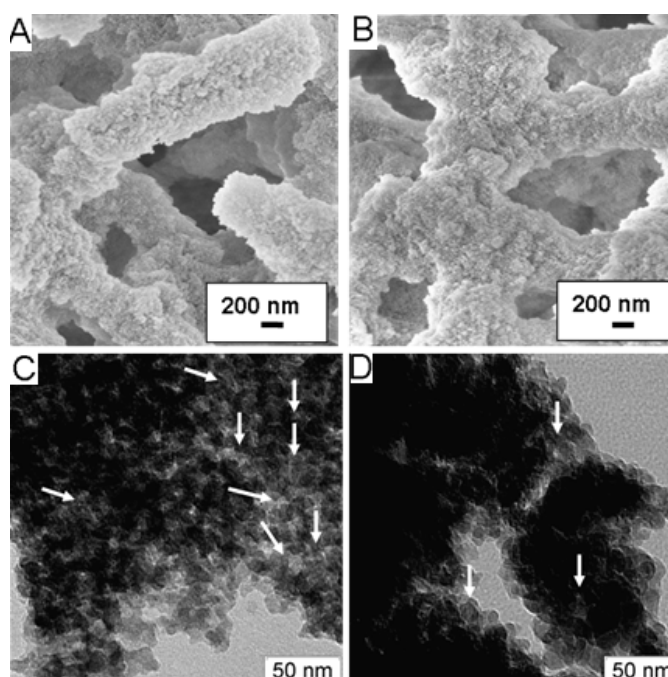


Figure 4-7: A,B) SEM micrographs and C,D) TEM micrographs of starting silica and thermoresponsive composite respectively

After the successful grafting of the polymers on silica monoliths is proven, the chromatographic performance of the final thermoresponsive composite was studied on the separation of a group of steroids in water. The results are discussed in the following sub-chapters.

4.1.3 Chromatographic Characterization

The chromatographic performance of the P(MEO₂MA-*co*-OEGMA)-grafted stationary phases were evaluated in purely aqueous media under isocratic conditions. First, a mixture of five steroids was investigated and their chemical structures are shown on Figure 4-8. The group of steroids shows rather similar structures but of different side groups and their differential solubilities can be calculated by a factor known as the partition coefficient ($\log P$). Under IUPAC definitions, ‘partition constant’ or $\log P^{98}$ is the ratio of concentrations of a compound in two phases of a mixture of two immiscible solvents at equilibrium, normally water and octanol. This value gives useful information on how readily the moieties can dissolve in water, especially in pharmacology, where drug delivery studies are determined by this factor.

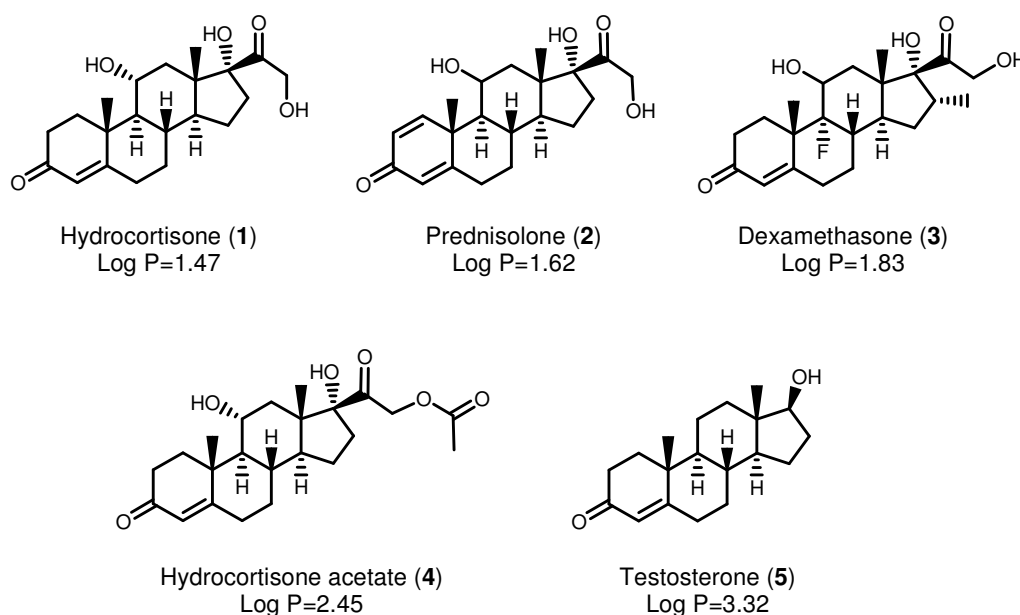


Figure 4-8: Chemical structures of the steroids involved in the separation processes and their corresponding partition coefficients (log P)

The lipophilicities of each compound can be calculated with Equation 4-6 and normally, hydrophilic substances have low log P values while the reverse is true for hydrophobic compounds.

$$\log P_{\text{oct/water}} = \log \left[\frac{[\text{solute}]_{\text{octanol}}}{[\text{solute}]_{\text{unionized water}}} \right] \quad \text{Equation 4-6}$$

Upon examination of their partition coefficients (log P), these steroids can be ranked by increasing hydrophobicity: hydrocortisone (1) < prednisolone (2) < dexamethasone (3) < hydrocortisone acetate (4) < testosterone (5).

The columns were evaluated under varying conditions such as temperature, molecular weight, and the amount of comonomer types on the separation of bioanalytes with the HPLC. UV detection was set at 254 nm and elution was run at 1 ml/min under isocratic aqueous conditions, with 10 μ l of analyte concentration and 10 mg/ml injected for each run.

In addition, this stationary phase was also tested for protein chromatography. Proteins are not only hydrophobic but contain also charged moieties. Previous attempts to separate proteins using thermoresponsive stationary phases employed PNIPAAm in combination with ion-

exchange polymers such as 2-(dimethylamino)ethyl methacrylate (DMAEMA), using a combination of hydrophobic and electrostatic interactions⁹⁹. Thus, in our preliminary experiments, we attempted the separation of two proteins, lysozyme (6) and myoglobin (7) using only hydrophobic-hydrophobic forces. The mobile eluent used for these experiments is purely aqueous 0.1 M phosphate buffer run at 0.5 ml/min.

4.1.3.1 Effect of Temperature on the Performance of the Column

The effect of varying temperatures of the columns was evaluated by running them below and above the polymers' LCSTs, in the case of our experiments, from 5 to 55 °C. Figure 4-9(a) shows a scheme of the behavior of the polymer covalently attached to the silica monolith at both its hydrophilic and hydrophobic states at low and high temperatures respectively. Figure 4-9(b) shows the turbidity measurement of particulate silica modified with polymer Composite e. At temperatures below the column's LCST (33 °C), polymer chains are hydrated with the aqueous mobile eluent and are extended, coinciding with the zero transmittance on (b) since the particles were well-dispersed in water solution. By increasing the temperature to above its LCST, the chains collapse as they are increasingly dehydrated of water molecules, thus rendering the column thermoresponsive. The turbidity of the polymer solution dropped when the particles are hydrophobic and settled below the cell, which is observed when the transmittance increased to 100%. This also coincides with the back pressure drop from 70 bars to 30 bars upon lowering the column temperature, as the silica support at its non-polar state encounters less resistance on eluent flow.

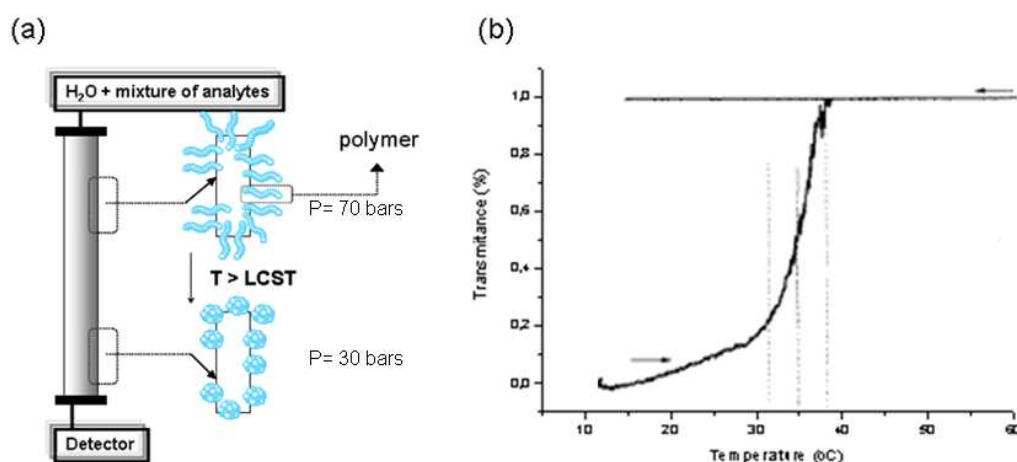


Figure 4-9: (a) Schematic diagram of the behavior of the polymer attached to silica monolith at high and low temperatures with corresponding column back pressures; (b) Turbidity measurement of particulate silica modified with polymer Composite e (LCST=33 °C)

Figure 4-10 shows the elution profiles for the separation of the mixture of five steroids below and above the LCST (43 °C) of the column packed with composite f. It can be observed that below 43 °C, this column separates analytes hydrocortisone (**1**) and prednisolone (**2**) while the more hydrophobic analytes dexamethasone (**3**) and hydrocortisone acetate (**4**) were eluted in a single peak. Testosterone (**5**), which has a much higher log P value (3.32) compared to that of the other steroids, was eluted in a single separate peak from the others. Significantly, by changing the temperature of the column above its LCST led to the separation of steroids **3** and **4** but **1** and **2** were observed to converge into a single elution peak. Fast separation profiles were achieved in less than ten minutes, and together with an increase in retention time for the more hydrophobic analytes, it seems to indicate that the driving forces for separation above LCST are hydrophobic-hydrophobic interactions between the analytes and the stationary phase. On the other hand, the reverse is true for the more lipophilic analytes; they seem to be only separated when the column is in its hydrophilic form.

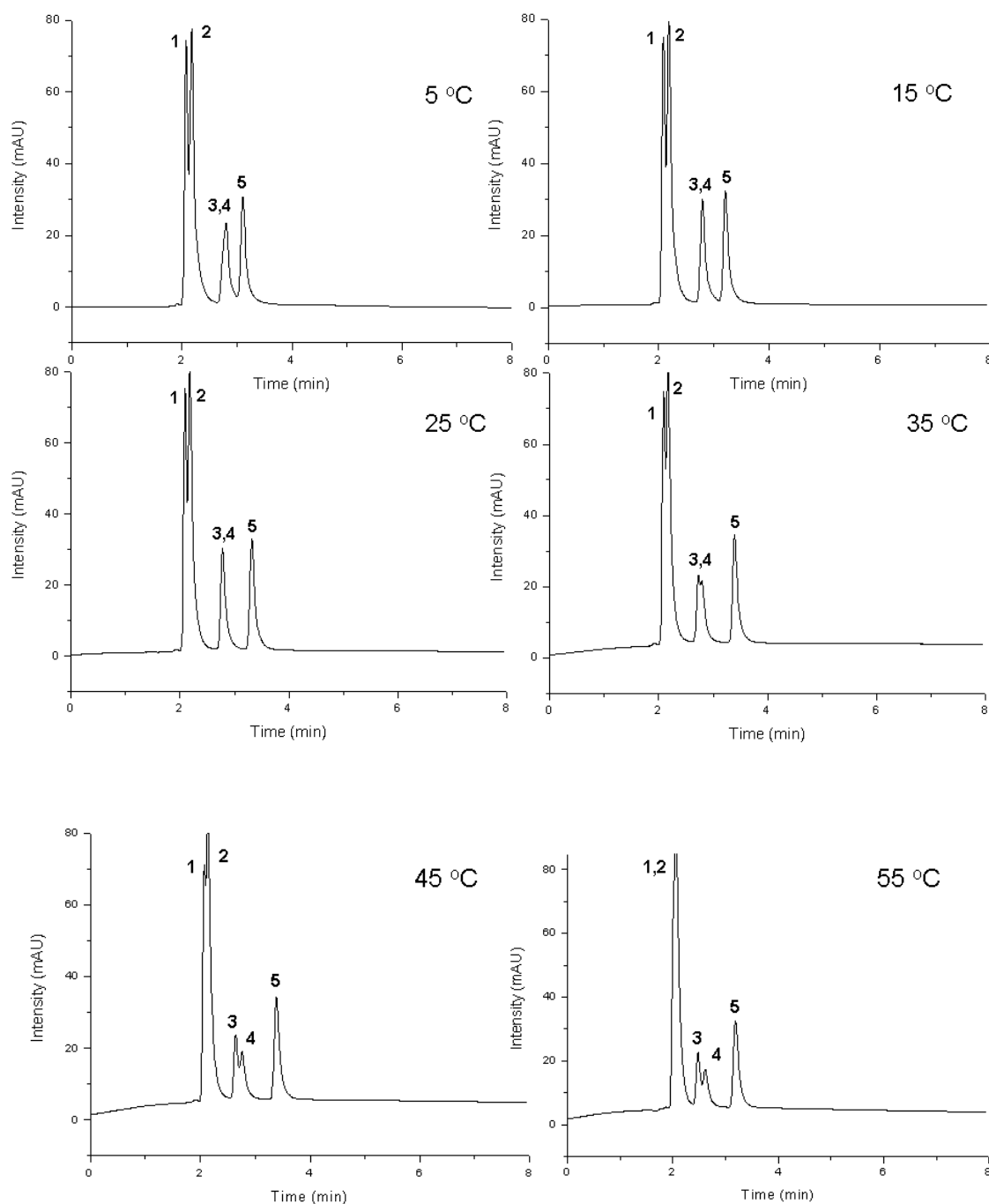


Figure 4-10: Elution profiles and changes in the retention times on five aqueous mixtures of steroids upon variation of temperature (composite f)

The efficiency of the separation was measured by the retention factor k using a benzene marker and the theoretical plate number N of the five steroids (Table 4-3) for elution profiles at 5 °C and 55 °C. Ideally, k should range from values 1 to 5, and values lower than 1 show very fast separations. It was also observed that k values increase with higher temperatures for the more hydrophobic analytes while the reverse is true for the hydrophilic analytes. N also

generally increases with the increase of temperature, showing the improved separation efficiency at the column's hydrophobic state.

Steroids	log P	k(5°C)	k(55°C)	N(5°C) (m ⁻¹)	N(55°C) (m ⁻¹)	HETP(5°C)	HETP(55°C)
Hydrocortisone	1.47	0.4	0.4	5295	1463	0.000019	0.000068
Prednisolone	1.62	0.5	0.4	3289	1463	0.000030	0.000068
Dexamethasone	1.83	0.9	0.6	2628	3312	0.000038	0.000030
Hydrocortisone Acetate	2.45	0.9	0.7	2628	3263	0.000038	0.000031
Testosterone	3.32	1.1	1.1	5997	4692	0.000017	0.000021

Table 4-3: Retention factors k, theoretical plate numbers N and heights equivalent to theoretical plate HETP for each of the five steroids at 5 °C and 55 °C (composite f)

The efficiency of the separation was studied by increasing the amount of polymers grafted onto the silica support and the results discussed below.

4.1.3.2 Effect of Grafting Density on the Performance of the Column

In order to study the effect of increasing grafting density, more polymers (250 mg of polymer per cycle of loading) were loaded onto the same column and varying temperature profiles carried out on the same separation analysis. From elemental analysis (EA) results, the grafting density of composite f increases from 235 to 483 $\mu\text{g}/\text{m}^2$ after the second loading cycle. On Figure 4-11, both elution profiles of composite f ($D_s=483 \mu\text{g}/\text{m}^2$) at 5 °C and 55 °C are shown:

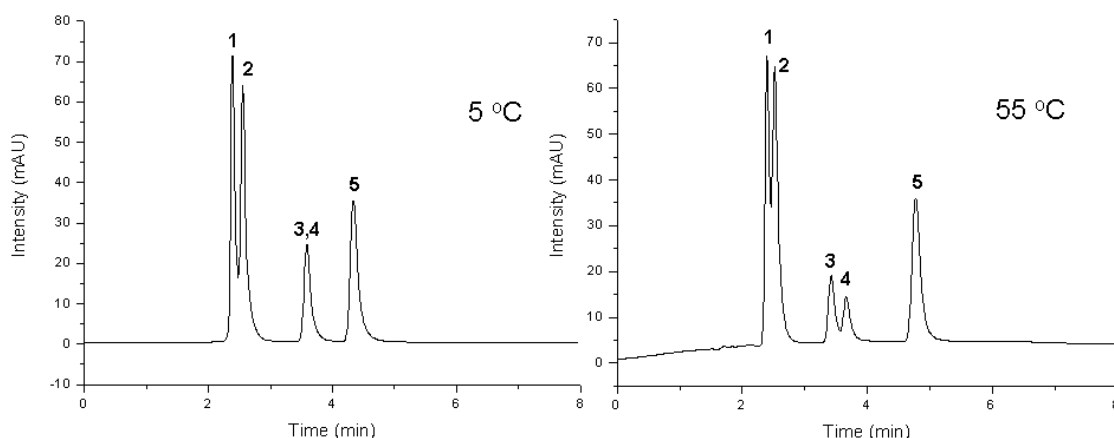


Figure 4-11: Elution profiles and changes in the retention times on five aqueous mixtures of steroids upon variation of temperature (composite f with $D_s=483 \mu\text{g}/\text{m}^2$)

It can be observed that when the silica monolith was modified with two times as much polymer composite f as previously, steroids **1** and **2** achieved better separations both at below and above column LCST. The column is also more hydrophobic as analytes **3** and **4** are better separated at high temperatures and **5** was seen to be more retained in the column as compared to column composite f ($D_s=235 \mu\text{g}/\text{m}^2$). The increased back pressure from 30 to 45 bars when running the column in the HPLC coincided with the results. The improved efficiency of this column is also measured with the following factors in Table 4-4:

Steroids	log P	k(5°C)	k(55°C)	N(5°C) (m ⁻¹)	N(55°C) (m ⁻¹)	HETP(5°C)	HETP(55°C)
Hydrocortisone	1.47	0.6	0.6	5671	3950	0.000018	0.000025
Prednisolone	1.62	0.7	0.7	5070	2932	0.000020	0.000034
Dexamethasone	1.83	1.4	1.3	5550	5136	0.000018	0.000019
Hydrocortisone Acetate	2.45	1.4	1.4	5550	5165	0.000018	0.000019
Testosterone	3.32	1.9	2.2	6491	6287	0.000015	0.000016

Table 4-4: Retention factors k, theoretical plate numbers N and heights equivalent to theoretical plate HETP for each of the five steroids at 5 °C and 55 °C (composite f with $D_s=483 \mu\text{g}/\text{m}^2$)

In order to better conclude the effect of variation of the grafting density of the polymer on the monolith on the resolution of steroids, a third cycle of polymer solution was introduced into the column. The grafting density of the resulting column from elemental analysis results

was shown to be increased to $550 \mu\text{g}/\text{m}^2$. The elution profiles at 5°C and 55°C are shown below on Figure 4-12. However, the performance of the this column decreased instead of achieving higher retention of solute analytes, with **1**, **2**, **3** and **4** not resolved well at both temperatures. The peak from steroid **5** appeared to broaden as the retention increases for the most hydrophobic moiety. The reason for this could be that a high amount of polymer grafting to surfaces could restrict the mesoporosity present in order to adsorb and thus, exert the necessary hydrophobic forces for steroid retention. Figure 4-13 shows the nitrogen sorption data indicating the decrease in surface area and average pore radius on the column with subsequent loading.

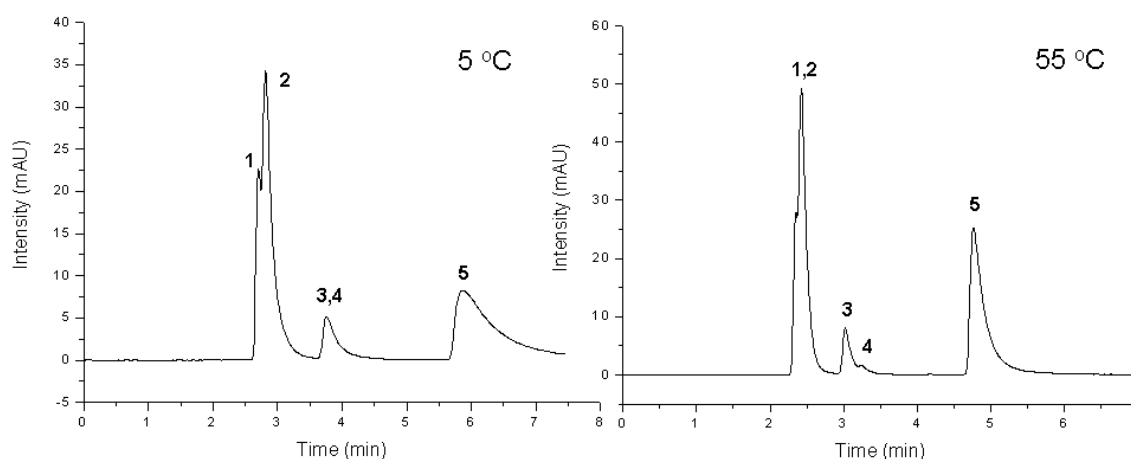


Figure 4-12: Elution profiles and changes in the retention times on five aqueous mixtures of steroids upon variation of temperature (composite f with $D_s=550 \mu\text{g}/\text{m}^2$)

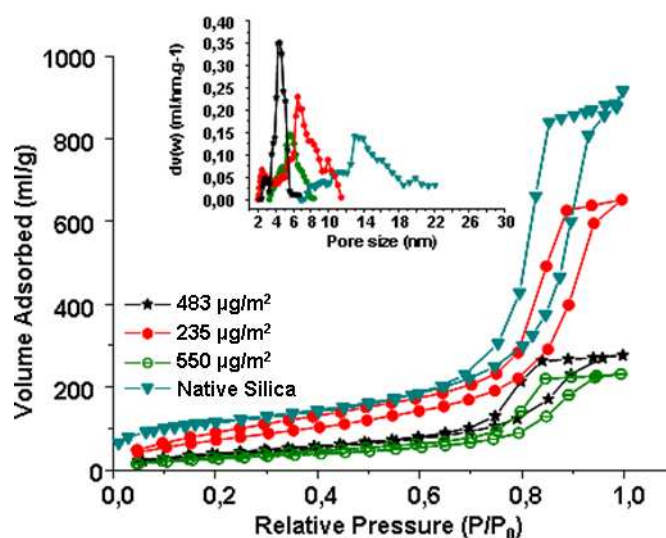


Figure 4-13: Nitrogen sorption data of the native silica and the final thermoresponsive composite with varying grafting densities

Similarly, the separation of steroids was also carried out with the other columns. The elution profiles of silica monolith grafted with Component e ($M_n=18\ 120$; $D_s=250\ \mu\text{g}/\text{m}^2$) are shown in Figure 4-14, in order to perform the same separation analysis with a column of higher hydrophobicity ($\text{LCST}=33\ ^\circ\text{C}$). With a grafting of only one polymer cycle, the elution profiles of column e already show improved separation of the five steroids and this is comparable to that of column f with two polymer cycles grafted ($483\ \mu\text{g}/\text{m}^2$). The former column also resolved analytes **3** and **4** at $35\ ^\circ\text{C}$ as compared to the other column at $45\ ^\circ\text{C}$ due to the difference in their LCSTs. This is also proven mathematically in Table 4-5 below, where column e's retention factors k and plate numbers N have larger values as compared to that of column f's at one polymer cycle grafting. The values are however observed to be comparable to column f's at second polymer cycle grafting.

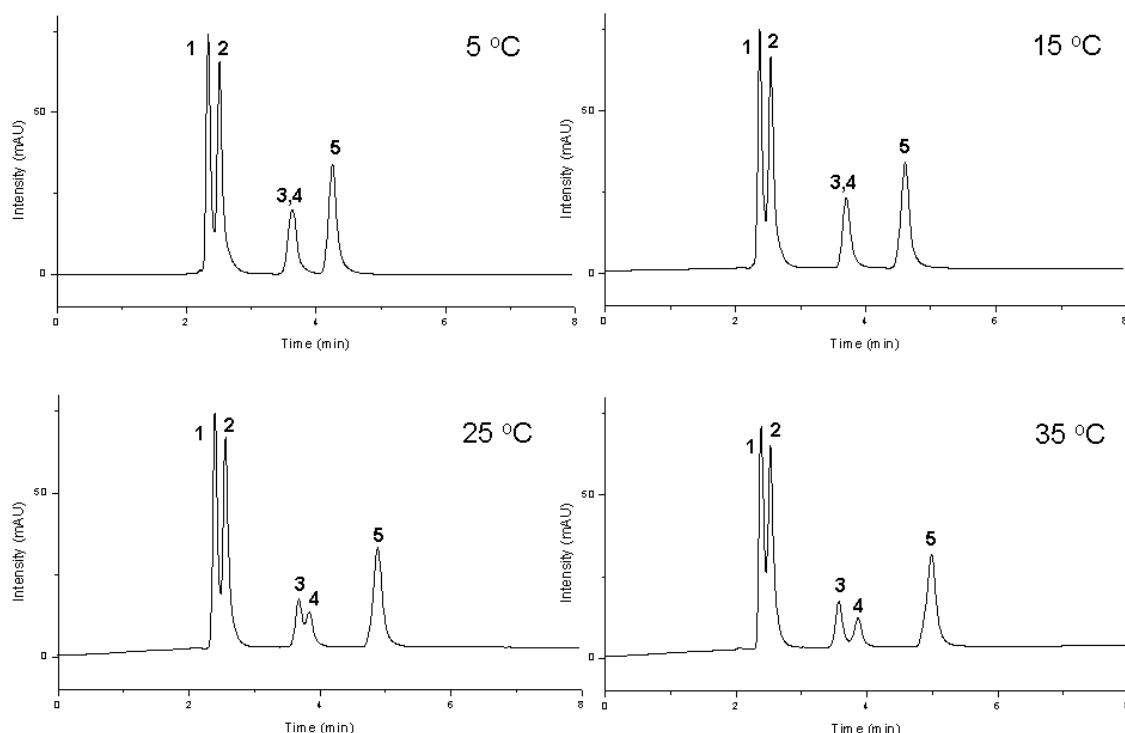


Figure 4-14: Elution profiles and changes in the retention times on five aqueous mixtures of steroids upon variation of the temperature on composite e ($D_s=250 \mu\text{g}/\text{m}^2$)

Steroids	log P	k(5°C)	k(55°C)	N(5°C) (m ⁻¹)	N(55°C) (m ⁻¹)	HETP(5°C)	HETP(55°C)
Hydrocortisone	1.47	0.6	0.6	5402	4911	0.000019	0.000020
Prednisolone	1.62	0.7	0.7	5097	4146	0.000020	0.000024
Dexamethasone	1.83	1.4	1.4	3327	5332	0.000030	0.000019
Hydrocortisone Acetate	2.45	1.4	1.6	3327	5153	0.000030	0.000019
Testosterone	3.32	1.8	2.3	5776	5863	0.000017	0.000017

Table 4-5: Retention factors k, theoretical plate numbers N and heights equivalent to theoretical plate HETP for each of the five steroids at 5 °C and 55 °C (composite e with $D_s=250 \mu\text{g}/\text{m}^2$)

As shown above, the effect of change in temperature of the P(MEO₂MA-co-OEGMA)-modified silica column has on the separation of steroids may prove to be important for the selective isolation of bioanalytes with different lipophilicities under very short analysis time. For an effective separation, the amount of polymer required to be grafted plays an important factor and an optimal amount balancing both density and accessible porosity has to be found.

Finally, a polymer with a lower LCST achieved the same effects in separation at lower grafting density as compared to one with higher LCSTs which can be compensated by higher grafting.

4.1.3.3 Effect of Molecular Weight of Grafted Copolymers on the Performance of the Column

In addition, the influence of some macromolecular parameters such as polymer molecular weight on the separation of the steroid mixture was investigated. For example, we observed that composites prepared with a polymer of high molecular weight (composite a) require only a small grafting density ($0.0078 \text{ chains/nm}^2$) on the silica support in order to achieve a reasonable separation of the five steroids at 55°C . On the other hand, with a lower molecular weight polymer (composite d), the grafting density has to be increased ($0.0295 \text{ chains/nm}^2$) to observe a similar performance. In order to observe this trend, polymer composites a to d with the same comonomer composition ($[\text{OEGMA}]:[\text{MEO}_2\text{MA}]=10:90$) and relatively similar cloud points ($39\text{--}41^\circ\text{C}$) but with varying molecular weights ((a)18 100, (b)15 690, (c)12 310, (d)6220) are compared in the elution of steroids.

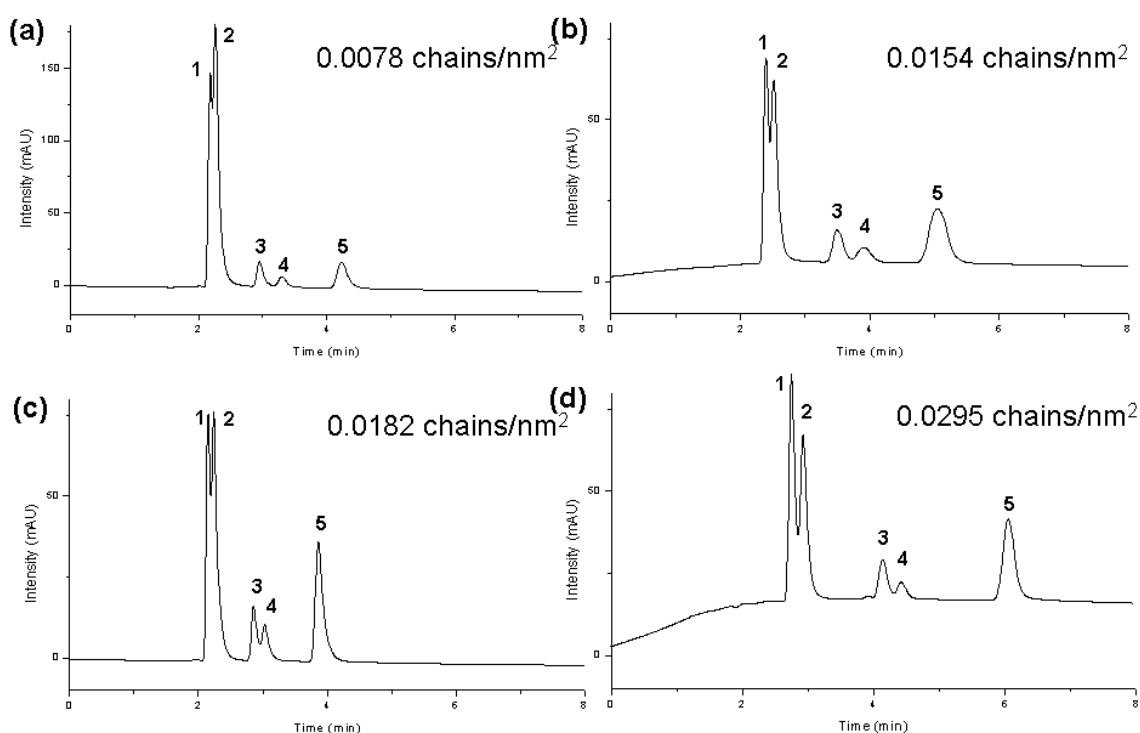


Figure 4-15: Elution profiles and changes in the retention times on five aqueous mixtures of steroids upon variation of the molecular weight at 55°C (composites a to d)

The grafting densities shown in Figure 4-15 are in accordance to the molecular weights of each polymer used in the column (comparing two parameters, molecular weight and D_s , a polymer with a four times shorter chain length requires four times more amount to be grafted). For example, the amount of polymer required for composite d to achieve optimal separation elution is approximately four times as much as that required for composite a. TGA was done on the four composites and the results were observed in Figure 4-16. Thus, to be able to achieve optimal control of the hydrophobicity of the column leading to an efficient separation, higher molecular weight polymers are preferred because a hydrophobic column would require a lower amount of grafting density. Indeed, over-grafting may lead to the blocking of mesopores, which are necessary for the adsorption and separation of bioanalytes.

Composite	Specific Surface Area (m ² /g)	Av. Pore Size Diameter (nm)	Av. Pore Volume (ml/g)
Native Silica	317	16	1.3
A	160	12	0.46
B	130	10	0.39
C	116	6	0.36
D	100	5	0.33

Table 4-6: Nitrogen sorption data of the starting native silica and the thermoresponsive composites a to d grafted with one cycle of polymer

The results from nitrogen sorption in Table 4-6 show the pores being increasingly blocked when polymers are grafted onto the silica surface. As a result of this, surface accessibility also decreased as more polymers are being attached.

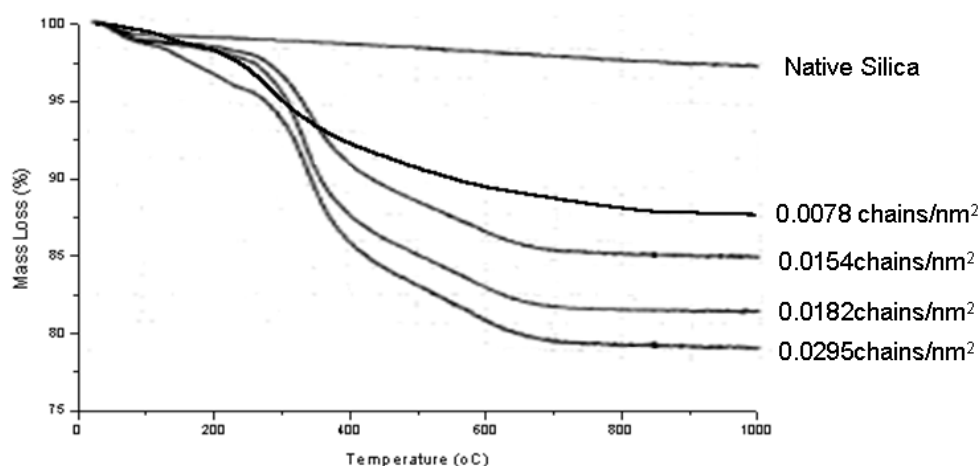


Figure 4-16: TGA profiles of native silica and polymer composites a to d

4.1.3.4 Effect of Varying Comonomers on the Performance of the Column

As mentioned, one important advantage of the P(MEO₂MA-*co*-OEGMA) copolymer is the possibility of tuning their thermo-sensitivity by adjusting their comonomer composition. In Figure 4-17, the chromatograms for the separation of the five steroids ran at 35 °C on two columns packed with composites prepared at different comonomer compositions and thus having different LCSTs are shown (composites e, f). Other parameters such as polymer molecular weights (~20 000) and grafting densities (233-250 µg/m²) are kept relatively similar. For the polymer with more hydrophobic monomer blocks thus a lower LCST (composite e), separation of the more hydrophobic analytes **3** and **4** can already be achieved at lower temperatures (33 °C), while the composite with a higher amount of hydrophilic blocks thus a higher LCST (composite f) can only perform this separation above 43 °C with a worse resolution.

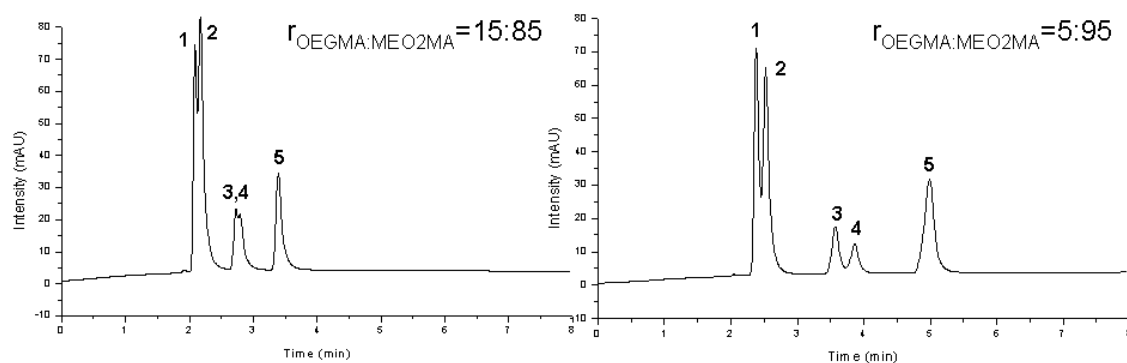


Figure 4-17: Elution profiles and changes in the retention times on five aqueous mixtures of steroids upon variation of the comonomer ratio at 35 °C

Thus, we could show that the separation temperature is closely correlated to the LCST of the polymer and that this could simply be adjusted by changing the comonomer composition of the P(MEO₂MA-*co*-OEGMA) thermoresponsive polymer. This feature has proven to be an advantage over PNIPAAm due to the ease of cloud point variations simply by the control of hydrophobic-hydrophilic components while other factors such as solution concentration and polymer molecular weight do not affect the LCST.

4.1.3.5 Performance of the Column in the Separation of Proteins

The P(MEO₂MA-*co*-OEGMA)-grafted stationary phases were tested for protein chromatography. As was described before, previous efforts to separate proteins using thermoresponsive stationary phases employing PNIPAAm pure analogues showed extensive retention times in pure aqueous eluents. Other attempts include using PNIPAAm in combination with ion-exchange polymers such as poly(acrylic acid) components for hydrophobic and electrostatic interactions.

In our preliminary experiments, we chose the most hydrophobic column (composite e) to attempt the separation of the two proteins with relatively close hydrophobicities, lysozyme (**6**) and myoglobin (**7**), utilizing a purely aqueous system of 0.1M phosphate buffer (pH 6). The eluents were run at a flow rate of 0.5 ml/min under isocratic conditions. At temperature below the LCST of column e (33 °C), the two proteins were eluted in a single peak (Figure 4-18). With an increase in the temperature, they achieved near baseline separation in a relatively short elution time based only on simple polymers, in contrast to that of the PNIPAAm-acrylic acid analogues. Also, their relatively short elution time is in contrast to that of the pure PNIPAAm analogue.

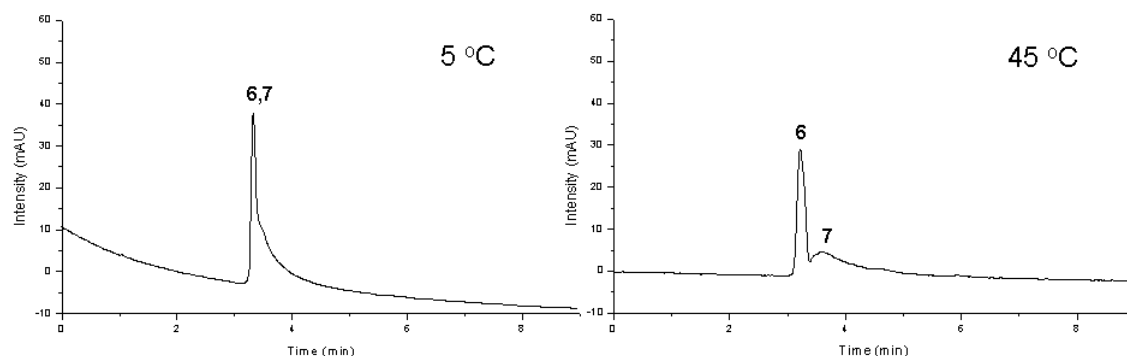


Figure 4-18: Elution profiles and changes in retention times with temperature variation on an aqueous mixture of two proteins, lysozyme (**6**) and myoglobin (**7**), using composite e ($D_s=250 \mu\text{g}/\text{m}^2$)

A reason for this observation may be for the fact that the non-linear poly(ethylene glycol)-like based polymer backbone and side chains are chemically inert, in contrast to the PNIPAAm analogue, which contains the amide bond, leading to some non-specific interactions and extension retention in the column. The absence of such interactions thus led to the fast elution of the proteins on the P(MEO₂MA-co-OEGMA) column. However, the broader peaks indicating tailing may also suggest the involvement of different types of interactions between proteins instead of just hydrophobic-hydrophobic forces, as demonstrated in the case of steroid separation.

The baseline separation of the proteins lysozyme and myoglobin was shown to be carried out in aqueous systems by a simple temperature switch instead of employing organic mobile phases with gradient elution in the C₁₈ system, thus demonstrating a huge step towards proteomics analyses based on isocratic water conditions.

4.1.3.6 Determination of the Hydrophobicity of the Monolithic Columns

The hydrophobicity of the monolithic columns can be determined by a standard test according to Engelhardt¹⁹, which is commonly used for evaluating hydrophobic properties of C₁₈ and C₈ RP columns. Normally, a standard group of tracer markers (Figure 4-19) involving phenol (**9**), toluene (**10**), ethylbenzene (**11**) and uracil (**8**) as a void marker can be injected into the column and the retention analyzed. Uracil has been recommended for use as a void volume marker compound for reversed phase chromatography. It is sparingly soluble in water and is insoluble in alcohol, thus slight retention is based solely on its solubility. Because its pK_a is 9.45, it is protonated at most pH values that are used in RP-LC. Thus, because it is ionized at these pH values, it would tend to be eluted quickly from most columns. For both RP columns

above, the isocratic elution is typically run in water/methanol 49:51 % (w/w) mixture. The retention of toluene and ethylbenzene reflect the hydrophobicity of the column.

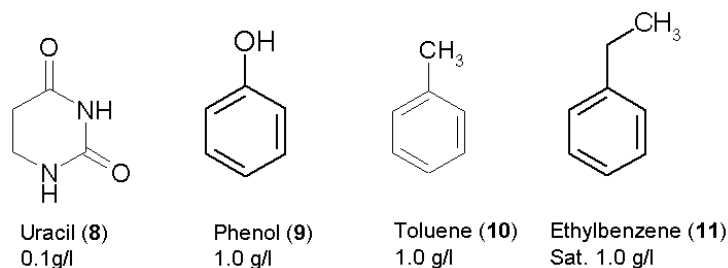


Figure 4-19: Group of tracer molecules used as analytes in the hydrophobicity test and their corresponding concentrations in a sample

According to the literature mentioned above, the retention coefficients k of the most hydrophobic compound ethylbenzene vary between 5 and 15 for RP18 columns and 2-11 for RP8 columns, the selectivity factor α of ethylbenzene over toluene ranges from 1.75 to 1.82 for RP18 columns and 1.7 for RP8 columns. The molecular markers were injected into two of the P(MEO₂MA-*co*-OEGMA)-modified columns, one grafted with polymer composite e (LCST=33 °C; $D_s=250 \mu\text{g}/\text{m}^2$) and with polymer composite f (LCST=43 °C; $D_s=235 \mu\text{g}/\text{m}^2$) at their collapsed states. Through the retention (Figure 4-20), the k (ethylbenzene) and α (ethylbenzene/toluene) factors were calculated and compared to that of benchmark RP18 (MERCK, Darmstadt) and RP8 (MERCK Darmstadt) monolithic columns.

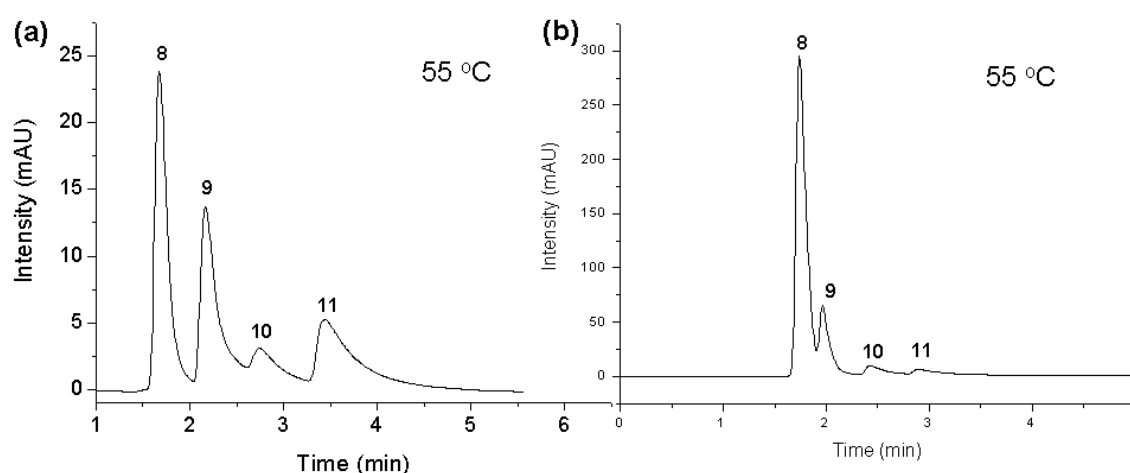


Figure 4-20: Performance of a column packed with polymer (a) composite e (LCST=33 °C); (b) composite f (LCST=43 °C) on the separation of a mixture of trace molecules uracil (8), phenol (9), toluene (10) and ethylbenzene (11) at 55 °C

The hydrophobicity results summarized below in Table 4-7 show that the retention of the hydrophobic analyte ethylbenzene is lower on the PEGylated columns at their hydrophobic states as compared to that on the reversed phase columns. The k (ethylbenzene) value of composite f-modified column (0.7) shows a lower retention than that of composite e (1.8) due to the difference in both their cloud point values, thus hydrophobicities. However, the selectivity factors α of ethylbenzene over toluene remain relatively similar among all four columns (~ 1.7), showing that the separation efficiency of ethylbenzene and toluene are close in performance.

Composite Column	Retention factor k (ethylbenzene)	Selectivity α (ethylbenzene/toluene)
C ₁₈	5-15	1.75-1.82
C ₈	2-11	1.7
e ($D_s=250 \mu\text{g}/\text{m}^2$)	1.8	1.7
f ($D_s=235 \mu\text{g}/\text{m}^2$)	0.7	1.7

Table 4-7: Retention factor k (ethylbenzene) and selectivity factor α (ethylbenzene/toluene) of columns e and f in comparison to RP18 (MERCK, Darmstadt) and RP8 (MERCK, Darmstadt) columns

The Engelhardt hydrophobicity test procedures were performed as seen above and the P(MEO₂MA-*co*-OEGMA) columns were compared against commercial RP-HPLC columns in order to characterize their hydrophobic properties in chromatography.

4.1.3.7 Effect of Polymer Type on the Performance of the Column

In order to study how the polymer type influences the separation of the mixture of five steroids, two other thermoresponsive polymers as mentioned before, the modification of silica monoliths with poly(*N*-isopropyl acrylamide) (PNIPAAm) and poly(2-oxazoline) are evaluated and compared to P(MEO₂MA-*co*-OEGMA)-modified columns.

a) Poly(*N*-isopropyl acrylamide) (PNIPAAm)

The grafting of PNIPAAm on silica monoliths and the resolution of the thermoresponsive column on steroids have been previously reported¹⁸. PNIPAAm was first synthesized by RAFT polymerization utilizing the RAFT agent 4-cyanopentanoic acid trithiododecane and

azobutyronitrile (AIBN) as an initiator. The reaction was carried out at 70 °C after three freeze dry cycles. According to GPC results done in NMP solvent, the final polymer product shows a molecular weight of approximately 14 700 (g/mol) with carboxylic end groups. In order to render the end groups more reactive for coupling to amino groups on silica monoliths as described before, *N*-hydroxysuccinimide was added. The final grafting density of PNIPAAm chains in the column was calculated from elemental analysis results to be 0.0096 chains/nm². The general mechanism of the polymerization and activation is shown in Figure 4-21.

The PNIPAAm-modified column was taken as a comparison to the P(MEO₂MA-*co*-OEGMA) copolymer-modified column in the separation of the mixture of five steroids in aqueous isocratic conditions. In order to make a comparison based only on the difference in polymer type, the other parameters are kept relatively similar and they are summarized for each polymer type in Table 4-8.

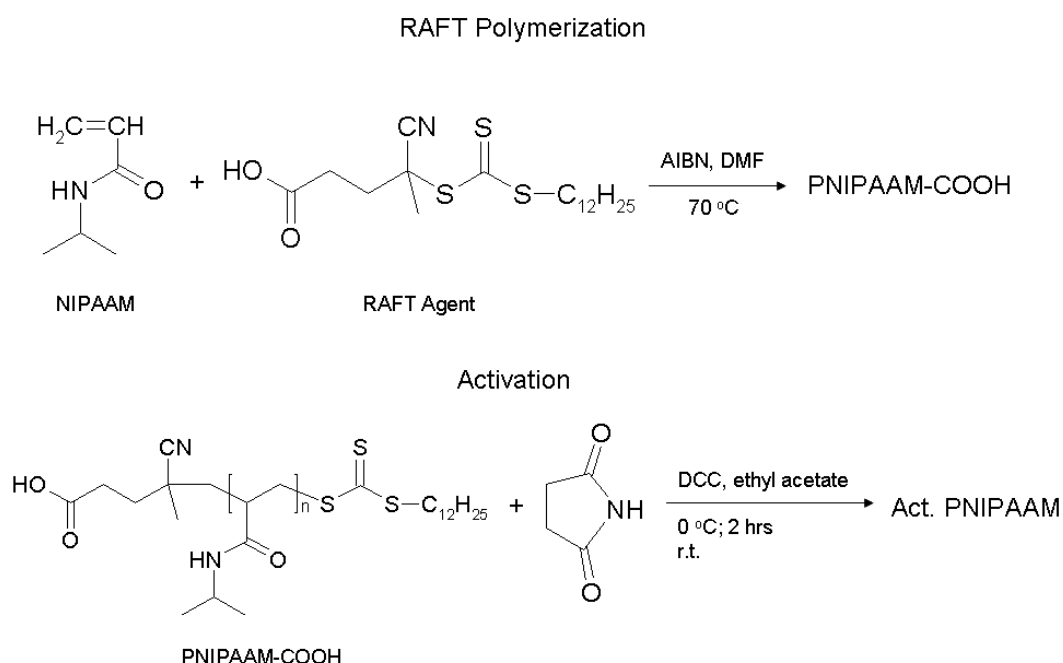


Figure 4-21: General reaction scheme of RAFT polymerization of NIPAAm and the activation of PNIPAAm

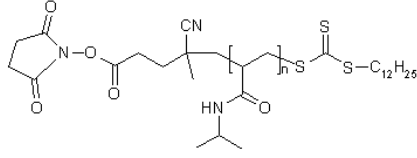
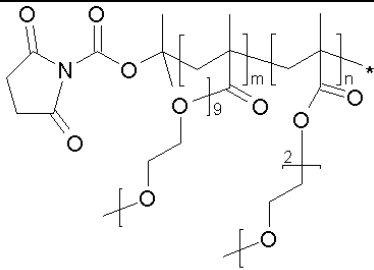
	(a) PNIPAAm	(b) P(MEO ₂ MA- <i>co</i> -OEGMA)
Structure of Polymer Grafted on Silica Monolith (MERCK)		
Molecular Weight (mol/g)	14 700	18 120
Cloud Point (°C)	32	33
Grafting Density (chains/nm ²)	0.0096	0.0093

Table 4-8: Characterization of the two columns used for polymer type comparison in the elution of a mixture of five steroids in water

The chromatograms of both columns showing their behaviors at their hydrophilic and hydrophobic states are compared in Figure 4-22. At column temperature below their LCSTs, it was observed that the PNIPAAm column (Figure 4-22(a)) could not resolve hydrocortisone (**1**), prednisolone (**2**), dexamethasone (**3**) and hydrocortisone acetate (**4**). Testosterone (**5**) was eluted as a single peak as its hydrophobicity ($\log P=3.32$) is much higher as compared to the other steroids. By increasing the temperature, all the analytes could be separated.

As for the P(MEO₂MA-*co*-OEGMA) column, the separation behavior has a significant difference in that different steroids are resolved according to the column's hydrophilic-hydrophobic states. Testosterone (**5**) was shown to be retained much longer in the first column due to its higher hydrophobicity at 45 °C. The constant order of elution for both columns suggests that the driving force for separation is hydrophobic-hydrophobic interactions.

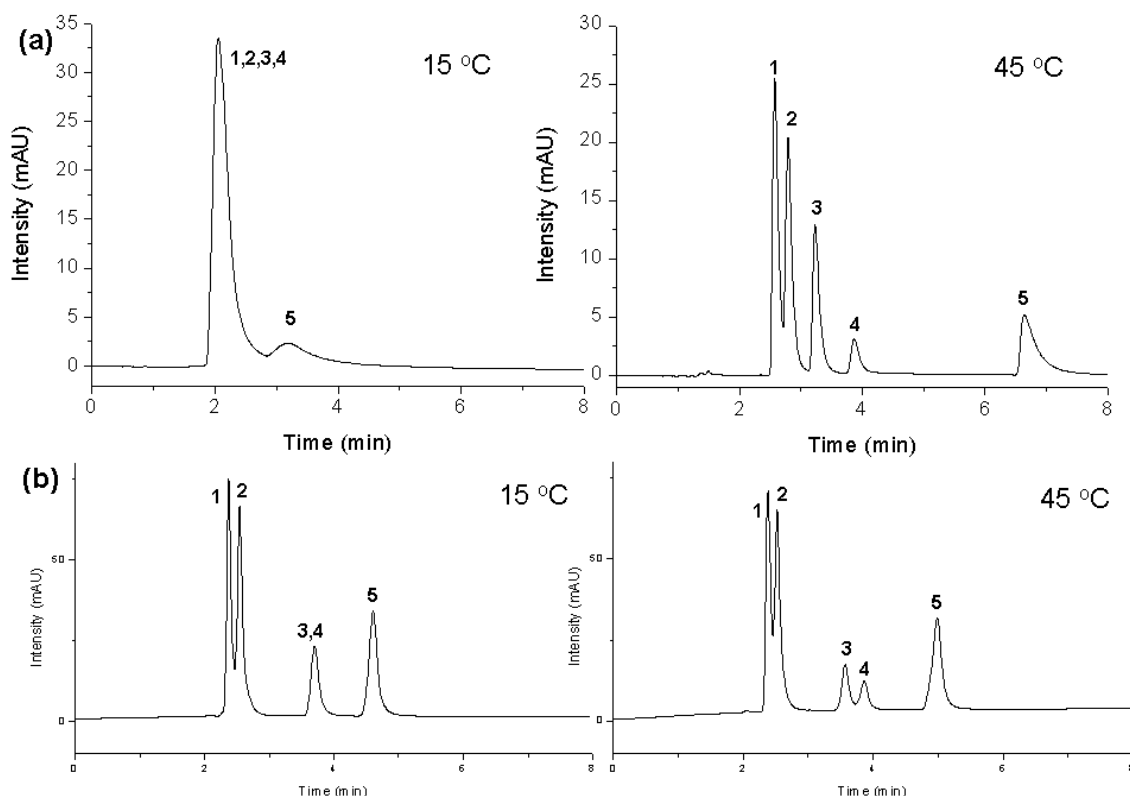


Figure 4-22: Elution profiles and changes in the retention time on five aqueous mixtures of steroids upon variation of temperature with (a) PNIPAAm column; (b) composite e ($D_s=250 \mu\text{g}/\text{m}^2$) column

The difference in elution behavior may be attributed to the structures of the polymers. From PNIPAAm's structure, the presence of the amide bond ($\text{C}=\text{O}(\text{N}-\text{H})$) within the side chains of the polymer constitutes to strong Van der Waal's forces, specifically hydrogen bonding even when the chains are in their collapsed state. Accessible oxygen atoms appearing on the side chains of the polymer on the PEGylated column cause it to be hydrophilic even at low temperatures, thus separating steroids (1) and (2), suggesting polar type of interactions between the polymer and the analytes. Once the temperature was raised, (3) and (4) were resolved due to strong Van der Waal's between hydrophobic polymer backbone and steroids.

Besides biocompatibility⁶⁵ and the promising ability to separate proteins as discussed previously, P(MEO₂MA-*co*-OEGMA)-modified columns have also demonstrated two apparent advantages over PNIPAAm columns as described before. The cloud points of the copolymer may be tailored accordingly to separation requirements and its separation behavior was selective, which makes it efficient in choosing either hydrophilic or hydrophobic analytes for catch and release mechanisms at different temperatures.

b) Poly(2-oxazoline)

As mentioned before, poly(2-oxazoline) is a structural isomer of PNIPAAm and it is a widely studied thermoresponsive material due to its potential for use as biomaterials in drug delivery systems and paint industries^{64, 100}. One could also linearly tune a specific cloud point temperature by copolymerizing two monomers each with different LCSTs: 2-*N*-propyl-2-oxazoline (NPOX) (23.8 °C) and 2-isopropyl-2-oxazoline (IPOX) (38.7 °C)¹⁰¹. The monomers could first be synthesized with ethanolamine and isobutyronitrile or *N*-butyronitrile to give IPOX or NPOX respectively in the presence of a cadmium catalyst. The synthesis of the copolymer was done by cationic ring opening polymerization and the initiator methyl *p*-tosylate (MeTos) and termination agent Boc-protected aminopiperidine were used under very dry conditions. The final Boc-protected polymer product was obtained from freeze drying and the deprotection with trifluoroacetic acid (TFA) activated the polymer chain ends with amino groups. Figure 4-23 shows the mechanism for the synthesis of each monomer and the polymerization of the copolymer P(IPOX-*co*-NPOX).

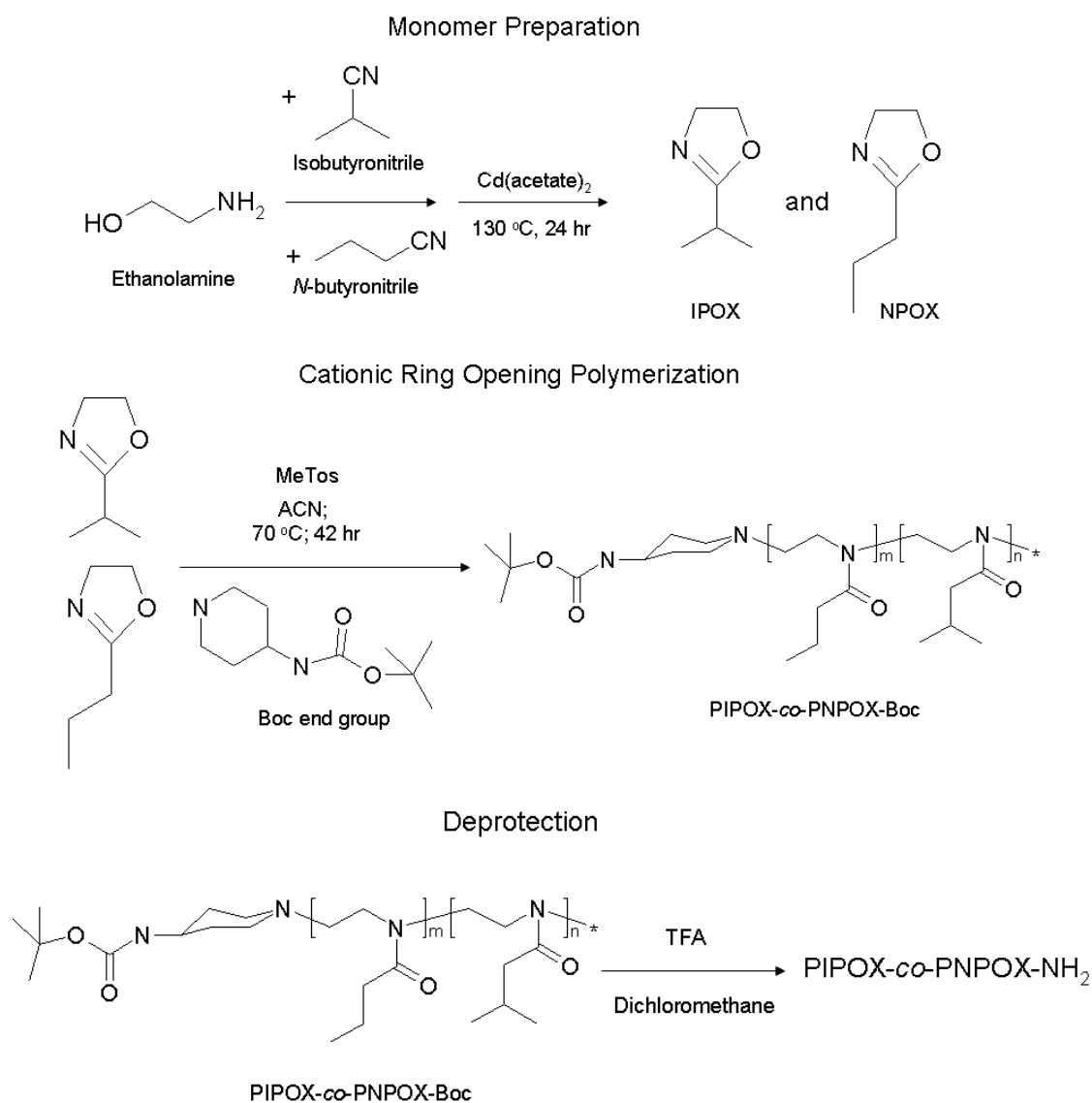


Figure 4-23: Reaction scheme of the synthesis of monomers IPOX and NPOX; the cationic ring opening polymerization and activation of polymer chain end group

From GPC done with NMP solvent, poly(IPOX-*co*-NPOX) with the desired comonomer units of 32:15 ([IPOX]:[NPOX]) showed a molecular weight of approximately 5000. In order to couple the amino chain end of the polymer to the silica monolith, 3-isocyanatopropyl triethoxysilane was used to modify the silica surface with cyano groups instead of amino. From elemental analyses, the amount of cyano groups immobilized onto the monolith was $504 \mu\text{g}/\text{m}^2$ and the grafting density from the first cycle polymer attachment was $0.06 \text{ chains}/\text{nm}^2$. Turbidity measurements confirmed the LCST in water at 1 wt.% to be 42°C . For comparison purposes, silica monolith grafted with P(MEO₂MA-*co*-OEGMA) from composite d was chosen.

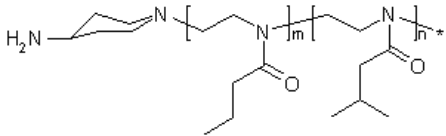
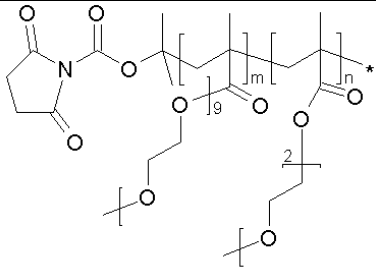
	(a) P(IPOX-co-NPOX)	(b) P(MEO ₂ MA-co-OEGMA)
Structure of Polymer Grafted on Silica Monolith (MERCK)		
Molecular Weight (mol/g)	5000	6220
Cloud Point (°C)	42	40
Grafting Density (chains/nm ²)	0.058	0.039

Table 4-9: Characterization of the two columns used for polymer type comparison in the elution of a mixture of five steroids in water

On Figure 4-24, the elution of steroids in water on both modified columns is shown at 55 °C with 1 ml/min flow rate under isocratic conditions.

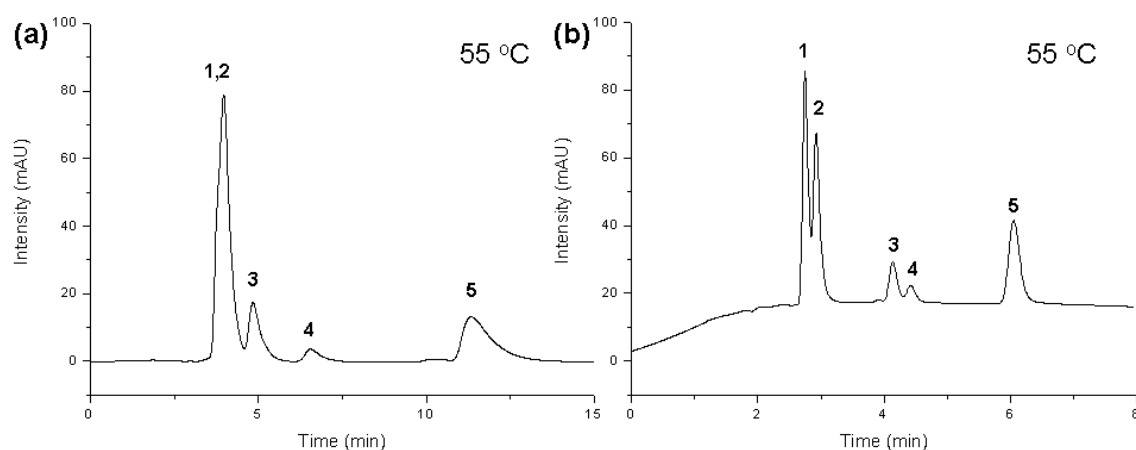


Figure 4-24: Elution profiles and changes in the retention time on five aqueous mixtures of steroids run at temperature 55 °C with (a) P(IPOX-co-NPOX) column; (b) composite d ($D_s=305 \mu\text{g}/\text{m}^2$) column

The column modified with poly(2-oxazoline)s at its optimal performance could only drive the separation of four peaks above the polymer's LCST (42 °C) even with successive loading of more polymers into the column. Apparently, the column was not hydrophobic enough to

resolve hydrocortisone (**1**) and prednisolone (**2**) which have relatively close log P values. The peak of testosterone (**5**) was broad and was observed to be retained longer than in the PEGylated column. The presence of the N moiety appears within the polymer chain backbone on P(IPOX-*co*-NPOX), thus the interactions the polymer has on the steroid analytes are different from the other columns. There was a lack of strong hydrogen bonding in this polymer as compared to the case of PNIPAAm and thus the isopropyl and *N*-propyl groups on the extended chains are not hydrophobic enough to separate all analytes. The polymer also lacks the oxygen moiety like in P(MEO₂MA-*co*-OEGMA); in the case of the latter hydrophilic interactions were apparent in the resolution of (**1**) and (**2**).

As was seen in the elution graphs above, the effect of the polymer type alters the hydrophobicity of the column in the process. However, the LCST of each polymer does not play a direct role in the separation processes; instead, each polymer structure influences the interactions between the grafted polymer and the group of steroids intrinsically.

4.1.4 Summary and Outlook

In conclusion, we have reported for the first time the preparation and chromatographic evaluation of a PEG-related thermoresponsive stationary phase, leading to the successful separation of a mixture of five steroids based on a simple temperature switch under environmentally friendly aqueous conditions. Studies on the influences of various parameters on the elution such as temperature, molecular weight of grafted polymer, grafting density, comonomer composition and polymer structures were explored.

The synthesis of P(MEO₂MA-*co*-OEGMA) employs the ‘living’ atom transfer radical polymerization (ATRP) method which gives narrow molecular weight distributions and the succinimidyl end groups could be easily ‘in-situ’ ‘grafted to’ amino surface-modified silica monoliths (MERCK, Darmstadt). An advantage of such a copolymer as compared to previously studied PNIPAAm is that the cloud point of the former could be specifically tuned to a desired value. Environmental factors such as pH, polymer concentrations and polymer molecular weights also do not largely affect its LCST.

Protein chromatography was attempted and the isocratic elution of two proteins in aqueous mobile phases showed initial near-baseline resolution. By further optimization of our system, proteomics based on isocratic water conditions may one day overcome current limitations.

In addition to the existing thermoresponsive polymeric block, other stimuli-responsive properties could be conferred to maximize the window for the potential applications in the separation of biomolecules. Employing the benefit of the living properties of the ATRP technique, the polymerization of P(MEO₂MA-*co*-OEGMA) could be easily re-initiated with a small amount of initiator AIBN and the polymerization process continued. Ternary copolymers could be designed for example, a pH-responsive polymer such as poly(acrylic acid) or 2-dimethylaminoethyl methacrylate (DMAEMA) could be added to introduce charged groups. Butyl methacrylate (BMA) could also be introduced as a hydrophobic monomer to the system. Thus the final grafted surface would be one with anionic or cationic thermoresponsive hydrogel, producing an alterable stationary phase with both thermally regulated hydrophobicity and charged density for the separation of other bioactive compounds without the use of organic mobile phases.

4.2 Biomass Derived Carbonaceous Materials for Chromatography

As already mentioned in the previous chapter, the search for alternative stationary phases for high performance liquid chromatography (HPLC) is not limited to only silica-based phases. The development of highly pH-stable and mechanical robustness type of materials was motivated by the limitations in stabilities of both silica¹⁰² and bonded-silica columns when exposed to aggressive conditions over long periods of time. Attention was drawn to carbon-based materials for packing after Knox *et al.*⁴¹ first proposed the use of porous graphitic carbon (PGC) as stationary phases combining chromatographic performance with mechanical strength. However, the synthesis of PGCs is not straightforward and requires high temperatures routes (>2500 °C) to carry out. After high temperature treatment, the surfaces usually become inert and hydrophobic.

Recently, much attention has been focused on the use of plant biomass to produce functional carbonaceous materials under comparatively mild synthesis conditions. In this study done within our working group, carbon materials with different morphologies, including modern carbon nanocomposites and hybrids have been produced and investigated for a variety of applications including catalysis¹⁰³, energy storage, water purification and CO₂ sequestration⁸⁶. The process known as hydrothermal carbonization (HTC) employs environmentally friendly and sustainable processes under mild carbonization conditions (<200 °C; < 20 hr). The precursors are thus partially carbonized in water, leaving polar functional groups on its surfaces. In our previous studies on thermoresponsive silica monoliths, the presence of surface functionalities on silica materials was also shown to play an important factor for the modification of support surfaces with thermoresponsive polymers. In our attempt to synthesize carbon-based stationary phases which boasts superior mechanical stability in comparison to silica-based supports for chromatography, we focus on the HTC process for the production of low cost nanostructured carbon materials with functionalization patterns which could be tailored for applications in chromatography.

In this chapter of my thesis, carbonaceous materials were obtained from a one-step HTC reaction under self-generated pressures of various carbohydrates such as xylose, glucose and sucrose. The structures of the precursors used are shown in Figure 4-25. The obtained hydrothermal carbons were studied for their morphology and reactive surface functionalities.

The performance of bare hydrophilic carbon particles in chromatography were initially demonstrated as both normal phase (NP) and reversed phase (RP) modes.

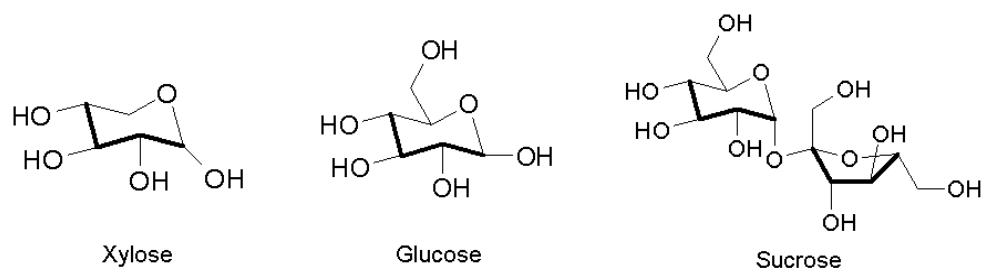


Figure 4-25: Chemical structures of carbohydrate precursors used for HTC

Furthermore, the hydrophilic surfaces present on carbon beads were subjected to modifications with the homo-polymer, poly(*N*-isopropyl acrylamide) (PNIPAAm) in order to confer a thermoresponsive property to the spheres. As described earlier, PNIPAAm was first synthesized by the RAFT technique. Similar to the modification steps undertaken for the silica monoliths, the polymer was grafted to the carbonaceous surfaces 'ex-situ'. The carbon particles were first tailored to give amino-rich surfaces, which were later chemically coupled with the activated succinimidyl end-groups of the polymer. Cloud point measurements were done to determine whether the polymer was indeed grafted to the surfaces by checking the behaviour of the modified solid in water with increasing temperature. Thus, the ease of functionalization of the hydrothermal carbons could be investigated and chromatographic tests were also carried out to develop hydrothermal carbon with alterable surfaces as a stationary support.

4.2.1 Hydrothermal Carbonization and the Incorporation of Functional Monomers

As described earlier in Chapter 2.4, the mechanism of HTC shows carbohydrates being dehydrated first to form a furan-like molecule (furfural aldehyde or 5-(hydroxymethyl)-2-furaldehyde) (HMF). Upon subsequent polymerization and carbonization, micrometer-sized carbonaceous spheres composed of a polyfuran hydrophobic core and a hydrophilic shell decorated with a high number of polar functionalities such as hydroxyl (OH), carbonyl (C(=O)H) or carboxylate (COOH) groups were produced.

In addition to the production of mono-dispersed carbon spheres from carbohydrates, it was found that organic functional monomers such as acrylic acid, acrylamide or cyano groups

could be easily incorporated to the surfaces of carbon microspheres through a cycloaddition process during the formation of the aromatic polyfuran core. Functionalities depending on the employed monomer could be conferred, giving a hybrid carbon nanocomposite upon the HTC of carbohydrates and a small amount of monomer in water. The reaction scheme for the cycloaddition of the acrylic acid monomer during HTC for example, is shown in Figure 4-26 below. In this case, the carbonaceous particles obtained are loaded with carboxylate rich groups which find important applications such as materials for the removal of heavy metals⁸⁸.

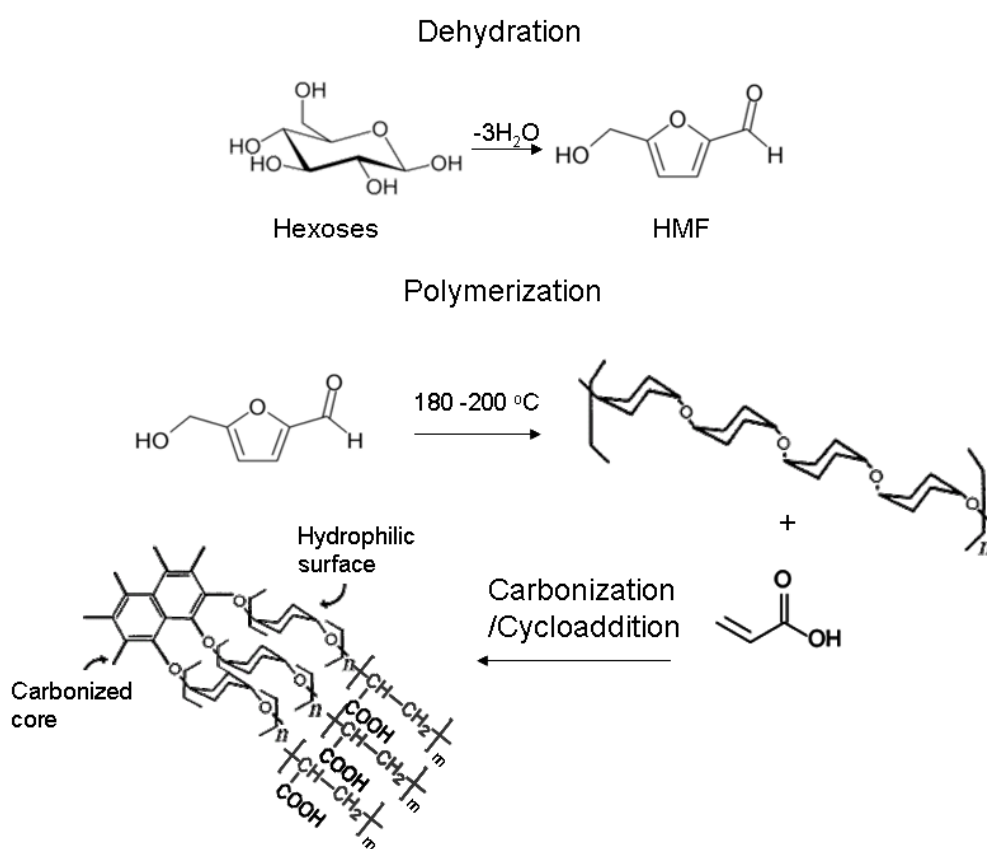


Figure 4-26: General reaction scheme of hydrothermal carbonization of glucose with the addition of acrylic acid

These functional microporous carbon nanocomposites are produced from a rather uncomplicated synthesis route, with the simple method of incorporation of desired functional monomers on the carbon surfaces. When carbonization is carried out with acrylamide as an additive instead, the final composite would be loaded with acrylamido groups on the surfaces. PNIPAAm could then be added directly without first modifying the surfaces with APS as described previously, thus one synthetic step could be skipped.

The final materials which are then packed into a stainless steel column (4.6 X 100; Knauer, Germany) could be tested as a potential cationic exchanger candidate for the separation of proteins, or in the case of thermoresponsive-modified composites, for the hydrophobic resolution of steroids in chromatographic applications. The synthesis and characterization of such chromatographic materials are reported below.

4.2.2 Synthesis and Characterization

a) Pure Carbohydrates

A series of parallel HTC reactions were carried out. To obtain monodispersed spherical carbonaceous particles, pure carbohydrates were first stirred and dissolved in pure water before carbonization.

In order to investigate the particulate formation with respect to varying concentrations of starting precursors, 10 wt.% and 30 wt.% of xylose were dissolved separately in water and both solutions were placed each in a glass cell, which were later inserted into a Teflon inlet, sealed in a stainless steel autoclave and the carbonization carried out at 180 °C for 18 to 20 hours. During the reaction, the pressure was observed to be less than 20 bars. After the reaction was done, the autoclaves were cooled down quickly and a black mass of solid was collected by centrifugation. The unreacted hydrothermal solution remaining from the reaction was discarded. The hydrothermal product was washed with water repeatedly and later dried in a vacuum oven at 80 °C. For the 10 wt.% and 30 wt.% xylose in solution as starting materials, the yields were observed to be 28% and 34.2% respectively. The SEM images of the hydrothermal product obtained from a lower concentration precursor (Figure 4-27 (A, B)) and a higher concentration precursor (Figure 4-27 (C, D)) as starting materials are shown below.

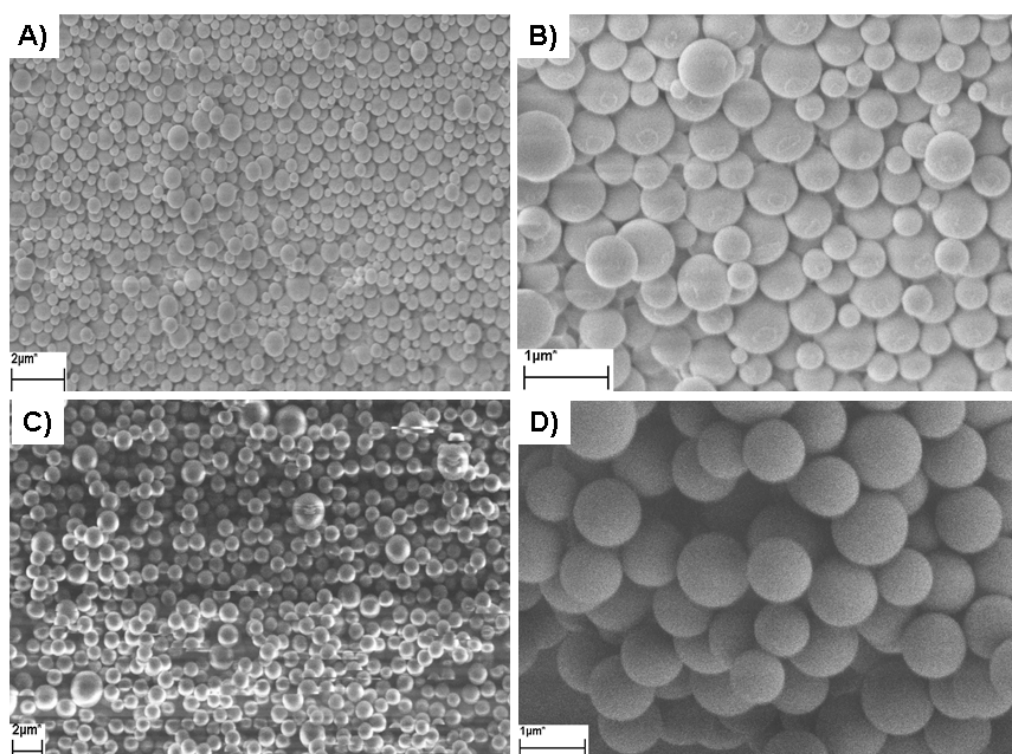


Figure 4-27: SEM images of hydrothermal carbon derived from HTC of A, B) 10 wt.% xylose; C, D) 30 wt.% xylose in water; 180 °C, 18-20 hrs

The hydrothermal carbon product obtained in each case appears to resemble clusters of fish eggs, with rather monodispersed spheres. As observed above, when the concentration of starting xylose is increased (from 10 to 30 wt.%), the diameter of the resulting spheres seem to grow more homogeneously with sizes staying at approximately 1 μm (Figure 4-27 (C, D)) while the spheres on Figure 4-27 (A, B) are not uniform (0.3 to 1 μm). This observation coincides with the mechanism of HTC of simple carbohydrates. As xylose was transformed into HMF and later carbon, the particles aromatize and grow in water spherically until the sugar is consumed. By using a higher concentration of carbohydrate in the solution, the final hydrothermal product will result in bigger spheres. This simple control of sphere morphology extends also to varying reaction time and temperature. The longer the synthesis time, the bigger the spheres will grow and higher reaction temperatures initiate the faster formation of particles.

As seen on the FT-IR spectra on Figure 4-28, the resulting carbon product shows aromaticity in its core ($\nu_{\text{C}=\text{C}}$ at 1800-1500 cm^{-1} for conjugated olefinic bonds) and the surface shells are decorated with hydroxyl (ν_{OH} at 3550-3200) hydrophilic groups due to the use of water as a reaction media. Bending and stretching at $\delta_{\text{C-H}}$ = 920-740 cm^{-1} and at 3100-2800 cm^{-1} also

show out of plane aromatic vibrations. Elemental analyses show N% of 0.015 % and C% of 68.16 %, where the high carbon content is expected.

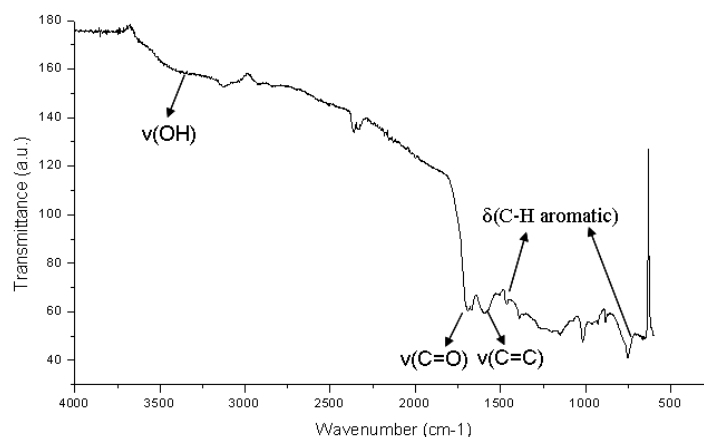


Figure 4-28: FT-IR spectra of hydrothermal carbon derived from HTC of 30 wt.% xylose in water; 180 °C, 18 hr

From BET measurements, the spheres however display a relatively low surface area ($\sim 28 \text{ m}^2/\text{g}$) as compared to that of silica ($\sim 350 \text{ m}^2/\text{g}$). This is presumably due to some micropore blocking with small organic molecules (levulinic acid) resulting from the decomposition of carbohydrates.

The same HTC procedure was carried out with 30 wt.% glucose solution at 180 °C for 18 to 20 hours. The final hydrothermal product obtained from glucose has a yield of 35 % with its morphology shown below in Figure 4-29.

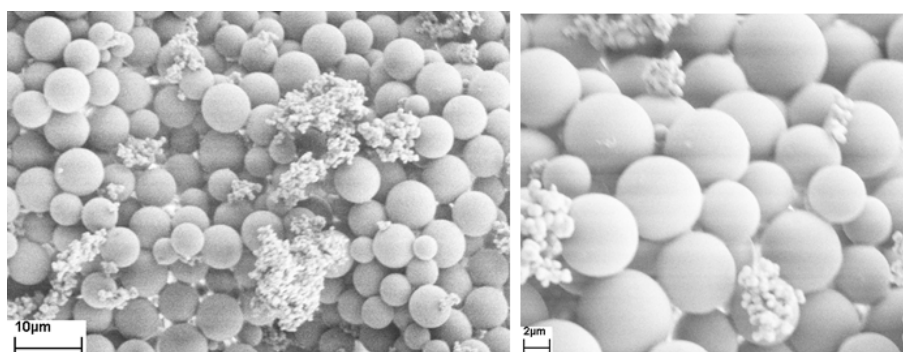


Figure 4-29: SEM image of hydrothermal carbon derived from HTC of 30 wt.% glucose in water; 180 °C, 18 hr

From the SEM image above, the carbonaceous product derived from using glucose as a precursor shows spheres with sizes ranging from 5 to 8 μm . The HTC product spherical size

is related to the solubilities of the carbohydrates in water, where the process converts dissolved sugar molecules more readily thus resulting into bigger spheres as compared to one which is less soluble in solution. Glucose has a solubility of 91 g per 100 ml of water at 25 °C while xylose is less soluble, with approximately 55 g dissolved per 100 ml at its saturation point at this temperature. However, the results show inhomogeneous particle morphology, with some residues of unreacted glucose precursor observed to be stuck between the spheres. The FT-IR was also done and is shown on Figure 4-30.

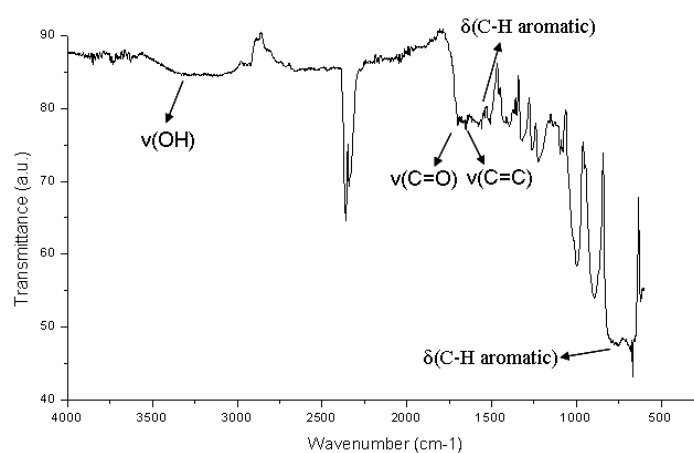


Figure 4-30: FT-IR spectra of hydrothermal carbon derived from HTC of 30 wt.% glucose in water; 180 °C, 18 hr

As expected, the glucose-based spherical product shows a hydrophilic surface (ν_{OH} at 3550-3200) with well-defined aromatic groups $\nu_{\text{C=C}}$ at 1800-1500 cm^{-1} for conjugated olefinic bonds. C content of 63.32 % is reported from elemental analyses. The surface area measured at $\sim 14.2 \text{ m}^2/\text{g}$ from BET is however, smaller than that of xylose-based particles ($\sim 28 \text{ m}^2/\text{g}$) and macropores are measured at approximately 460 nm.

Figure 4-31 shows the SEM images of the hydrothermal product obtained from carbonizing sucrose under the same conditions as described with xylose and glucose. The main difference lies chiefly in their morphologies; spherical carbon showing a small amount of aggregation was obtained from xylose and glucose while spheres showing an interconnected network with through-pores in between (approximate core diameter of 540 nm) was the result of the HTC of sucrose. This could be due to the fact that sucrose is a disaccharide of glucose and fructose, thus a network of joint spherical cores grows simultaneously, as compared to a single aromatic core in monosaccharides. As mentioned already, where solubility of the

carbohydrates affects the end-result of hydrothermal carbon produced, the relatively high amount of sucrose which can be dissolved in 100 ml of water at 25 °C (200 g per 100 ml) resulted in higher homogeneity. From elemental analyses, the C% content is 65.61%.

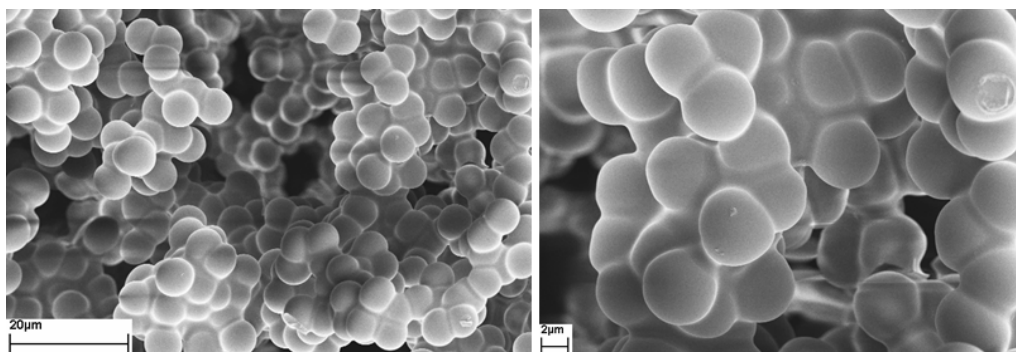


Figure 4-31: SEM image of hydrothermal carbon derived from HTC of 30 wt.% sucrose in water; 180 °C, 18 hr

The FT-IR spectra (Figure 4-32) of the carbon obtained from the HTC of sucrose also shows hydrophilic surfaces (ν_{OH} at 3550-3200) and a pronounced absorption band indicating that carboxylate (COOH) surface groups ($\nu_{\text{C=O}}$ at 1700 cm^{-1}) are present.

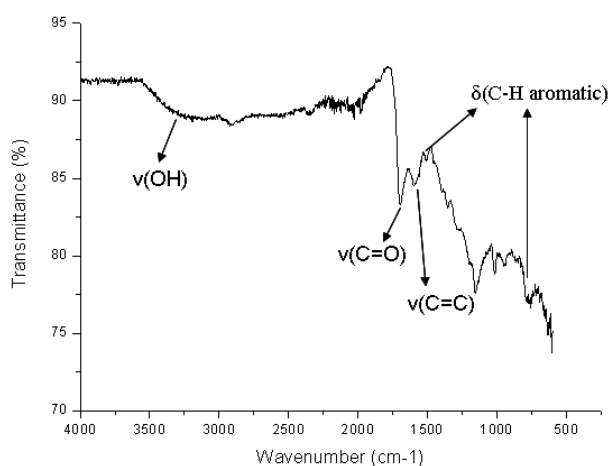


Figure 4-32: FT-IR spectra of hydrothermal carbon derived from HTC of 30 wt.% sucrose in water; 180 °C, 18 hr

In order to investigate the ease of surface functionalization of these hydrothermal carbonaceous products, glucose-based spheres (5 μm) were modified in a reaction flask (*ex-situ*) using the procedures that were previously done on silica monoliths: amination with 3-aminopropyl-triethoxysilane (APS) to produce amino-functionalized materials; grafting of a range of amounts of poly(*N*-isopropyl acrylamide) (PNIPAAm) ($M_w = 20\,000$ mol/g from

GPC) synthesized by RAFT polymerization with a tailored succinimidyl end-group as described before to introduce a thermoresponsive surface property. This procedure involving the grafting of a thermoresponsive polymer to carbonaceous compounds has also been previously described for functional tubular carbon nanotubes¹⁰⁴. The general reaction scheme of the modification of carbon spheres with amino groups and the final grafting of PNIPAAm on its surfaces are described below in Figure 4-33.

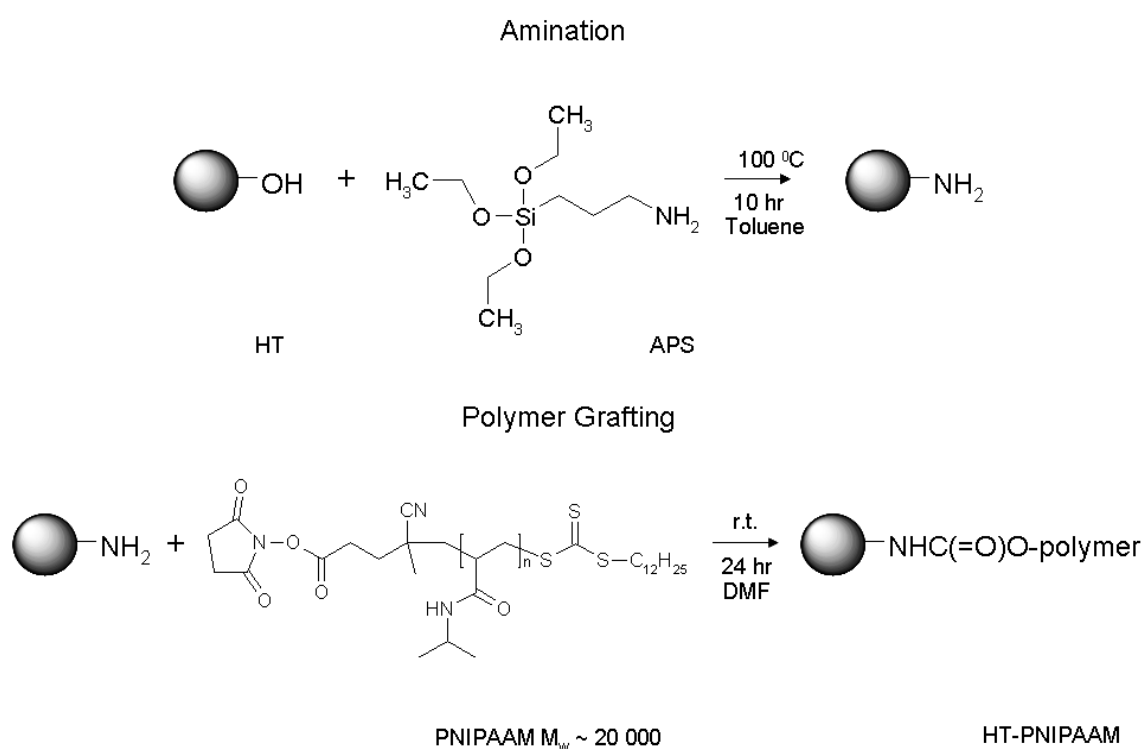


Figure 4-33: General reaction scheme of the amination of hydrothermal carbon (HT) and grafting with PNIPAAm

In order to determine the amount of polymer that is chemically coupled to the hydrothermal carbon spheres, changes in the N% content from elemental analyses were considered. Elemental analyses done on the starting carbon and the final thermoresponsive composite show an increase in N% content from 0.105% to 1.7% and the C% value dropped from 63.32% to 57.675% respectively. With references to Equations 4-1 to 4-4 used for calculating grafting densities of polymer loaded on silica monoliths via elemental analyses, the amount of grafting densities of the final polymer on the carbon surface can be similarly computed. The amount of APS attached to the carbon particles are calculated from Equations 4-7 and 4-8:

$$m_N = \frac{\Delta N}{100 - [\Delta N \times M_{w,APS} / M_N]} \quad \text{Equation 4-7}$$

$$D_{s,APS} = m_N / M_N \quad (\text{mol/g}) \quad \text{Equation 4-8}$$

Where m_N is the weight of nitrogen content of the grafted APS per gram of bare carbon support, ΔN is the %N increase after amination, $M_{w,APS}$ is the weighted average molecular weight of APS, M_N is the weighted average molecular weight of the N fraction of APS, $D_{s,APS}$ is the grafting density of APS on carbon particles. The amount of polymer immobilized on carbon can be calculated with Equations 4-9 and 4-10 below:

$$m_p = \frac{\%N_p \times 10^6}{\%N_{p,theory} [1 - \%N_p / \%N_{p,theory} - \%N_i / \%N_{i,theory}] \times S} \quad (\mu\text{g/m}^2) \quad \text{Equation 4-9}$$

$$D_{s,p} = \frac{m_p \times 10^{-6} \times N_A}{M_{w,polymer}} \quad (\text{chains/m}^2) \quad \text{Equation 4-10}$$

Where m_p is the amount of grafted polymer in μg per m^2 of support, $\%N_p$ is the increase in N% after grafting of polymers, $\%N_{p,theory}$ is the calculated weight %N in a monomer repeat unit, $\%N_i$ is the increase in N% after amination, $\%N_{i,theory}$ is the calculated weight %N in one initiator APS unit, S is the specific surface area of the solid support in m^2/g , $D_{s,p}$ is the grafting density of the polymer in chains/m^2 , N_A is the Avogadro's constant at 6.022×10^{23} and $M_{w,p}$ is the molecular weight of the grafted polymer. According to the computations, the final amount of PNIPAAm grafted onto the carbon surface (500 mg of polymer used) is effectively 3 mg/m^2 .

FT-IR spectras were taken from unmodified hydrothermal carbon spheres (HT) and that of the final thermoresponsive composite (HT-PNIPAAm) in order to determine that the surface functionalities were indeed grafted with a layer of polymer. It was shown on Figure 4-34 below that new absorption bands at 2900 cm^{-1} ($\nu_{(C-H)}$), 1650 and 1700 cm^{-1} corresponding to the amide band and 1540 cm^{-1} corresponding to the N-H amide are observed, thus confirming the grafting of PNIPAAm to the surface of carbon spheres. The band intensifies at $3200\text{-}3500$

($\nu_{\text{(N-H)}}$) for HT-PNIPAAm, showing the excess ungrafted hydrophilic groups (NH_2) after amination with APS.

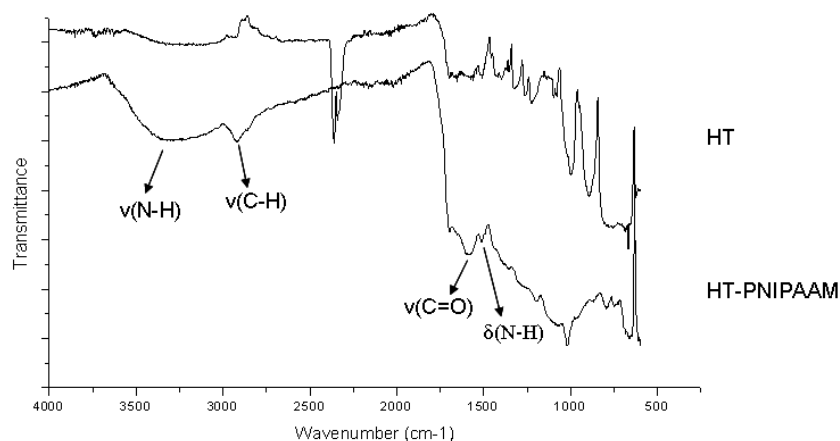


Figure 4-34: FT-IR spectra of starting hydrothermal carbon (HT) and the final thermoresponsive carbon-polymer composite (HT-PNIPAAm)

The ^{13}C CP-MAS solid state NMR of the starting pure carbon (HT) (top spectra) and the final composite HT-PNIPAAm (bottom spectra) was also done (Figure 4-35). The peaks between 100 and 160 ppm accounts for the sp^2 hybridized (aromatic) carbons, the small peak at 175 ppm due to the small amount of carboxylate (COOH) groups on the surfaces and at 200 ppm, it shows the resonance of small amounts of ketones ($\text{C}=\text{O}$) and aldehydes ($\text{C}(=\text{O})\text{H}$). The large peak ranging from 14 to 75 ppm indicates the presence of aliphatic ($\text{C}-\text{C}$) and ether ($\text{C}-\text{O}-\text{C}$) groups. As observed, the aliphatic groups on the HT-PNIPAAm spectra increased (14-60 ppm) in intensity after grafting of the polymer while the ether groups (75 ppm) are shown to decrease, proving that the polymer was indeed coupled to the carbon surface. The decrease in the ether groups after coupling shows the reduction in available surface $\text{C}-\text{O}-\text{C}$ groups that have yet to be modified with PNIPAAm. Since the two spectra remain relatively similar, it was concluded that the grafting process did not change the shape and composition of the carbon spheres in any way, except for the modification in surface functionalities.

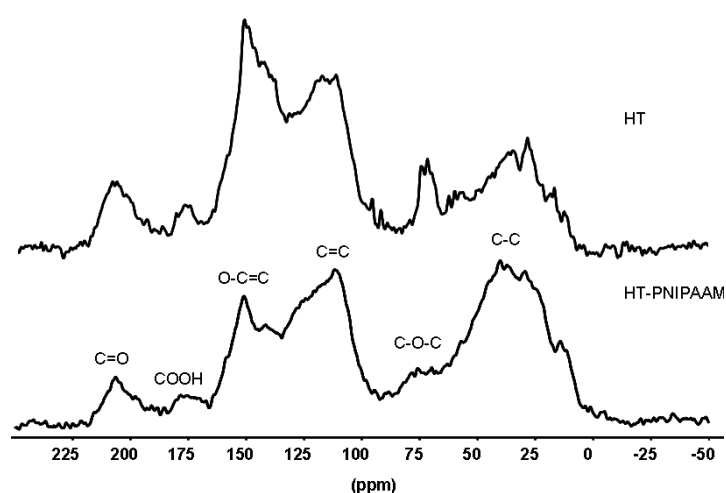


Figure 4-35: ^{13}C solid state NMR of carbon spheres (HT) and those modified with PNIPAAm ($M_w = 20\,000$) (HT-PNIPAAm)

On Figure 4-36 below, the cloud point measurements (heating and cooling cycles) are shown on the thermoresponsive composite (0.25 wt.% in water) with a $1\text{ }^{\circ}\text{C}$ increment-decrement per minute measured from 10 to $60\text{ }^{\circ}\text{C}$. The suspension was first sonicated for 30 minutes before measurements in order to disperse the micrometer-sized particles in water. On the graph, intensity of the light transmittance starts at 0% since when the thermoresponsive polymer is in its hydrophilic form thus dispersing the carbon composite particles in water. As the temperature reaches $35\text{ }^{\circ}\text{C}$, the transmittance was shown to increase, which corresponds approximately to the LCST of PNIPAAm ($32\text{ }^{\circ}\text{C}$). The particles sediment completely at the bottom of the measurement cell as the temperature reaches $45\text{ }^{\circ}\text{C}$, thus allowing 100% of the light transmittance. However, cooling of the sedimentation after does not seem to disperse the particles in water again as carbon remained at the bottom of the measuring cell. Thus it was shown that the stirring action at the bottom of the measuring cell was not strong enough to disperse the heavy carbon sedimentation, that the particles are too large such that they precipitated fast in water. Stronger dispersion strength such as sonication was required to disperse the particles evenly in water. By sonicating while cooling the carbon particles in water, it was also shown that the particles re-dispersed, thus proving the reversibility of the polymer structure from hydrophobic to hydrophilic upon decreasing the temperature.

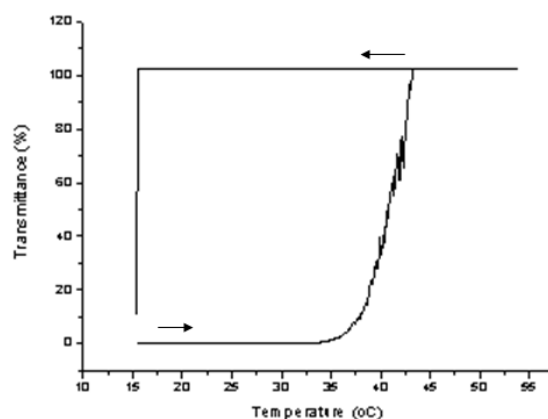


Figure 4-36: Turbidity curve (heating and cooling cycles) of carbon spheres modified with PNIPAAAM ($M_w = 20\,000$) (HT-PNIPAAAM) taken at 0.25 wt.% in water, $1^\circ\text{C}/\text{min}$

As was discussed above, the HTC of pure carbohydrates such as glucose or sucrose produces carbonaceous spheres in the range of 1 to 8 microns under controlled conditions. The size of the spheres obtained depends on the type of sugar used as a precursor, its concentration in water and other reaction conditions such as reaction time and temperature^{87, 105}. The resulting spherical hydrothermal carbons are decorated with a layer of hydrophilic shell, in which the ease of functionalization was demonstrated by attempting to graft the thermoresponsive polymer PNIPAAAM ($M_w=20\,000$ g/mol) on a 5 micron glucose-based particle surfaces. Since the surface area of carbon-based particles are much smaller (10 to $30\text{ m}^2/\text{g}$) and thus surface areas less accessible as compared to that of silica's ($350\text{ m}^2/\text{g}$), the modification of the carbon was done 'ex-situ' in a flask under reflux to induce a higher amount of grafting through harsher reaction conditions before packing it into empty HPLC columns. Characterization methods done on the final HT-PNIPAAAM composite proved that the hydrothermal carbonaceous particles were indeed grafted with a layer of polymer ($3\text{ mg}/\text{m}^2$).

b) Carbohydrates and Additives

The inherent disadvantage of hydrothermal carbon spheres as characterized above is their low surface areas, unlike silica supports with high surface areas of approximately $350\text{ m}^2/\text{g}$. This renders modifiable hydrophilic hydroxyl groups less accessible, especially when surface interactions play an important role in chromatographic analyses. A solution would be to have a one-step synthesis reaction which incorporates the necessary active groups directly so as to eliminate for example, the amination step previously done on silica monoliths, or to find a

way to greatly increase the amount of functional amino groups on carbonaceous product during modification.

It was found that when 10 wt.% of additives like acrylamide or acrylic acid were added to a 10 wt.% glucose solution, stabilization of the particles and change in morphology occur during HTC⁸⁸. This step was also found to incorporate the functional groups of the additive on the final carbon product. Raspberry-like structures (~250 nm) with micro- and macropores form as a result. For example, when acrylamide is used as an additive, the final product is hydrothermal carbon showing surface incorporated acrylamido functional groups.

In order to perform HTC on the same glucose solution with an acrylamide as an additive, the following solution is prepared and stirred before sealing it in an autoclave: 10 wt.% of glucose and 10 wt.% of acrylamide were added to pure water. The reaction mixture was heated up to 200 °C for 19 to 20 hours. After the reaction, the autoclave was cooled down quickly and the final hydrothermal product collected and washed repeatedly with water. After drying, the carbonaceous particles with 10.1 % yield were observed to show monodispersed microspheres formed out of small aggregated particles as shown in the SEM images below (Figure 4-37). In contrast to the product obtained from the HTC of pure carbohydrates^{89, 106}, the surfaces of the particles appeared not smooth. The low yields obtained are accounted by stabilization of the particles with the organic monomer added, thus preventing further size growth as occurred with the pure sugar case. Later on in the process, the polymerized particles assembled into micrometer ‘raspberry-like’ structures¹⁰⁷.

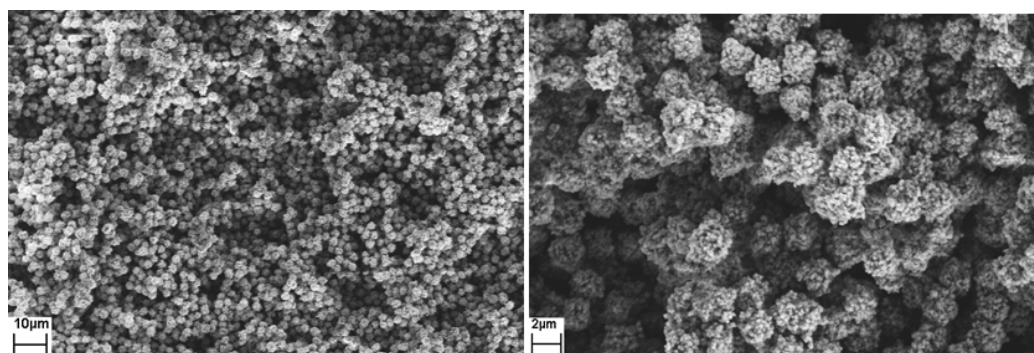


Figure 4-37: SEM image of hydrothermal carbon derived from HTC of 10 wt.% glucose in water with 10 wt.% acrylamide as an additive; 200 °C, 19 hr

These particles show a C% content of 65 % and an N% content of 6.39 % due to doping from the acrylamide monomer additive. The remaining 29.59% is accounted for O% and H%. From the FT-IR spectra as shown in Figure 4-38, hydrophilic groups ($\nu_{\text{(N-H)}}$) including amino from acrylamido C(=O)-NH_2 additive can be observed, which coincides with the elemental analysis results proving the incorporation of reactive functionalities to the surfaces of the final carbon particles.

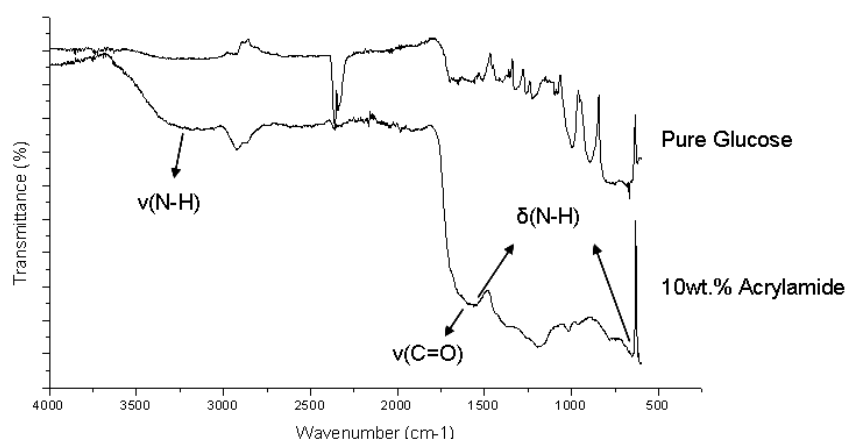


Figure 4-38: FT-IR spectra of hydrothermal carbon derived from HTC of 10 wt.% glucose in water with 10 wt.% acrylamide as an additive; as compared to that of pure glucose; 200 °C, 19 hr

Mercury (Hg) intrusion porosimetry was done to determine the sample's macroporosity. On Figure 4-39 below, the Hg intrusion profile shows that the macropore size lie in the value of approximately 360 nm, and BET measurements done in parallel determined the sample's microporosity in the value of approximately 1 nm (Figure 4-40). The sample shows a surface area of approximately 40 m²/g and a total pore volume of 0.16 cm³/g.

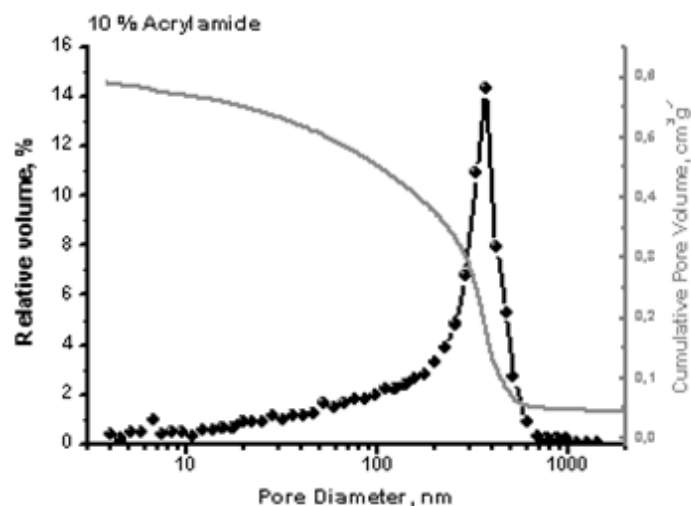


Figure 4-38: Hg intrusion profile of hydrothermal carbon derived from HTC of 10 wt.% glucose in water with 10 wt.% acrylamide as an additive; 200 °C, 19 hr

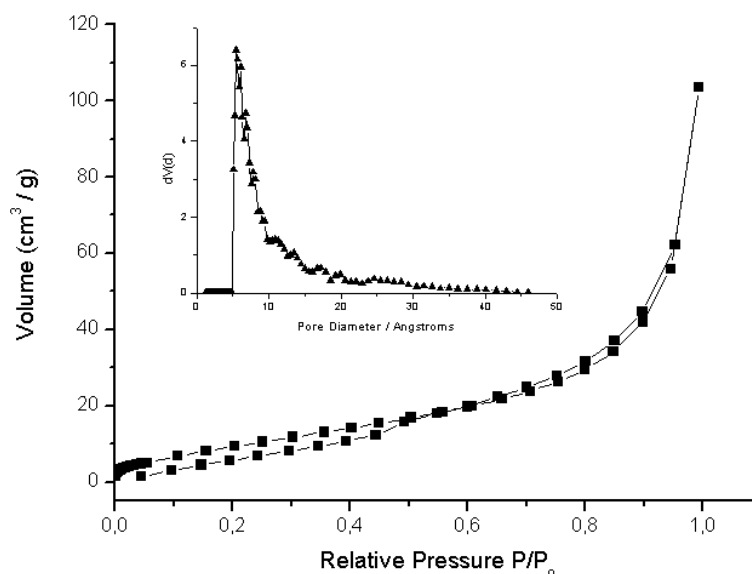


Figure 4-40: Nitrogen sorption data and DFT analysis of hydrothermal carbon derived from HTC of 10 wt.% glucose in water with 10 wt.% acrylamide as an additive; 200 °C, 19 hr

The same aggregated particle morphology (~250 nm diameter structures) can be obtained by carbonizing glucose with 10 wt.% acrylic acid as an additive under the same conditions as previously which was described by Demir-Cakan⁸⁸ (Figure 4-41). Instead of incorporating an amide linkage on the surfaces of the carbon particles, a high amount of carboxylic (COOH) groups would be present instead. The yield of the final product was 10%, with elemental analysis results showing C% at 59.915% and N% at 0.2%. As expected, the sample exhibits a low surface area of 45 m²/g.

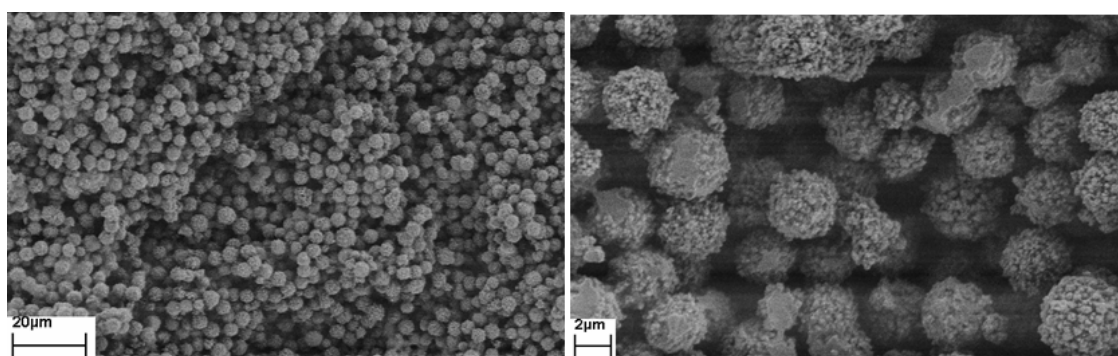


Figure 4-41: SEM image of hydrothermal carbon derived from HTC of 10 wt.% glucose in water with 10 wt.% acrylic acid as an additive; 200 °C, 19 hr

The presence of carboxylic groups on the surface was proven by FT-IR measurements (Figure 4-42). As compared to the surface functionalities of the HTC product obtained from pure glucose, it was shown that the intensity of the absorption band at 1700 cm^{-1} corresponding to the carboxylate groups increased with the addition of the stabilizing acrylic acid into the HTC sample. The adsorption at 1620 cm^{-1} shows the C=C double bonds, C-OH stretching and OH bending vibrations ($1000\text{--}1300\text{ cm}^{-1}$) show hydrophilic functionality present on its surface.

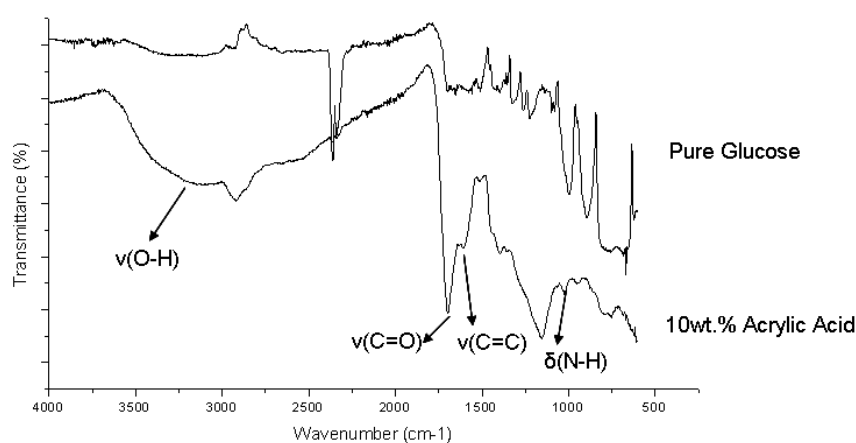


Figure 4-42: FT-IR spectra of hydrothermal carbon derived from HTC of 10 wt.% glucose in water with 10 wt.% acrylic acid as an additive; as compared to that of pure glucose; 200 °C, 19 hr

In addition, TGA was done for both hydrothermal carbon samples obtained from pure glucose and one with a 10 wt.% of acrylic acid. In the profiles shown in Figure 4-43, the pure glucose product shows a lower final mass loss (50%) as compared to that of the nanocomposite (65%), proving that the monomer was indeed incorporated into the final carbon composite.

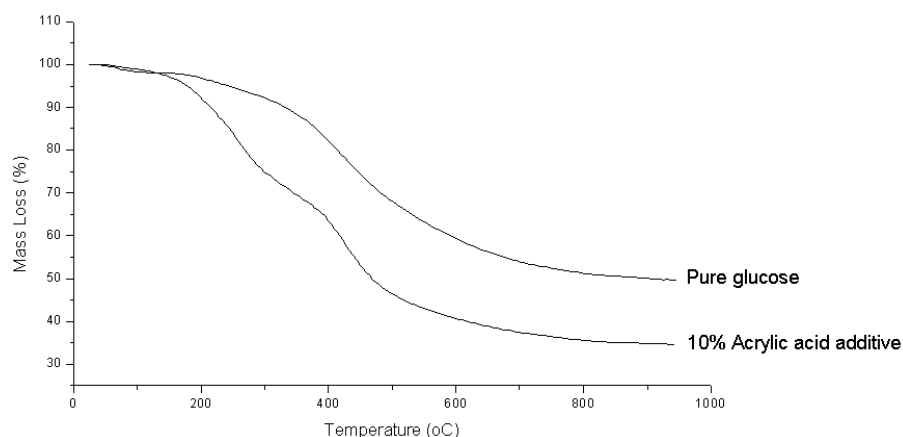


Figure 4-43: TGA profiles of the hydrothermal product obtained from pure glucose and that of the product obtained from glucose with 10 wt.% acrylic acid additive

On the hydrothermal carbon product obtained from the HTC of glucose with 10 wt.% acrylamide monomer, activated PNIPAAm polymer was immobilized onto the surfaces. The reaction solution was heated up in order to initiate the coupling. After the coupling reaction, the raspberry-like morphologies seem to be retained, thus it was proven that the grafting of the polymer does not change the core structures of the particles (Figure 4-44). From elemental analyses, the N% after grafting is increased slightly from 6.39% to 6.56%. The grafting density is calculated to be 0.4 mg/m^2 using Equation 4-8.

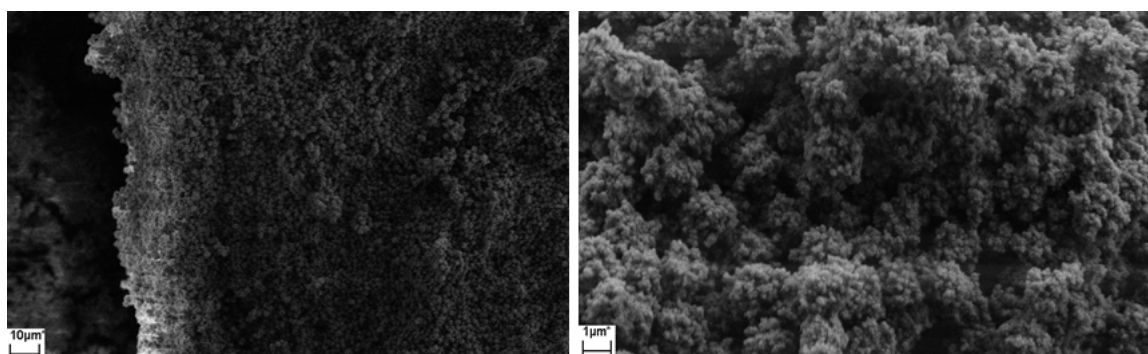


Figure 4-43: SEM image of hydrothermal carbon derived from HTC of 10 wt.% glucose in water with 10 wt.% acrylamide as an additive, modified with PNIPAAm

Figure 4-45 shows the FT-IR spectra of both the unmodified hydrothermal carbon obtained from the HTC of glucose with a 10 wt.% of acrylamide and the PNIPAAm-modified composite. These two spectra are relatively similar due to the amide linkage on both samples. However, at 1540 cm^{-1} , 1650 cm^{-1} and 1700 cm^{-1} corresponding to the amide bonds on the PNIPAAm-modified compound are more pronounced, showing surface modification.

Thus it was seen that functional groups incorporated into carbon microparticles can be synthesized by the simple hydrothermal carbonization of glucose in the presence of an organic monomer with desired functionalities such as acrylic acid (carboxylate surface) or acrylamide (acrylamido surface). The addition of the monomer allows nanostructuring and thus stabilizes the carbon particles chemically and morphologically. Using the surface shells which were finally incorporated with a layer of active groups, thermoresponsive PNIPAAm was then grafted to the carbon in one coupling step. The amount of polymer grafted was calculated to be effectively 0.4 mg/m^2 . This amount is lower than the coupling shown for glucose-based spheres due to less accessible reactive groups directly available on the carbon surfaces.

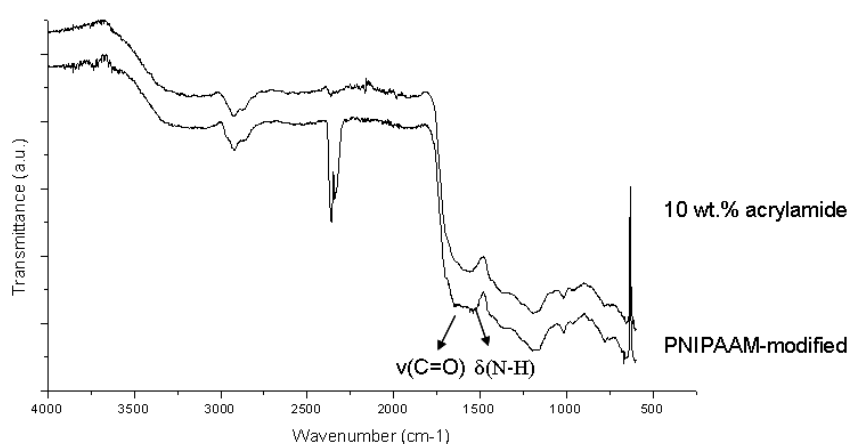


Figure 4-45: FT-IR spectra of starting unmodified 10 wt.% acrylamide-based HT and the final thermoresponsive carbon-polymer composite

The final compounds could then be suspended in toluene and packed into an empty stainless steel column (4.6 X 100 mm; Knauer, Germany) with a HPLC pressure pump (Jasco, Germany) for chromatography.

4.2.3 Chromatographic Characterization

The column packed with non-porous hydrothermal carbon spheres obtained from the HTC of pure glucose (5 μm) was evaluated for its chromatographic performance both as a normal phase (NP) and a reversed phase (RP) modes. The column was assumed to portray both hydrophobic and hydrophilic characters due to its aromatic core and its polar surface groups present respectively. Both the structures could be 'chromatographically visualized' depending on the mobile phases used in each run. Thus, the bi-functional characteristics of the carbon

spheres used as a stationary support are demonstrated using two different HPLC experiment runs. Figure 4-45 shows a series of gallates, gallic acid (**12**), gallic acid methylester (**13**), gallic acid ethylester (**14**) and gallic acid propylester (**15**) used as analytes. The test compounds give different polarities: the hydrophobic character increases with the order from analyte (**12**) to analyte (**15**) while the reverse is true for their hydrophilicities.

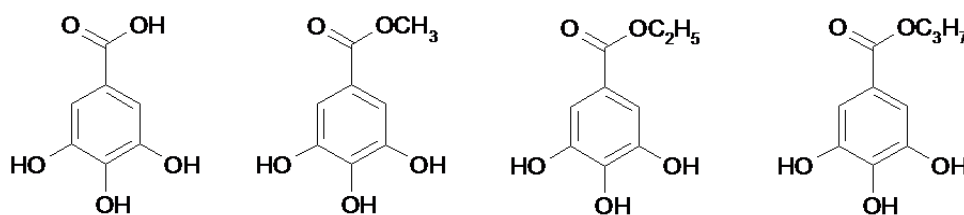


Figure 4-46: Chemical structures of the gallates involved in the NP and RP separation processes

In the first HPLC run, the column was first conditioned with a relatively non-polar solvent, a mixture of isooctane/ dioxane (50/50 (v/v)) for approximately 30 minutes before the test compounds were injected (10 μ l). The flow rate used was 1.5 ml/min, with the UV detector set at 254 nm at room temperature. The back pressure observed was stable at 90 bars. The elution conditions suggested a NP character to the column. On Figure 4-47(b), the same elution profile was carried out with a rehydroxylated silica column (Si300, 5 μ m; 4.6 X 100 mm; Kromasil) in order to compare it with the hydrothermal carbon (HT) column.

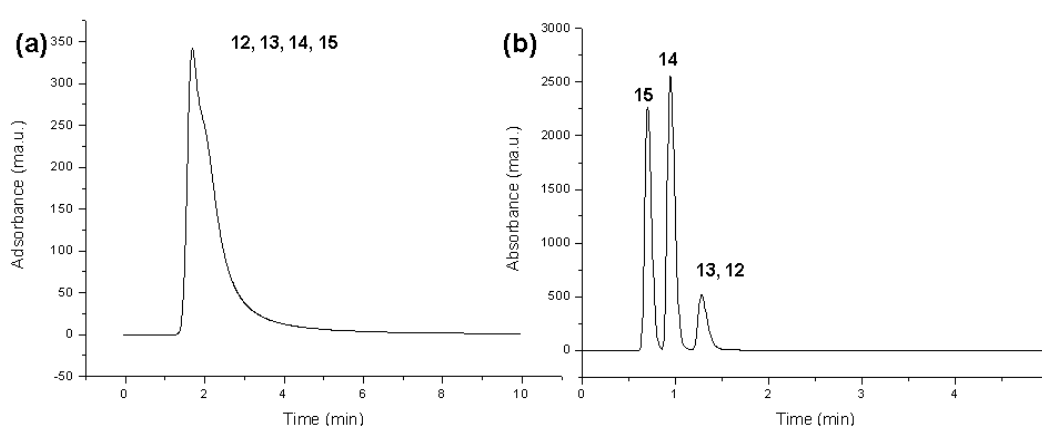


Figure 4-47: Elution profiles and changes in the retention time on four mixtures of gallates under NP mode upon variation of types of stationary phases with (a) hydrothermal carbon column; (b) rehydroxylated silica column

It was shown that while the rehydroxylated silica column eluted three peaks, with the more polar compounds (**12**) and (**13**) not resolved, the hydrothermal carbon column did not resolve

the mixture of analytes at all under isocratic elution. Hence it was concluded that the polarity of the packed carbon particles is not strong enough to neither resolve nor retain gallates under NP conditions.

Subsequently, the columns were also conditioned with a water-rich eluent, phosphate buffer/ acetonitrile (pH 3.0; 95/5 (v/v)) with similar parameters as before. This time, the elution conditions suggested a RP mode for the column. Figure 4-48 shows the elution profiles of the mixture of gallates using the HT column (a) and the silica column (b) under water-rich mobile phases. On the carbon column, it was shown that analytes (**12**) and (**13**) were eluted quickly in less than three minutes in two peaks while the more hydrophobic compounds (**14**) and (**15**) were eluted last in one single broad peak. In contrast, bare silica surfaces are not efficient in resolving gallates while acting as a RP column.

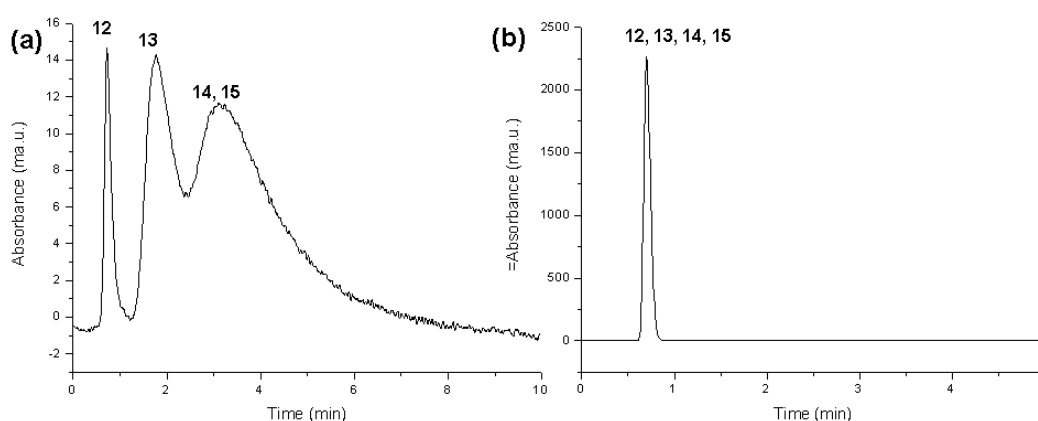


Figure 4-48: Elution profiles and changes in the retention time on four mixtures of gallates under RP mode upon variation of types of stationary phases with (a) hydrothermal carbon column; (b) rehydroxylated silica column

Based on the chromatograms above, the hydrophobicity present in the aromatic cores of hydrothermal carbon spheres was demonstrated to show a certain extent of resolution of gallates under RP conditions more efficiently than when it was acting as a NP stationary phase. The reverse is true for non-bonded polar silica stationary supports.

In order to further characterize the hydrothermal carbon column as a working stationary phase, another set of chromatographic evaluation was carried out with a mixture of benzenes: butylbenzene (**16**) and nitrobenzene (**17**) (Figure 4-49) and their efficiency calculated by plate numbers. A mobile eluent rich in non-polar phase (heptane/ ethyl acetate (95:5)) was run at 1

ml/min under isocratic elution. The wavelength utilized was set at 254 nm. This was done alongside to the previously mentioned rehydroxylated silica column (Kromasil, 5 μ m, 300 Angstroms).

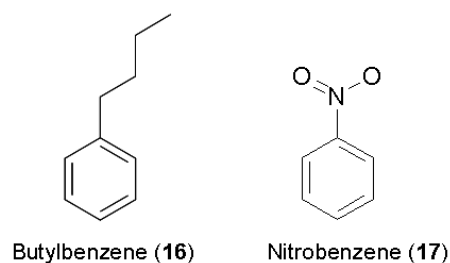


Figure 4-49: Chemical structures of the benzenes involved in the NP separation processes

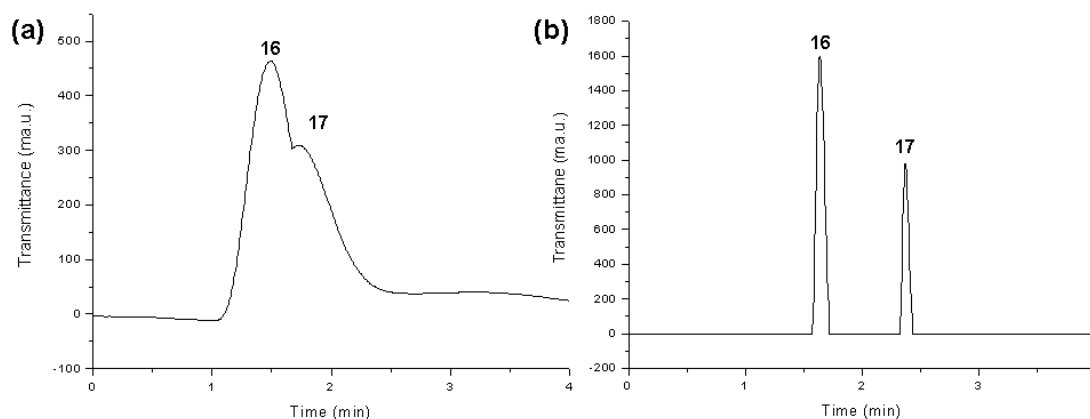


Figure 4-50: Elution profiles and changes in the retention time on two mixtures of benzenes upon variation of types of stationary phases with (a) hydrothermal carbon column; (b) rehydroxylated silica column

The test chromatograms are shown below in Figure 4-50. Since the test mode was under normal phase conditions, the more hydrophilic component, nitrobenzene (**17**) was observed in both cases to be more retained. The carbon column (a) suggested initial separation of both benzene analytes although it was demonstrated previously that it was not hydrophilic enough to separate gallates as a NP stationary phase. The chromatographic performances of both the silica and carbon columns were finally characterized by plate numbers (Table 4-10). However, based on the values of the plate numbers (N) for the carbon column, it was indicated that the performance of the hydrothermal carbon stationary phase was indeed not hydrophilic enough for NP separations.

Column	$t_{R(16)}$	$t_{R(17)}$	$N_{(16)} (m^{-1})$	$N_{(17)} (m^{-1})$	HETP ₍₁₆₎	HETP ₍₁₇₎
Kromasil 300-5	1.63	1.49	2342	5797	0.00004	0.00002
Glucose-based HT Carbon	2.37	1.73	62	46	0.0016	0.0022

Table 4-10: Retention factors k , theoretical plate numbers N and heights equivalent to theoretical plate HETP for each of the benzene analytes for both silica and hydrothermal carbon columns

The HT column's back pressure is relatively stable at 90 bars when subjected to elution for a couple of HPLC runs. However, the pressure began to increase to as high as 300 bars upon repeated chromatography. In order to check if the morphology is still stable after the repeated HPLC runs, the frits were removed from the column and the carbon particles removed and collected. After drying in a vacuum oven overnight, SEM was done on the sample to check the structures.

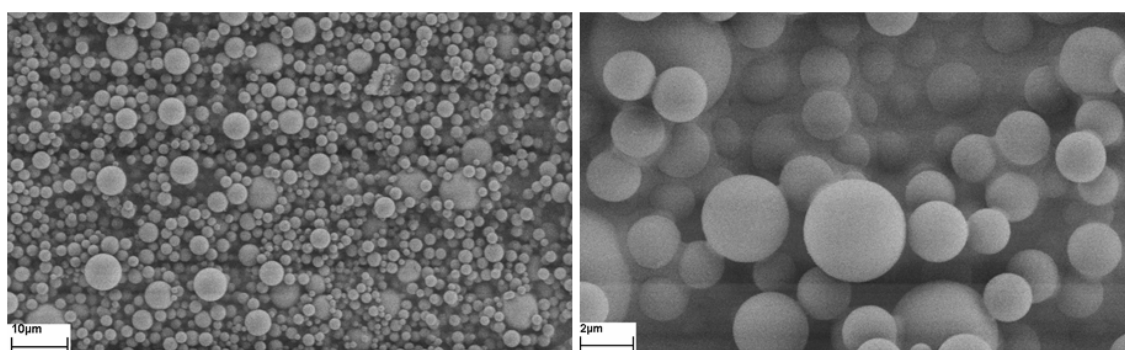


Figure 4-51: SEM image of hydrothermal carbon derived from HTC of 30 wt.% glucose in water; 180 °C, 18 hr; post HPLC runs

From the SEM images shown in Figure 4-51, it was shown that there were a majority of particles present in the post-HPLC run sample with an average size of 100 to 200 nm, including some bigger particles of approximately 500 nm in size. This is a contrast to the pre-HPLC run glucose-based sample, which previously showed bigger spheres in the range of 500 to 800 nm. Moreover, the picture on the right from Figure 4-51 shows spheres which seem to be in a structurally collapsed state. This could thus be proof for the rise in back pressure observations on subsequent HPLC runs using a column packed with glucose-based hydrothermal carbons. The aromatic cores of the carbon seemingly degraded over time when

exposed to mobile phases under high pressures, thus decreasing the sizes of the microspheres. Finally, the spheres are compressed together, forming a block of impenetrable carbon which caused the clogging of the frits and column, thus explaining the continued pressure rise which disrupted analyses.

The stability of bare silica beads was explained previously to be not fully resistant to prolonged exposure towards extreme pH conditions and organic phases. As was discussed, the modification of chromatographic surfaces is a useful method which prolongs the performance life of silica-based columns. Thus, the same postulation towards hydrothermal carbon beads could be made. The glucose-based hydrothermal carbon (HT) materials obtained, which was subjected to grafting with a layer of PNIPAAm ($M_w = 20\,000$ g/mol), is discussed below on the separation of the same group of steroid mixtures (hydrocortisone (1), prednisolone (2), dexamethasone (3), hydrocortisone acetate (4) and testosterone (5)) used previously on thermoresponsive silica monoliths. Stability of the column was also discussed. On Figure 4-52, chromatography characterization of two HT carbon columns, each with a different amount of polymer grafting density (1 mg/m^2 and 3 mg/m^2) done at $55\text{ }^\circ\text{C}$, under pure aqueous conditions isocratically are shown.

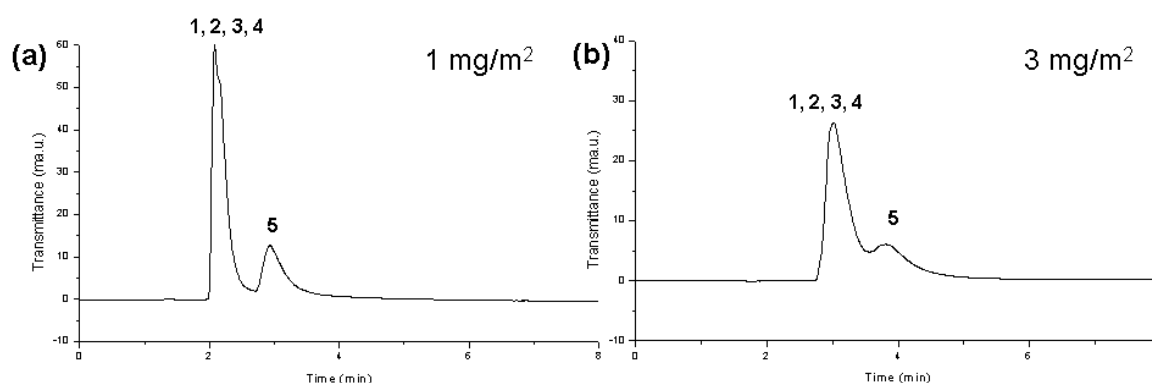


Figure 4-52: Elution profiles and changes in the retention times on five aqueous mixtures of steroids upon variation of the grafting density (a) 1 mg/m^2 and (b) 3 mg/m^2 at $55\text{ }^\circ\text{C}$ (glucose-based HT carbon column)

At the columns' hydrophobic states both at low (a) and higher amount (b) of PNIPAAm grafting, all the steroids were observed to be inefficiently resolved. By introducing a higher amount of polymer to carbon beads thus increasing the column's hydrophobicity, the peaks were shown to be shifted, showing a higher retention of the steroids in the column. However, the resolution was observed to slightly decrease instead.

4.2.4 Summary and Outlook

In conclusion, the attempt to utilize hydrothermal carbons as chromatographic supports for a series of HPLC separations was reported in this chapter. Carbonaceous materials are chosen in my work as a potential alternative to conventional silica-based supports since the former has been known to exhibit superior mechanical strength and chemical stability after porous graphitic carbon (PGC) was proposed as a stationary phase by Knox⁴¹. The inexpensive and environmentally friendly process which was used for the production of carbon particles for chromatography in my work was described as hydrothermal carbonization (HTC).

Pure carbohydrates were carbonized in order to obtain macro- and microporous spheres which boast hydrophobic aromatic cores with polar surface functionalities (OH, C(=O)H, COOH). The desired sphere size were shown to be adjustable by varying certain reaction parameters including type of precursor used, concentration in water, temperature and reaction time. Glucose-based carbon particles (5 μm) were chosen and they were packed first into an empty stainless steel column (4.6 X 100 mm; Knauer, Germany). The column was then tested for its chromatographic performance both in the normal phase (NP) and the reversed phase (RP) modes with a mixture of gallates by changing the mobile eluents in each case. The chromatographic results were shown side by side in a comparison to silica beads-packed column (Si300, 5 μm ; Kromasil 4.6 X 100 mm). It was reported that the performance of the carbons acting as RP column performed relatively better as when it was a NP one. After subjected to repeat HPLC runs under high back pressures (90-300 bars), the structures of the spheres were shown to collapse.

Furthermore, the ease of derivatization of the hydrothermal carbon was demonstrated by attempting to modify and graft PNIPAAm polymer on its surfaces. It was indeed shown that the polymer was attached on the carbon surfaces and turbidity measurements show that the thermoresponsive property was conferred after modification. These polymer-modified carbon beads were later characterized chromatographically as a hydrophobic column in the resolution of steroids in water, where the separation of all the analytes was shown to be less efficient as compared to the same studies conducted previously on silica monoliths.

In addition, functional nanocomposites were produced when a small percent of organic monomer such as acrylic acid or acrylamide was added to the HTC of carbohydrates. The

particles were stabilized when functional groups were loaded onto their surfaces. Incorporated functional groups could provide the necessary ‘active’ surfaces required in our case for the grafting of PNIPAAm. Thus, the amination step discussed before during modification of surfaces could be skipped.

However, the small particulate sizes and the lack of porosity present provided challenges of high back pressures in the HPLC system. Also as was described, the carbonaceous materials collected directly after HTC typically possesses a small surface area (as compared to activated carbon and silica beads). Therefore, this characteristic presents huge challenges as proposed candidates of chromatographic supports. In the chromatographic studies shown on silica with the separation of steroids, mesoporosity was deemed to be an important factor for the adsorption of molecules, thus the lack of porosity in microporous HT could well impede resolution processes. Currently, a lot of attention^{89, 108, 109} is thus turned to techniques which increase surface areas in these carbons. It was reported that pore systems could be imprinted if the HTC of carbohydrates takes place in the presence of templates or additives. For example, mesoporous hydrothermal carbons or hollow spheres could be produced in the presence of nanostructural silica templates⁸⁹ and by using a non-porous template respectively under mild carbonization conditions. Thus, the possibility of using non-porous core/ porous shell HTC particles as chromatographic supports could be introduced. Sponge-like aerogels obtained from the hydrothermal treatment of glucose in the presence of ovalbumin protein were also recently demonstrated that mesopores could be introduced¹¹⁰.

Besides the technique of introducing porosity to allow a higher number of surface sites for the adsorption and retention of analytes, the reduction of non-specific interactions on the surfaces of carbon materials could also be a solution towards efficient chromatography. Further work could be done to further carbonize the hydrothermal carbon materials, by calcining them to temperatures up to 950 °C. The calcined carbon beads will thus display ‘pseudo’ graphitic structures, in which the high amount of specific interactions on its surface would be lost in addition to the introduction of porosity during the process.

5 CONCLUSION

The aim of this work is to synthesize novel stationary phases for high performance liquid chromatography (HPLC) in separation processes which are environmentally benign thus contributing to the field of 'green' chromatography. The first part of the thesis focused on the synthesis of chromatographic supports for the separation of a mixture of hydrophobic analytes in pure water under isocratic elution. Such conditions are important as they allow the retention of the solute biological activities of biocompounds. This was successfully achieved by grafting a layer of thermoresponsive polymer onto mesoporous silica monolithic column (4.6 X 100 mm; MERCK, Darmstadt), thus modifying its surface properties. The second part of the thesis described the synthesis of carbonaceous beads obtained from natural precursors in which they were packed manually after and used as alternate backbone material to silica in chromatography.

In conclusion, we have reported for the first time the preparation and chromatographic evaluation of a PEG-related thermoresponsive stationary phase, leading to the successful separation of a mixture of five steroids based on a simple temperature (hydrophilic-hydrophobic) switch under environmentally friendly aqueous conditions. Oligo(ethylene glycol)-based polymers have been proposed recently as an interesting thermoresponsive alternative to PNIPAAm as they are composed of biocompatible units and could be synthesized with commercially available monomers. Environmental factors such as pH, polymer concentrations and polymer molecular weights were also known to not largely affect its LCST. The synthesis of P(MEO₂MA-*co*-OEGMA) employs the 'living' atom transfer radical polymerization (ATRP) method which gives narrow molecular weight distributions and the final LCSTs of the block copolymers could be linearly tuned according to the amount of comonomer used. Thus, six copolymers with a range of LCSTs (33 °C– 43 °C) and varying chain lengths were used to study the separation processes. As was also shown, by using the tailored succinimidyl end groups of the copolymer, they could be easily 'in-situ' 'grafted to' amino surface-modified silica monoliths.

The experimental results show that below the copolymer's LCST, the five steroids showed separation of the more hydrophilic steroids hydrocortisone and prednisolone, while the more hydrophobic analytes hydrocortisone acetate and testosterone could only be resolved above the column's LCST. This unusual separation behavior of P(MEO₂MA-*co*-OEGMA)-modified

column is a contrast to that of PNIPAAm-grafted ones; PNIPAAm (LCST 32 °C) could only resolve all steroids at its hydrophobic state. Thus a new observation over the latter column was demonstrated, in that P(MEO₂MA-*co*-OEGMA)-modified silica monoliths could selectively separate steroids with different hydrophobicities relative to different elution temperatures. The hydrophobicities of the resultant columns at 55 °C were observed to be in the same range as for the commercial benchmark RP-8 column.

Studies on the influences of various parameters on the elution such as molecular weight of grafted polymer, grafting density, comonomer composition and polymer structures were explored.

The performance of the column was shown to depend on the grafting density of the loaded polymer. As demonstrated on column composite f (LCST 43 °C), it was proven that at low grafting densities (235 µg/m²), the hydrophobicity of the column was not able to separate all five steroids at 55 °C. As more polymer was loaded ($D_s=483 \mu\text{g/m}^2$), the column was then able to resolve all analytes at 55 °C. Similarly, at 5 °C, the column's hydrophilic state was also shown to resolve the more hydrophilic analytes hydrocortisone and prednisolone more efficiently. This effect proves that P(MEO₂MA-*co*-PEGMA)-modified silica monoliths show enhanced performance in both hydrophilic and hydrophobic interactions with steroids upon the increase in polymer grafting density. However, when the D_s reaches 550 µg/m², the performance of the column was observed to decrease. Thus an optimal amount of polymer could be grafted to achieve desired separation effects which also in turn, do not block mesopores to allow efficient elution.

The molecular weight of the grafted polymer is another parameter that affects steroid elution. When a high molecular weight polymer ($M_w=18\,100 \text{ g/mol}$) was grafted to the monolith, it was observed that a lower amount ($D_s=0.0078 \text{ chains/nm}^2$) was required to achieve optimal performance as compared to one ($D_s=0.0295 \text{ chains/nm}^2$) that was grafted with a lower molecular weight polymer ($M_w=6220 \text{ g/mol}$). Since the differences in chain lengths of the polymer do not affect its LCST in water, it is desired that a low amount of grafting density could achieve the same degree of separation since the blocking of pores could then be avoided.

Studying the effect of the variation of comonomer composition of the grafted polymer revealed that their LCSTs could be tuned accordingly to the composition of comonomers used. Thus, the lower the cloud point of the polymer (composite e at LCST 33 °C), the faster the resolution of the steroids at lower temperatures as compared to a column with an LCST of 43 °C (composite f). This feature was proven to be desirable due to the ease of variation of the copolymer's cloud point.

From the HPLC chromatograms discussed in this chapter, P(MEO₂MA-*co*-OEGMA) displays interesting separation properties that are different from other thermoresponsive polymer types PNIPAAm and P(IPOX-*co*-NPOX). Comparing the homo-polymer PNIPAAm in the same steroid separation analysis, it was observed that the PEGylated copolymer of approximately similar molecular weight, LCST and amount of grafting density showed different separation behavior combining the separation of both hydrophilic and hydrophobic bioanalytes while the PNIPAAm-modified monolith was observed to show direct structural change behavior towards the analytes. As for the copolymer P(IPOX-*co*-NPOX), its performance is less efficient as it was unable to resolve all five steroids at 55 °C. This specific character present in P(MEO₂MA-*co*-OEGMA) allows selective interactions with the simple variation of temperature, thus it may be a potential material as catch-release 'bio-gates' in biological applications.

In addition, since this copolymer is biocompatible and the scope of its applications can be further extended to biomedical technology. Protein chromatography was attempted with the pure copolymer analogue and the isocratic elution of two proteins (lysozyme and myoglobin) in aqueous mobile phases showed initial near-baseline resolution. The results shown far surpass previous efforts to separate proteins employing thermoresponsive polymers like PNIPAAm, which was known to extensively retain the compounds. By further optimization of our system, proteomics based on isocratic water conditions may one day overcome current limitations. Further work could also branch out to the introduction of other stimuli-responsive polymers such as a pH-responsive block or molecularly imprinted segments to the existing copolymer block for the separation of other biological analytes such as useful drug compounds.

Finally, a new approach was tried in the attempt to utilize spherical hydrothermal carbons as chromatographic supports for a series of HPLC separations which was reported in Chapter 4.2. Carbonaceous materials are chosen in my work as a potential alternative to conventional silica-based support since the former has been known to exhibit superior mechanical strength and chemical stability after porous graphitic carbon (PGC) was described as a stationary phase by Knox⁴¹. Various reports on the process known as hydrothermal carbonization (HTC) have been shown in our working group to describe the production of carbon materials using ‘green’ technology. The one-step process is inexpensive and environmentally benign since it requires cheap precursors obtained from biomass or biomass products. The operating conditions involve mild temperatures (< 200 °C) and pressures (< 20 bars) under purely water solutions, which avoid aggressive synthesis routes like in the production of PGC.

Within this study, various precursors were chosen (xylose, glucose, sucrose) for HTC. Pure carbohydrates were carbonized in order to obtain spheres which boast stable hydrophobic aromatic cores decorated with polar surface functionalities (OH, C(=O)H, COOH). The desired sphere size could be well adjusted by varying certain reaction parameters including type of precursor used, concentration in water, temperature and reaction time. It was observed that when the concentration of xylose in water to be carbonized increased from 10 wt.% to 30 wt.%, the resultant particles grew in size (from below 1 µm to uniform 1µm spheres). When a different sugar precursor, glucose, was used, the obtained particles were shown to be bigger (5- 8 µm) than that of xylose. The hydrothermal carbon obtained from carbonizing sucrose, however, shows an agglomerated network with emerging spherical forms with an average diameter of 540 nm. These phenomena could be explained from the solubilities of the starting precursor in water: glucose is more soluble than xylose and sucrose, which is a disaccharide of glucose and fructose, is more soluble than glucose, thus the uniform interconnected spheres.

Glucose-based carbon particles (average 500 nm) were chosen and they were packed first into an empty stainless steel column (4.6 X 100 mm; Knauer, Germany). The column was tested for its chromatographic performance both in the normal phase (NP) and the reversed phase (RP) modes with a mixture of gallates by changing the mobile eluents in each case. It was found that the performance of the carbons acting as RP column (resolved three gallates) performed relatively better as when it was a NP one (no resolution). The hydrophobic

interactions from the aromatic particle core are stronger than the hydrophilic groups present on its surfaces. After subjected to repeat HPLC runs at high back pressures (90 to 300 bars), the structures of the spheres were however shown to collapse.

Furthermore, the ease of derivatization of the hydrothermal carbon was demonstrated by attempting to modify and graft PNIPAAm polymer ($M_w=20\,000$ g/mol) on its surfaces. It was indeed shown that the polymer was attached on the surfaces and turbidity measurements show that the thermoresponsive property was indeed grafted after modification. As much as 3 mg/m^2 of PNIPAAm was observed to be grafted on the carbonaceous spheres. Previous modification steps done on silica could be used as a benchmark. Carbon surfaces were observed to be modified and in the process, their morphologies remained unchanged except for their final surface properties. The packed carbon beads (with D_s of 1 mg/m^2 and 3 mg/m^2) were then subjected to chromatography of a mixture of five steroids under isocratic elution. However, the performance of the column at its hydrophobic state did not show satisfactory separation results as compared to thermoresponsive silica chromatographic supports.

In addition, it was also described that functional nanocomposites could be produced when a small percent of organic monomer such as acrylic acid or acrylamide was added to the HTC of carbohydrates. The particles were stabilized when functional groups were loaded onto their surfaces. Incorporated functional groups could provide the necessary 'active' surfaces required in our case for the grafting of PNIPAAm. Thus, the amination step discussed before during modification of surfaces could be skipped. The polymer was directly attached and results show a grafting density of 0.4 mg/m^2 . However, chromatographic characterization faced challenges of high back pressures (pressure immediately reaching 200 bars) due to small particle sizes and microporosities. The system still has to be further optimized in order for it to be used as a chromatographic support.

From the experiments shown above, the low surface areas of the described hydrothermal materials still present huge challenges as proposed candidates of chromatographic supports. More work would be required to optimize hydrothermal carbon spheres, such as surface chemical functionalization or conferring porosity, in order to maximize its working potential as a promising stationary support in the future.

The studies conducted in this research work could therefore be concluded that they are aimed towards the development of novel stationary phases for ‘greener’ separation processes which are environmentally benign in order to meet the growing needs of biotechnology.

6 APPENDIX

6.1 Characterization

Elemental Analyses (EA) (C, H, N, S) were carried out on Vario EL Elementar (Elementar Analysensysteme, Hanau, Germany).

Fourier Transform Infrared (FT-IR) spectras were recorded on a Varian 600 spectrometer (Bio-Rad). All systems were measured using the KBr method.

Nitrogen Sorption measurements were obtained with a Quantochrome Autosorb-1 or Quadrosorb SI at liquid nitrogen temperature conditions (77 K). Prior to measurements, the silica samples were degassed at 80 °C for 20 hours using a masterprep degasser. For carbon, they were degassed at 150 °C for 16 hours. Evaluation of the results was done with BET and NLDFT models provided by the Quantochrome program, equipped with an automated surface area and pore size analyzer. Pore size analyses were done by the use of the equilibrium model for the adsorption and desorption isotherms of nitrogen on silica and carbon under the assumption that pores are cylindrical.

Mercury (Hg) Intrusion Porosimetry probes were sent to Martin Luther Universitaet Halle Wittenberg, Department of Chemistry for measurements.

Thermogravimetric Analyses (TGA) were done on a Netzsch thermoanalyzer model TG 209 F1 at a heating rate of 10 K/min under N₂. Samples were measured under nitrogen environment, starting at room temperatures up to 1000 °C.

Scanning Electron Microscopy (SEM) was performed on a LEO 1550 Gemini instrument. The samples were first loaded onto stubs coated with carbon, and sputtered with a Au/Pd alloy prior to imaging.

Transmission Electron Microscopy (TEM) images were taken using a Zeiss EM 912 Ω operated at an acceleration voltage of 120 kV. Samples were first grounded in a ball mill and dispersed in ethanol. One droplet of the suspension was applied to a 400 mesh carbon-coated copper grid and left to dry under air.

Gel Permeation Chromatography (GPC) measurements were performed to determine molecular weights and molecular weight distributions at 25 °C in THF (flow rate 1 ml/min), using four 5 μ -SDV columns (one guard column and three columns at 4×10^3 , 3×10^5 , 2×10^6 Angstroms). The detection was carried out with a RI (DN-1000, WGE Dr. Bures) and a UV/VIS detector (UV 2000; 260 nm). For calibration, linear polystyrene standards (PSS, Germany) were used.

Proton Nuclear Magnetic Resonance (^1H NMR) were recorded on a Bruker Avance DPX 400 Spectrometer at 300 MHz in deuterated chloroform CDCl_3 . The results obtained were analysed with 1D WINNMR program provided by Bruker. The chemical shift reference was tetramethylsilane (TMS).

Solid State ^{13}C Magic Angle Spinning (MAS) Nuclear Magnetic Resonance (^{13}C NMR) probes were sent to University of Pierre et Marie Curie (Paris, France) for measurements. They were obtained using Bruker Avance 300 MHz (7 T) spectrometer using 4 mm zirconia rotors as sample holders spinning at a MAS rate of 14 kHz. The chemical shift reference was tetramethylsilane (TMS).

Lower Critical Solution Temperatures (LCST) were measured on a turbidimetric photometer TP1 (Elmer Tepper, Mainz, Germany) at a heating and cooling rates of 0.1 °C/min and 1 °C/min with temperatures ranging from 5 to 60 °C. The concentration of polymers taken for measurements was 1 wt.% dissolved in bidistilled water. They were measured after its complete dissolution. Transmittance of polymer solutions in deionized water at 670 nm was monitored as a function of temperature (cell path length: 12 mm). As for silica or carbon particles modified with polymers, the suspension was first sonicated with a Bandelin Sonorex Digitec sonicator for 30 minutes before taking measurements.

High Performance Liquid Chromatography (HPLC) measurements were performed using an Agilent 1200 series equipped with a 3D quaternary pump with a degasser and a diode array detector. The mobile phases used were of HPLC grade and the elution monitored with the UV detector set at 254 nm.

6.2 Experimental Section

6.2.1 Materials

a) Chemicals

2-(2-Methoxyethoxy)ethyl methacrylate (95%) and poly oligo(ethylene glycol) methyl ether methacrylate ($M_n = 475$ g/mol) were obtained from Aldrich. 2,2' bipyridyl (Bipy) (Fluka, 98%) *N,N'*-diclycohexylcarbodiimide (DCC) (Acros, 99%), 2-bromoisobutyric acid (Aldrich, 98%) and *N*-hydroxysuccinimide (Aldrich, 98%) were used as received. Copper (I) chloride (Acros, 95%) was washed with glacial acetic acid in order to remove any soluble oxidized species, filtered, washed with ethanol and dried. *N*-isopropylacrylamide (NIPAAM) (Acros 99%) was purified from recrystallization with hexane before use. Si-100 and Si-300 porous colloidal silica, rehydroxylated cladded silica monolith columns (100 X 4.6 mm), RP-8 and RP-18 silica columns (100 X 4.6 mm) and analytical grade acetonitrile, ethylacetate and 1 M sodium hydroxide solution were kindly provided by MERCK, Darmstadt. (3-Aminopropyl) triethoxysilane (APS) (98%) was purchased from Fluka. 2,2-azobisisobutyronitrile (AIBN) and 4-*N*-Boc-aminopiperidine (98%) were obtained from Acros and were purified from recrystallization with methanol. The steroids hydrocortisone, prednisolone, dexamethasone, hydrocortisone acetate and testosterone, void marker benzene and phenol were purchased from Sigma Aldrich. Uracil, ethylbenzene, dry toluene, diethyl ether, dimethylformamide (DMF), trifluoroacetic acid (99.5%) and dichloromethane were provided by Acros. 2-propanol was purchased from Alfa Aeser and Milli-Q bidestilled water was taken from a Seral purification system (PURELAB Plus) with a conductivity of 0.06 $\mu\text{S}/\text{cm}$. α -D(+)-glucose monohydrate and D-xylose were purchased from Roth, and sucrose from Fluka. Acrylic acid (99.5%, stabilized) and acrylamide (98%) monomers were supplied by Acros. The gallates gallic acid (98%), methyl gallate (99%) and propyl gallate (98%) were also provided by Acros. Ethyl gallate was purchased from Fluka. Potassium hydrogen phosphate (Alfa Aeser) and potassium phosphate monobasic (Riedel de Haen) were used as received. Isopropyloxazoline, n-propyloxazoline monomers, methyl p-tosylate (MeTos) and calcium hydride were used as received from Aldrich.

b) Monoliths and columns

Column	Charge	Type
Chromolith Si-2 Monolith	CL027/2	MERCK, Darmstadt (Research sample) 100 X 4.6 mm; 50 X 4.6 mm
Chromolith RP-8e Monolith	Si2065/801	MERCK, Darmstadt (Research sample) 100 X 4.6 mm
Chromolith RP-18e Monolith	UM8122/054	MERCK, Darmstadt (Research sample) 100 X 4.6 mm
Kromasil 100-5NH2 Packed beads	E53034	Akzo Nobel 100 X 4.6 mm
Kromasil 300-5SIL Packed beads	E53043	Akzo Nobel 100 X 4.6 mm
MonoBis SIL Monolith	09043	Kyoto University (research sample) 50 X 3.2 mm
Stainless steel Empty	-	Knauer 100 X 4.6 mm; 150 X 4.6 mm
Vertex Plus Stainless steel Empty	A2106-1	Knauer 30 X 4.6 mm

6.2.2 Experimental

Synthesis of the ATRP initiator *N*-succinimidyl 2 bromoisobutyrate

The synthetic procedure was adapted from the following reference: D.-H. Han, C.-Y. Pan, *Polymer*, 2006, 47, 6956-6962. Typically, 2-bromoisobutyric acid (6.68 g, 0.04 mol) and *N*-hydroxy-succinimide (5.52 g, 0.048 mol) were dissolved in 200 ml of anhydrous CH₂Cl₂. *N,N'*-dicyclohexylcarbodiimide (DCC) (8.25 g, 0.04 mol) was added into the solution. The reaction mixture was stirred at room temperature for 24 h. A white by-product was separated by filtration. The filtrate was washed with distilled water three times for removal of the unreacted *N*-hydroxysuccinimide, and then dried over anhydrous sodium sulfate for 12 h. After removal of the solvent under reduced pressure, the residue was crystallized from hexane, and then the pure ATRP initiator was obtained in 70% yield. ¹H NMR (300 MHz, CDCl₃): δ 2,08 ppm (s, 6H, Br-C(CH₃)₂-CO-), 2,86 (s, 4H, succinimide).

Atom Transfer Radical Polymerization (ATRP) of MEO₂MA and OEGMA monomers

Copper(I) chloride and 2,2'-bipyridyl (Bipy) were added to a Schlenk tube sealed with a septum. The tube was purged with dry argon for a few minutes. Then, a degassed mixture of poly(ethylene glycol) methyl ether methacrylate, 2-(2-methoxyethoxy) ethyl methacrylate, *N*-succinimidyl 2-bromo-2-methylpropionate and ethanol were added through the septum with a degassed syringe. The mixture was heated at 60 °C in an oil bath for 1 day. The experiment was stopped by opening the flask and exposing the catalyst to air. The solution was diluted with deionized water and subsequently purified by dialysis against water (Roth, ZelluTrans membrane, molecular weight cut-off: 4000-6000). Last, water was removed by rotary evaporation.

Reversible Addition Fragmentation chain Transfer (RAFT) polymerization of NIPAAM

A 4 g amount (35 mmol) of *N*-isopropylacrylamide (NIPAAM) monomer was dissolved in 6 ml of dry DMF. 40 mg (0.1 mmol) of RAFT agent 4-cyanopentanoic acid trithiododecane and 2.6 mg (0.024 mmol) of azobisisobutyronitrile (AIBN) initiator were added to this solution. After three freeze-dry cycles, the reaction mixture was heated up to 70 °C for 24 hours. PNIPAAM polymer was obtained by precipitation into diethyl ether, followed by drying

overnight under vacuum at 50 °C. From GPC, the molecular weight of the polymer was determined to be 14 700 g/mol.

Activation of carboxylated PNIPAAm

4 g (0.14 mmol) of carboxylated PNIPAAm was activated with 115 mg (1 mmol) of *N*-hydroxysuccinimide and 206 mg (1 mmol) of *N,N'*-dicyclohexylcarbodiimide (DCC) in 10 ml of ethyl acetate, and the mixture was stirred at 0 °C for 2 hours, followed by stirring overnight at room temperature. The activated polymer solution was filtered, and the polymer isolated by precipitation in diethyl ether followed by a drying step overnight under vacuum at 50 °C.

Synthesis of 2-isopropyl-2-oxazolin and 2-n-propyl-2-oxazoline monomers

204 g (3.34 mol) of 2-aminoethanol was added dropwise to a suspension consisting of 218 g (3.16 mol) of isobutyronitrile and 42.6 g (0.16 mol) of cadmium acetate dehydrate run at 130 °C. The solution was stirred under this temperature for 24 hours and fractional distillation was carried out after to isolate the 2-isopropyl-2-oxazoline (IPOX) monomer. ¹H NMR (400 MHz, CDCl₃): δ/ ppm= 0.93 (6H, ³J= 7.1 Hz, CH₃), 2.30 (1H, ³J= 7.1 Hz, CH), 3.55 (2H, ³J= 9.6 Hz, CH₂), 3.96 (2H, ³J= 9.6 Hz, CH₂).

The synthesis of 2-n-propyl-2-oxazoline (NPOX) was carried out with similar procedures as above. ¹H NMR (400 MHz, CDCl₃): δ/ ppm= 0.90 (3H, ³J= 7.4 Hz, CH₃), 1.59 (2H, ³J= 7.4 Hz, CH₂), 2.18 (2H, ³J= 7.4 Hz, CH₂), 3.75 (2H, ³J= 9.5 Hz, CH₂), 4.15 (2H, ³J= 9.5 Hz, CH₂).

Cationic Ring Opening Metathesis Polymerization (ROMP) of IPOX and NPOX

Prior to polymerization, all the chemicals were dried over calcium hydride. 10 ml of IPOX (9.39 g, 0.083 mol) and 4.14 ml of NPOX (4.03 g, 0.036 mol), 0.36 ml of the initiator methyl p-tosylate (MeTos) (0.44 g, 0.00238 mol) were dissolved in 29 ml of acetonitrile. The polymerization was carried out at 70 °C for 42 hours. After the reaction, the solution was cooled down to room temperature. 1.43 g of termination agent Boc-protected aminopiperidine (0.00714 mol) was added and the flask heated further at 70 °C for 5 hours. Finally, the acetonitrile was removed by evaporation under vacuum and the remaining polymer re-

dissolved in water. Dialysis against water was carried out to purify the product. Finally, the pure P(IPOX_{32-co}-NPOX₁₅) was obtained by freeze drying.

Activation of P(IPOX-co-NPOX)

6.2 g of the Boc-protected block copolymer was dissolved in 47 ml of dichloromethane. 11.7 ml of trifluoroacetic acid (TFA) was added and the mixture stirred for 30 minutes. After, 138 ml of 1 M sodium hydroxide (NaOH) was added with the reaction flask submerged in an ice bath to cool down the exothermic neutralization. The organic layer was extracted three times with dichloromethane and the water phase discarded. The solvent was later removed by evaporation under vacuum and the remaining polymer was re-dissolved in water. Dialysis against water was done to purify the final product and activated solid polymer obtained upon freeze drying.

Functionalization of rehydroxylated silica monoliths

The synthetic procedure was adapted from the following reference: F. Roohi, M. Antonietti, M.-M. Titirici, *Journal of Chromatography A*, 2008, 1203, 160-167. A 1 ml volume of APS was dissolved in 50 ml dry toluene. 10 ml of the solution was pumped to the cladded rehydroxylated silica monolithic column using an HPLC pump equipped with a degasser. The column was closed and heated up to 65 °C for 24 h. After the reaction, the column was washed with 10 ml of toluene and methanol respectively. 5 ml of the polymer solution dissolved in DMF (0.05 g per ml) was then pumped through the column with the same procedures. The column was closed at both ends and left overnight at room temperature. For characterization, the same reaction was done on free standing monoliths.

Synthesis of carbonaceous materials from carbohydrates

To obtain mono-dispersed carbonaceous spheres, a solution of 30 wt.% xylose in milliQ bi-distilled water (7.7 g sugar, 18 g water) was stirred before it was sealed into a Teflon inlet in an autoclave and hydrothermally treated at 180 °C for 18 to 20 hours. After the reaction, the resulting black carbon materials were centrifuged and the unreacted solution discarded. The solid was washed with water and the solute removed. This washing procedure was repeated

several times. Finally, the carbon was dried in a vacuum oven at 80 °C overnight. In order to study how the concentration of the carbohydrate solution affects the resulting sphere morphology, a 10 wt.% of xylose solution was carried out with the same HTC procedure. In parallel, a 30 wt.% of glucose and 30 wt.% of sucrose solutions were also carried out.

Synthesis of carbonaceous materials with a high degree of functionality

In order to obtain carbonaceous materials with a high degree of functionality, a 10 wt.% of monomer (acrylic acid or acrylamide) was added to a 10 wt.% glucose with respect to water (2 g monomer, 2 g glucose, 18 g water). The reaction mixture was first stirred till it was dissolved, sealed in a Teflon inlet in an autoclave and hydrothermally treated at 190 to 200 °C for 16 to 20 hours. Finally, the obtained materials were centrifuged and the unreacted solute discarded. The remaining solid mass was washed several times with water and the liquid part removed. This procedure was repeated several times. The resulting solid was dried in a vacuum oven at 80 °C overnight.

Functionalization of polar hydrothermal carbon spheres

Approximately 1.5 g of hydrothermal carbon obtained from the HTC of pure glucose was suspended in 50 ml dry toluene in a reaction flask. 1 ml of APS was added and the suspension kept under stirring. Prior to reaction, the mixture was degassed with Argon for 10 minutes, in which it was after heated up to 100 °C under reflux conditions. The reaction was carried out for 12 hours. After the reaction was finished, the flask was cooled down, the mixture was filtered under vacuum with a por4 Buchner filter funnel. The solute was removed and the solid collected was washed with 2 X 50 ml toluene and 2 X 50 ml of methanol to remove unreacted APS. Finally, the amino-rich hydrothermal carbon spheres were dried under vacuum oven at 60 °C overnight. On 1 g of amino-modified hydrothermal carbon spheres, 6 ml of dioxane solution was added and the suspension stirred in a reaction flask. Approximately 50 mg per grafting cycle (up to 500 mg polymer used) of PNIPAAm ($M_w = 20\,000$) was dissolved in 4 ml of dioxane and the polymer solution added to the carbon suspension. The reaction was stirred overnight under room temperature. After the grafting process, the carbon-polymer composite was filtered under vacuum with a por4 Buchner filter funnel and the solute removed. The composite was washed with 2 X 50 ml dioxane, 2 X 50

ml ethanol, 2 X 50 ml methanol, 2 X 50 ml methanol/water (50:50 (v/v)) and 2 X 50 ml water. The polymer-grafted carbon spheres were then collected and dried in a vacuum oven under 50 °C overnight.

Grafting of PNIPAAm to acrylamido-rich hydrothermal carbon

Approximately 1 g of carbon materials obtained from the HTC of glucose with 10 wt.% acrylamide monomer were suspended in 6 ml of dioxane. 50 mg of PNIPAAm per grafting cycle (up to 500 mg) was dissolved in 4 ml of dioxane and the solution added to the suspension. The reaction was stirred and carried out at 50 °C overnight. After the reaction, the suspension was filtered with a por4 Buchner filter funnel under vacuum, the solute removed and the solid washed with 2 X 50 ml dioxane, 2 X 50 ml ethanol, 2 X 50 ml methanol, 2 X 50 ml methanol/water (50:50 (v/v)) and 2 X 50 ml water. The final carbon-polymer composite was left to dry in a vacuum oven at 50 °C.

6.3 Symbols and Abbreviations

Abbreviations

AIBN	2,2-azobisisobutyronitrile
ACN	acetonitrile
APS	3-(aminopropyl)-triethoxysilane
ATRP	atom transfer radical polymerization
BET	Brunauer-Emmet-Teller
Bipy	bipyridyl
BJH	Barrett-Joyner-Halenda
BMA	butyl methacrylate
CROP	cationic ring opening polymerization
DCC	<i>N,N</i> -dicyclohexylcarbodiimide
DFT	density functional theory
DMAEMA	2-(dimethylamino)ethyl methacrylate
DMF	dimethyl formamide
EA	elemental analysis
ED	electron diffraction

EDXS	energy-dispersive X-ray spectroscopy
EELS	electron energy loss spectroscopy
EM	electron microscope
EMLC	electrically modulated liquid chromatography
FT-IR	fourier transform infrared
GCMC	grand canonical Monte Carlo
GPC	gel permeation chromatography
HETP	height equivalent to a theoretical plate
Hg	mercury
HILIC	hydrophilic interaction liquid chromatography
HMF	5-hydroxymethyl-furfural-1-aldehyde
HPLC	high performance liquid chromatography
HT	hydrothermal
HTC	hydrothermal carbonization
IEC	ion exchange chromatography
Iniferter	initiaton, transfer, terminate
IPOX	2-isopropyl-2-oxazoline
IUPAC	International Union of Pure and Applied Chemistry
LCST	lower critical solution temperature
MAS	magic angle spinning
MEO ₂ MA	2-(2-methoxyethoxy)ethyl methacrylate
MeTos	methyl p-tosylate
MS	mass spectrometer
NLDFT	non-local density functional theory
NMR	nuclear magnetic resonance
NMP	nitroxide mediated polymerization
NPC	normal phase chromatography
NPOX	2- <i>N</i> -propyl-2-oxazoline
OEGMA	oligo(ethylene glycol) methacrylate
PDI	polydispersity index
PEG	polyethylene glycol
PEO	polyethylene oxide
PGC	porous graphitic carbon

PIPOX	poly(isopropyl oxazoline)
PNIPAAm	poly <i>N</i> -isopropylacrylamide
RAFT	reversible addition fragmentation chain transfer
ROMP	ring opening metathesis polymerization
RPC	reversed phase chromatography
SEC	size exclusion chromatography
SEM	scanning electron microscopy
Si	silica
TEM	transmission electron microscopy
TEMPO	2,2,6,6-tetramethylpiperidine-1-oxyl
TFA	trifluoroacetic acid
TGA	thermogravimetric analysis
UCST	upper critical solution temperature
UV	ultraviolet (light)
Vis	visible (light)

Symbols

[]	concentration
M_n	average molecular weight
t_R	analyte retention time
t_M	dead time of marker
α	selectivity factor
k	retention factor
$w_{0.5}$	peak width at half height (chromatogram)
N	plate numbers
L	length of HPLC column
$DP_{n,th}$	theoretical degree of polymerization
m_C	weight of carbon content of the grafted APS per gram of bare support
m_N	weight of nitrogen content of the grafted APS per gram of bare support
ΔC	%C increase (from elemental analysis)
ΔN	%N increase (from elemental analysis)
M_w	weighted average molecular weight

$M_{w,APS}$	weighted average molecular weight of APS
$M_{w,polymer}$	weighted average molecular weight of polymer
M_C	weighted average molecular weight of the C fraction of APS
M_N	weighted average molecular weight of the N fraction of APS
D_s	grafting density
$D_{s,APS}$	grafting density of APS
$D_{s,p}$	grafting density of polymer
m_p	amount of grafted polymer per m^2 of support
$\%C_p$	increase in C% after grafting of polymer
$\%N_p$	increase in N% after grafting of polymer
$\%C_{p,theory}$	calculated weight %C in a monomer repeat unit
$\%N_{p,theory}$	calculated weight %N in a monomer repeat unit
$\%C_i$	increase in C% after amination
$\%N_i$	increase in N% after amination
$\%C_{i,theory}$	calculated weight %C in one initiator APS unit
$\%N_{i,theory}$	calculated weight %N in one initiator APS unit
S	specific surface area
N_A	Avogadro's constant 6.022×10^{23}
T	temperature
P	pressure
P_o	saturated pressure
n_M	monolayer capacity (BET)
C	BET constant
E	heat of adsorption (BET)
ν	wavenumber (FT-IR)

7 REFERENCES

1. J. M. S. Pearce, *European Neurology*, 2008, **60**, 51-52.
2. H. Schägger and G. von Jagow, *Analytical Biochemistry*, 1987, **166**, 368-379.
3. T. P. Hennessy, R. I. Boysen, M. I. Huber, K. K. Unger and M. T. W. Hearn, *J. Chromatogr., A*, 2003, **1009**, 15-28.
4. R. Skudas, B. A. Grimes, E. Machtejevas, V. Kudirkaite, O. Kornysova, T. P. Hennessy, D. Lubda and K. K. Unger, *Journal of Chromatography A*, 2007, **1144**, 72-84.
5. M. N. Guy, G. M. Roberson and L. D. Barnes, *Anal. Biochem.*, 1981, **112**, 272-277.
6. B. J. Ledwith, M. K. Cahill, L. S. Losse, S. M. Satiritz, R. S. Eydeloth, A. L. Dallob, W. K. Tanaka, S. M. Galloway and W. W. Nichols, *Anal. Biochem.*, 1993, **213**, 349-355.
7. J. Kobayashi, A. Kikuchi, K. Sakai and T. Okano, *Analytical Chemistry*, 2001, **73**, 2027-2033.
8. B. F. Roettger and M. R. Ladisch, *Biotechnology Advances*, 1989, **7**, 15-29.
9. K. Adachi and T. Asakura, *Journal of Chromatography B: Biomedical Sciences and Applications*, 1987, **419**, 303-307.
10. T. Arakawa, *Archives of Biochemistry and Biophysics*, 1986, **248**, 101-105.
11. A. J. Alpert, *Journal of Chromatography*, 1990, **499**, 177-196.
12. A. J. Alpert, *Analytical Chemistry*, 2008, **80**, 62-76.
13. J. H. Knox, B. Kaur and G. R. Millward, *Journal of Chromatography*, 1986, **352**, 3-25.
14. H. Giesche, K. K. Unger, U. Esser, B. Eray, U. Trudinger and J. N. Kinkel, *Journal of Chromatography*, 1989, **465**, 39-57.
15. K. K. Unger, G. Jilge, J. N. Kinkel and M. T. W. Hearn, *Journal of Chromatography*, 1986, **359**, 61-72.
16. K. K. Unger, G. Jilge, R. Janzen, H. Giesche and J. N. Kinkel, *Chromatographia*, 1986, **22**, 379-380.
17. H. Kanazawa, K. Yamamoto, Y. Matsushima, N. Takai, A. Kikuchi, Y. Sakurai and T. Okano, *Analytical Chemistry*, 1996, **68**, 100-105.
18. F. Roohi, M. Antonietti and M.-M. Titirici, *Journal of Chromatography A*, 2008, **1203**, 160-167.
19. K. K. Unger and E. Weber, *A Guide to Practical HPLC*, GIT VERLAG GMBH, Darmstadt, 1999.
20. F. C. Leinweber and U. Tallarek, *Journal of Chromatography A*, 2003, **1006**, 207-228.
21. B. Bidlingmaier, K. K. Unger and N. von Doehren, *Journal of Chromatography A*, 1999, **832**, 11-16.
22. K. Nakanishi, H. Minakuchi, N. Ishizuka and N. Soga, in *Sol-Gel Synthesis and Processing*, eds. S. Komarneni, S. Sakka, P. P. Phule and R. M. Laine, Editon edn., 1998, vol. 95, pp. 139-150.
23. T. Ikegami, H. Fujita, K. Horie, K. Hosoya and N. Tanaka, *Analytical and Bioanalytical Chemistry*, 2006, **386**, 578-585.
24. D. Wagrowski-Diehl, E. Grumbach, K. Van Tran, U. Neue and J. Mazzeo, *Abstracts of Papers of the American Chemical Society*, 2002, **224**, 068-ANYL.
25. B. W. Pack and D. S. Risley, *Journal of Chromatography A*, 2005, **1073**, 269-275.
26. B. Mayr, F. Sinner and M. R. Buchmeiser, *Journal of Chromatography A*, 2001, **907**, 47-56.
27. W. Sugrue, P. N. Nesterenko and B. Paull, *Journal of Chromatography A*, 2005, **1075**, 167-175.

-
28. S. Rokushika, D. Y. Huang, Z. Y. Qiu and H. Hatano, *Journal of Chromatography*, 1985, **332**, 15-18.
 29. P. Erlandsson, L. Hansson and R. Isaksson, *Journal of Chromatography*, 1986, **370**, 475-483.
 30. H. W. Jarrett, *Journal of Chromatography A*, 1987, **405**, 179-189.
 31. V. A. Davankov, A. A. Kurganov and K. K. Unger, *Journal of Chromatography A*, 1990, **500**, 519-530.
 32. G. Masci, L. Giacomelli and V. Crescenzi, *Macromol. Rapid Commun.*, 2004, **25**, 559-564.
 33. F. Ganachaud, M. J. Monteiro, R. G. Gilbert, M.-A. Dourges, S. H. Thang and E. Rizzardo, *Macromolecules*, 2000, **33**, 6738-6745.
 34. T. Otsu, T. Matsunaga, A. Kuriyama and M. Yoshioka, *Eur. Polym. J.*, 1989, **25**, 643-650.
 35. M. Ejaz, S. Yamamoto, K. Ohno, Y. Tsujii and T. Fukuda, *Macromolecules*, 1998, **31**, 5934-5936.
 36. Y. Nakayama and T. Matsuda, *Macromolecules*, 1996, **29**, 8622-8630.
 37. M. Husseman, E. E. Malmstrom, M. McNamara, M. Mate, D. Mecerreyes, D. G. Benoit, J. L. Hedrick, P. Mansky, E. Huang, T. P. Russell and C. J. Hawker, *Macromolecules*, 1999, **32**, 1424-1431.
 38. X. Huang and M. J. Wirth, *Macromolecules*, 1999, **32**, 1694-1696.
 39. R. A. Sedjo, B. K. Mirous and W. J. Brittain, *Macromolecules*, 2000, **33**, 1492-1493.
 40. B. de Boer, H. K. Simon, M. P. L. Werts, E. W. van der Vegte and G. Hadziioannou, *Macromolecules*, 1999, **33**, 349-356.
 41. J. H. Knox, K. K. Unger and H. Mueller, *Journal of Liquid Chromatography*, 1983, **6**, 1-36.
 42. S. K. Poole and C. F. Poole, *Analytical Communications*, 1997, **34**, 247-251.
 43. Z. Li and M. Jaroniec, *Journal of the American Chemical Society*, 2001, **123**, 9208-9209.
 44. T. Hanai, *Journal of Chromatography*, 2004, **1030**, 13-16.
 45. A. Tornkvist, K. E. Markides and L. Nyholm, *Analyst*, 2003, **128**, 844-848.
 46. S. Wang and M. D. Porter, *Journal of Chromatography A*, 1998, **828**, 157-166.
 47. J. L. Gundersen, *Journal of Chromatography A*, 2001, **914**, 161-166.
 48. B. Kaur, *Lc Gc-Magazine of Separation Science*, 1990, **8**, 468-&.
 49. Y. Daali, S. Cherkaoui, X. Cahours, E. Varesio and J. L. Veuthey, *Journal of Separation Science*, 2002, **25**, 280-284.
 50. I. Clarot, D. Clédad, S. Battu and P. J. P. Cardot, *Journal of Chromatography A*, 2000, **903**, 67-76.
 51. M. Davies, K. D. Smith, A. M. Harbin and E. F. Hounsell, *Journal of Chromatography*, 1992, **609**, 125-131.
 52. E. Forgacs, *Chromatographia*, 1994, **39**, 740-742.
 53. J. C. Berridge, *Journal of Chromatography*, 1988, **449**, 317-321.
 54. H. G. Schild, *Progress in Polymer Science*, 1992, **17**, 163-249.
 55. M. Torres-Lugo and N. A. Peppas, *Macromolecules*, 1999, **32**, 6646-6651.
 56. D. A. VandenBout, W. T. Yip, D. H. Hu, D. K. Fu, T. M. Swager and P. F. Barbara, *Science*, 1997, **277**, 1074-1077.
 57. H. Kanazawa, K. Yamamoto, Y. Kashiwase, Y. Matsushima, N. Takai, A. Kikuchi, Y. Sakurai and T. Okano, *Journal of Pharmaceutical and Biomedical Analysis*, 1997, **15**, 1545-1550.
 58. F. Roohi and M. Magdalena Titirici, *New Journal of Chemistry*, 2008, **32**, 1409-1414.
 59. P. M. Mendes, *Chemical Society Reviews*, 2008, **37**, 2512-2529.

-
60. M. Heskins and J. E. Guillet, *Journal of Macromolecular Science, Chemistry*, 1968, **2**, 1441-1455.
 61. C. d. I. H. Alarcon, S. Pennadam and C. Alexander, *Chemical Society Reviews*, 2005, **34**, 276-285.
 62. J. A. Mackay and A. Chilkoti, *International journal of hyperthermia : the official journal of European Society for Hyperthermic Oncology, North American Hyperthermia Group*, 2008, **24**, 483-495.
 63. H. Uyama and S. Kobayashi, *Chemistry Letters*, 1992, 1643-1646.
 64. N. Adams and U. S. Schubert, *Advanced Drug Delivery Reviews*, 2007, **59**, 1504-1520.
 65. J.-F. o. Lutz, A. z. r. Akdemir and A. Hoth, *Journal of the American Chemical Society*, 2006, **128**, 13046-13047.
 66. J. Nicolas, V. S. Miguel, G. Mantovani and D. M. Haddleton, *Chemical Communications*, 2006, 4697-4699.
 67. J.-F. o. Lutz and A. Hoth, *Macromolecules*, 2005, **39**, 893-896.
 68. M. Chanana, S. Jahn, R. Georgieva, J.-F. o. Lutz, H. Bañumler and D. Wang, *Chemistry of Materials*, 2009, **21**, 1906-1914.
 69. E. Wischerhoff, K. Uhlig, A. Lankenau, H. G. Borner, A. Laschewsky, C. Duschl and J. F. Lutz, *Angewandte Chemie-International Edition*, 2008, **47**, 5666-5668.
 70. E. Wischerhoff, S. Glatzel, K. Uhlig, A. Lankenau, J.-F. o. Lutz and A. Laschewsky, *Langmuir*, 2009, **25**, 5949-5956.
 71. J. M. G. Cowie, 2008.
 72. M. Szwarc and A. Rembaum, *Journal of Polymer Science*, 1956, **22**, 189-191.
 73. M. Szwarc, M. Levy and R. Milkovich, *Journal of the American Chemical Society*, 1956, **78**, 2656-2657.
 74. A. L. J. Beckwith, V. W. Bowry, M. O'leary, G. Moad, E. Rizzardo and D. H. Solomon, *Journal of the Chemical Society-Chemical Communications*, 1986, 1003-1004.
 75. J. Krstina, G. Moad, E. Rizzardo, C. L. Winzor, C. T. Berge and M. Fryd, *Macromolecules*, 1995, **28**, 5381-5385.
 76. C. L. McCormick and A. B. Lowe, *Accounts of Chemical Research*, 2004, **37**, 312-325.
 77. J. Chiefari, Y. K. Chong, F. Ercole, J. Krstina, J. Jeffery, T. P. T. Le, R. T. A. Mayadunne, G. F. Meijjs, C. L. Moad, G. Moad, E. Rizzardo and S. H. Thang, *Macromolecules*, 1998, **31**, 5559-5562.
 78. M. Destarac, D. Charmot, X. Franck and S. Z. Zard, *Macromolecular Rapid Communications*, 2000, **21**, 1035-1039.
 79. R. T. A. Mayadunne, E. Rizzardo, J. Chiefari, J. Krstina, G. Moad, A. Postma and S. H. Thang, *Macromolecules*, 2000, **33**, 243-245.
 80. R. Francis and A. Ajayaghosh, *Macromolecules*, 2000, **33**, 4699-4704.
 81. G. Moad, E. Rizzardo and S. H. Thang, *Australian Journal of Chemistry*, 2005, **58**, 379-410.
 82. J. S. Wang and K. Matyjaszewski, *Journal of the American Chemical Society*, 1995, **117**, 5614-5615.
 83. K. Matyjaszewski and N. V. Tsarevsky, *Nature Chemistry*, 2009, **1**, 276-288.
 84. G. Kickelbick and K. Matyjaszewski, *Macromolecular Rapid Communications*, 1999, **20**, 341-346.
 85. T. E. Patten and K. Matyjaszewski, *Advanced Materials*, 1998, **10**, 901-+.
 86. M. M. Titirici and M. Antonietti, *Chemical Society Reviews*, **39**, 103-116.
 87. M.-M. Titirici, M. Antonietti and N. Baccile, *Green Chemistry*, 2008, **10**, 1204-1212.

-
88. R. Demir-Cakan, N. Baccile, M. Antonietti and M.-M. Titirici, *Chemistry of Materials*, 2009, **21**, 484-490.
 89. M. M. Titirici, A. Thomas and M. Antonietti, *Advanced Functional Materials*, 2007, **17**, 1010-1018.
 90. R. J. White, M. Antonietti and M.-M. Titirici, *Journal of Materials Chemistry*, 2009, **19**, 8645-8650.
 91. X. M. Sun and Y. D. Li, *Angewandte Chemie-International Edition*, 2004, **43**, 597-601.
 92. S. Brunauer, P. H. Emmett and E. Teller, *Journal of the American Chemical Society*, 1938, **60**, 309-319.
 93. E. P. Barrett, L. G. Joyner and P. P. Halenda, *Journal of American Chemical Society*, 1951, **73**, 373-380.
 94. K. S. W. Sing, *Advances in Colloid and Interface Science*, 1998, **76-77**, 3-11.
 95. H. Kanazawa, Y. Kashiwase, K. Yamamoto, Y. Matsushima, A. Kikuchi, Y. Sakurai and T. Okano, *Analytical Chemistry*, 1997, **69**, 823-830.
 96. H. Kanazawa, T. Sunamoto, Y. Matsushima, A. Kikuchi and T. Okano, *Analytical Chemistry*, 2000, **72**, 5961-5966.
 97. J. F. Lutz, *Journal of Polymer Science Part a-Polymer Chemistry*, 2008, **46**, 3459-3470.
 98. A. Leo, C. Hansch and D. Elkins, *Chem. Rev.*, 1971, **71**, 525-616.
 99. H. Kanazawa, M. Nishikawa, A. Mizutani, C. Sakamoto, Y. Morita-Murase, Y. Nagata, A. Kikuchi and T. Okano, *Journal of Chromatography A*, 2008, **1191**, 157-161.
 100. M. Meyer and H. Schlaad, *Macromolecules*, 2006, **39**, 3967-3970.
 101. C. Diehl, P. Cernoch, I. Zenke, H. Runge, R. Pitschke, J. Hartmann, B. Tiersch and H. Schlaad, *Soft Matter*, **6**, 3784-3788.
 102. A. Berthod, *Journal of Chromatography A*, 1991, **549**, 1-28.
 103. P. Makowski, R. D. Cakan, M. Antonietti, F. Goettmann and M.-M. Titirici, *Chemical Communications*, 2008, 999-1001.
 104. S. Kubo, I. Tan, R. J. White, M. Antonietti and M.-M. Titirici, *Chemistry of Materials*, **22**, 6590-6597.
 105. N. Baccile, G. Laurent, F. Babonneau, F. Fayon, M.-M. Titirici and M. Antonietti, *J. Phys. Chem. C*, 2009, **113**, 9644-9654.
 106. Q. Wang, H. Li, L. Chen and X. Huang, *Carbon*, 2001, **39**, 2211-2214.
 107. R. Demir-Cakan, N. Baccile, M. Antonietti and M.-M. Titirici, *Chem. Mater.*, 2009, **21**, 484-490.
 108. H.-S. Qian, S.-H. Yu, L. Luo, J. Gong, L. Fei and X. Liu, *Chem. Mater.*, 2006, **18**, 2102-2108.
 109. J. C. Yu, X. Hu, Q. Li, Z. Zheng and Y. Xu, *Chemistry – A European Journal*, 2006, **12**, 548-552.
 110. N. Baccile, M. Antonietti and M. M. Titirici, *Chemsuschem*, **3**, 246-253.

ACKNOWLEDGEMENTS

I would like to humbly express my sincere thanks to all who have given me guidance and support in completing my Ph.D work or 'Doktorarbeit'. The knowledge and encouragement I have received from this period is invaluable. First of all, I would like to thank my 'Doktorvater' Prof. Dr. Markus Antonietti, for giving me the opportunity to do my Ph.D at one of the most prestigious institutes not only in Germany but worldwide. Many many thanks go to my supervisor, Dr. Maria-Magdalena Titirici, with whom I share not only many constructive discussions at work, but for making the start of my Berlin life more interesting with the great weekends. Thanks for being very straightforward and patient all this time.

With special mention to Dr. Jean-Francois Lutz and Zoya Zarafshani from the Fraunhofer Institute for Applied Polymer Research (IAP), for their total support and discussions on some aspects of my work, without which the conclusion of my project will not be possible.

I would like to thank Prof. Dr. Klaus Unger whom I am real honoured to have met in Hohenroda, but whose summer school I have had no chance to attend yet, for his knowledge and interest in my field which served as a huge inspiration. Prof. Dr. Wolfgang Lindner (University Vienna, Austria) and Dr. Ales Podgornik (BIA Separations, Slovenia) are acknowledged for providing the opportunities for me to vocalize my project in Euroanalysis 2009 and BIA Summer School 2010 respectively. Thank you for the endless encouragements and support. Because of you, I believe that there are people out there who always have the time to enjoy science.

Many thanks to Dr. Klaus Tauer for his 'good temper'; it is definitely enjoyable to say 'hello' everyday. I express my absolute gratitude to Regina Rothe for keeping our lab in a tip-top condition, and for the nice time we had in the last two class trips. Thank you Regina, for your friendship and the delicious cookies. I am deeply indebted to Marlies Graewert (GPC) for measuring my large amount of samples, and being really efficient in them. I really appreciate that every time I ran into technical problems, Marlies is the one who helped me solve them. Sylvia Pirok is acknowledged for the quick elemental analyses, Irina Shekova for the TGA measurements, Rona Pitscke and Heike Runge for SEM/ TEM pictures. Thanks to Frau

Anette Pape and Annemarie Schulz for making all administrative matters a breeze. I owe my SEM/ TEM measurements also to Jelena, Camillo and Steffi.

Without these people I am about to mention, my working life in Golm would be less bearable. Many thanks go to my office mate Jekaterina Jeromenok, who is a great company in difficult times. Shiori, you would probably be the only person who shares the same ‘Asian in Europe’ dilemma as I do, thank you for always being there. Jelena, thank you for the long chats and for sharing common interests like theatre and music, and simply just for the friendship. I will also never forget the memorable ‘Bratwurst on Friday’ and the countless German phrases that Alex and Daniel have taught me. A very big thank you to the rest of my group mates and ‘coffee corner informants’ Nico, Camillo, Robin, Steffi, Tim, Fillipe, Li, Hiro, Su Jeong, Ling Hui, Clara, Stefan, Betti, Nina, Admir, thank you for the extremely funny times in Golm or in CCCP. As for the people who have since left Golm, Jerome, Niki, Fernando, Jules, Alfonso, Rafi, Andreas, Marina, Mari-Luz, Andi Picker, Farnoosh, Zoya, Rezan, I will always remember the personal times I shared with each of you.

I would also like to extend a really huge appreciation to the good friends who have gone a long way together with me, despite the ups and downs we went through, you stuck around. You may not know that I’ve dedicated a little space to thank you because you may never read a scientific thesis ever. Suzanne, Crystal, Jocelyn, Cheryl, Arakah, Juuso, Mathias Boeck, Aslinda, Houy-Sy, you deserve a mention and a big hug. Your support means a lot to me. To the people who made life in Berlin and Germany bearable, Vedi, Florian, Tobias Richter, Tobias Keye, Bastl, Lotte, Niels, Axel, Carlos, Boedi, Sonia, Claudia, Christine and more I have not mentioned, you all know who you are, I owe everyone a huge thank you.

Before I run out of space, I have to express my deepest gratitude to one person who has been and will always be thanked in all my theses, Matthias Range. As clichéd as it is always, I am especially grateful for your patience and love. The tremendous support you lend me is irreplaceable, even though you might have difficulty understanding my job. Last but not least, I express my heartfelt thanks to my family, whose encouragement and patience have served as the biggest motivation throughout my thesis work.

EIDESSTATTLICHE ERKLÄRUNG / STATUTORY DECLARATION

“Hiermit erkläre ich an Eides statt, dass ich die vorliegende Dissertation selbständig und ohne Hilfe verfasst, andere als die angegeben Quellen und Hilfsmittel nicht benutzt und die benutzen Quellen wörtlich oder inhaltlich entnommenen Stellen als solche kenntlich gemacht habe.”

Potsdam, im Februar 2011

“I herewith formally declare that I myself have written the submitted dissertation independently. I did not use any outside support except for the quoted literature and all the other sources which I employed producing this academic work, either literally or in content.”

Potsdam, February 2011-02-01

Tan, Irene